

PHYSICOCHEMICAL AND ADHESION PROPERTIES OF SOY PROTEIN BASED
ADHESIVES

by

MIN JUNG KIM

B.S., Sunshin Women's University, 2003

M.S., Hanyang University, 2007

AN ABSTRACT OF A DISSERTATION

submitted in partial fulfillment of the requirements for the degree

DOCTOR OF PHILOSOPHY

Department of Grain Science and Industry
College of Agriculture

KANSAS STATE UNIVERSITY
Manhattan, Kansas

2015

Abstract

Soy protein is one of the most promising bio-degradable adhesives as an alternative to synthetic petroleum-based adhesives for wood composite industries. In this study, soy protein was modified to improve adhesion properties and water resistance, which could facilitate the industrialization of soy protein-based adhesives. Furthermore, we attempted to identify a reliable indicator to predict the adhesion properties of soy protein by establishing the correlation of physical and mechanical properties with adhesion properties of soy protein.

One of the objectives in this work was to investigate if inorganic calcium silicate hydrate (CSH) hybrids could improve adhesion properties of soy protein-based adhesives. 3-aminopropyltriethoxysilane (APTES) was used as a crosslinking agent between organic soy protein and inorganic CSH phases. APTES helped to form a crosslinked interface between soy protein and CSH, which was confirmed by changes in thermal, rheological, spectroscopic, and morphological properties with aging effect. More entangled structure and reduction of water-sensitive functional groups could lead to improvements in adhesion strength compared to unmodified soy protein-based adhesives.

The second objective was to identify reliable indicators to predict shear adhesion properties by building the correlation between physical properties and adhesion properties of enzymatically modified soy protein-based adhesives (ESP). ESP was prepared with three independent variables (X_1 : trypsin concentration, X_2 : incubation time, and X_3 : glutaraldehyde (GA) concentration as a crosslinker) using a response surface methodology (RSM) called a central composite design (CCD). The important physical properties of viscosity (Y_1), tacky force (Y_2), and water resistance (Y_3) were measured and investigated their relationship with adhesion strength. Viscosity, tacky force and water resistance showed solid correlation with adhesion

strength of ESP and they were used to predict adhesion performance of soy protein modification system in this work.

In addition, we studied the correlation between film strength and adhesion strength of another soy protein system. Because cohesion among protein molecules plays an important role in film and bonding mechanisms, we assumed that the film strength may be a reliable indicator to predict the adhesion strength of soy protein. The mechanical properties of the film and adhesion properties of soy protein on cherry wood were measured in terms of different concentrations of plasticizer (poly (propylene glycol) bis (2-aminopropyl ether) ($H_2N-PPG-NH_2$)). The results found out the low correlation between film and adhesion strength of soy protein in the presence of the plasticizer. We believe this might be caused by different curing conditions for film and adhesive applications of soy protein. Curing conditions greatly affect the thermal and curing behavior as well as mechanical properties of final materials. Thus, similar or comparable curing conditions should be required to obtain the information on the relationship between film and adhesion strength of soy protein.

PHYSICOCHEMICAL AND ADHESION PROPERTIES OF SOY PROTEIN BASED
ADHESIVES

by

MIN JUNG KIM

B.S., Sunshin Women's University, 2003
M.S., Hanyang University, 2007

A DISSERTATION

submitted in partial fulfillment of the requirements for the degree

DOCTOR OF PHILOSOPHY

Department of Grain Science and Industry
College of Agriculture

KANSAS STATE UNIVERSITY
Manhattan, Kansas

2015

Approved by:

Major Professor
Xiuzhi Susan Sun

Copyright

MIN JUNG KIM

2015

Abstract

Soy protein is one of the most promising bio-degradable adhesives as an alternative to synthetic petroleum-based adhesives for wood composite industries. In this study, soy protein was modified to improve adhesion properties and water resistance, which could facilitate the industrialization of soy protein-based adhesives. Furthermore, we attempted to identify a reliable indicator to predict the adhesion properties of soy protein by establishing the correlation of physical and mechanical properties with adhesion properties of soy protein.

One of the objectives in this work was to investigate if inorganic calcium silicate hydrate (CSH) hybrids could improve adhesion properties of soy protein-based adhesives. 3-aminopropyltriethoxysilane (APTES) was used as a crosslinking agent between organic soy protein and inorganic CSH phases. APTES helped to form a crosslinked interface between soy protein and CSH, which was confirmed by changes in thermal, rheological, spectroscopic, and morphological properties with aging effect. More entangled structure and reduction of water-sensitive functional groups could lead to improvements in adhesion strength compared to unmodified soy protein-based adhesives.

The second objective was to identify reliable indicators to predict shear adhesion properties by building the correlation between physical properties and adhesion properties of enzymatically modified soy protein-based adhesives (ESP). ESP was prepared with three independent variables (X_1 : trypsin concentration, X_2 : incubation time, and X_3 : glutaraldehyde (GA) concentration as a crosslinker) using a response surface methodology (RSM) called a central composite design (CCD). The important physical properties of viscosity (Y_1), tacky force (Y_2), and water resistance (Y_3) were measured and investigated their relationship with adhesion strength. Viscosity, tacky force and water resistance showed solid correlation with adhesion

strength of ESP and they were used to predict adhesion performance of soy protein modification system in this work.

In addition, we studied the correlation between film strength and adhesion strength of another soy protein system. Because cohesion among protein molecules plays an important role in film and bonding mechanisms, we assumed that the film strength may be a reliable indicator to predict the adhesion strength of soy protein. The mechanical properties of the film and adhesion properties of soy protein on cherry wood were measured in terms of different concentrations of plasticizer (poly (propylene glycol) bis (2-aminopropyl ether) ($H_2N-PPG-NH_2$)). The results found out the low correlation between film and adhesion strength of soy protein in the presence of the plasticizer. We believe this might be caused by different curing conditions for film and adhesive applications of soy protein. Curing conditions greatly affect the thermal and curing behavior as well as mechanical properties of final materials. Thus, similar or comparable curing conditions should be required to obtain the information on the relationship between film and adhesion strength of soy protein.

Table of Contents

List of Figures	xi
List of Tables	xiii
Acknowledgements.....	xiv
Chapter 1 - INTRODUCTION	1
1.1. GENERAL BACKGROUND.....	1
1.2. OBJECTIVE	4
1.3. REFERENCES	5
Chapter 2 - LITERATURE REVIEW	7
2.1. STRUCTURE OF SOY PROTEIN	7
2.2. SOY PROTEIN AS A WOOD ADHESIVE	8
2.2.1. Adhesive application to wood.....	8
2.2.2. Theories of adhesion	9
2.3. PERFORMANCE OF SOY PROTEIN ADHESIVES.....	11
2.3.1. PARTICLE SIZE	11
2.3.2. NATURE OF SURFACE AND SUBSTRATE.....	12
2.3.3. VISCOSITY	12
2.3.4. PROCESSING PARAMETERS.....	13
2.4. SOY PROTEIN ADHESIVES AND MODIFICATION	14
2.4.1. DENATURATION AND CLEAVAGE OF SOY PROTEINS.....	14
2.4.2. ENZYMATIC MODIFICATION.....	16
2.4.3. CROSSLINKING	17
2.4.4. NANO TECHNOLOGY.....	18
2.5. REFERENCES	18
Chapter 3 - ADHESION PROPERTIES OF SOY PROTEIN CROSSLINKED WITH ORGANIC CALCIUM SILICATE HYDRATE HYBRID	22
3.1. ABSTRACT.....	22
3.2. INTRODUCTION	22
3.2.1. Reaction mechanism hypothesis	25

3.3. EXPERIMENTAL PROCEDURES	27
3.3.1. MSP sample preparation	27
3.3.2. Synthesis of hybrid organic CSH and adhesive preparation.....	27
3.3.3. Differential scanning calorimetry (DSC).....	27
3.3.4. Dynamic viscoelastic measurement	28
3.3.5. FT-IR spectroscopy.....	28
3.3.6. Scanning Electron Microscopy	28
3.3.7. Two ply plywood specimen preparation	29
3.3.7. Three ply plywood specimen preparation.....	29
3.3.8. Shear strength measurement	29
3.4. RESULTS AND DISCUSSION	30
3.4.1. Thermal Properties	30
3.4.2. Dynamic Viscoelastic Properties	33
3.4.3. FT-IR Spectroscopic properties	34
3.4.5. Morphological Properties.....	36
3.4.6. Shear Adhesion Strength.....	37
3.5. CONCLUSION.....	38
3.6. REFERENCES	38
Chapter 4 - CORRELATION BETWEEN PHYSICAL PROPERTIES AND SHEAR	
ADHESION STRENGTH OF ENZYMATICALLY MODIFIED SOY PROTEIN-BASED	
ADHESIVES	56
4.1. ABSTRACT.....	56
4.2. INTRODUCTION	57
4.3. EXPERIMENTAL PROCEDURES	58
4.3.1. Materials	58
4.2.2. Experimental design.....	59
4.2.3. MSP and ESP sample preparation	60
4.2.4. Physicochemical properties measurement	60
4.2.4.1. Viscosity Measurement.....	60
4.2.4.2. Tacky force	60
4.2.4.3. Water resistance	61

4.2.5. Mechanical plywood properties	62
4.2.5.1. Two ply plywood specimen preparation.....	62
4.2.5.2. Shear strength measurement	62
4.4. RESULTS AND DISCUSSION	63
4.3.1. Model fitting	63
4.3.2. Interpretation of response surface model	65
4.3.3. Relationship between three responses and shear adhesion properties	68
4.3.3.1. Viscosity	68
4.3.3.2. Tacky force	70
4.3.3.3. Water resistance	71
4.4. CONCLUSION.....	72
4.5. REFERENCES	72
Chapter 5 - CORRELATION BETWEEN FILM STRENGTH AND ADHESION STRENGTH OF SOY PROTEIN	87
5.1. ABSTRACT.....	87
5.2. INTRODUCTION	87
5.2. EXPERIMENTAL PROCEDURES.....	89
5.2.1. Materials and SPI separation	89
5.2.2. SPI Separation and soy protein based biopolymer preparation.	90
5.2.3. Preparation of soy protein-based films	90
5.2.4. Characterization of physical and mechanical properties of the film.....	90
5.2.4.1. Tensile strength and Elongation at Break of the film	90
5.2.4.2. Water resistance of the film	91
5.2.4.3. Two ply plywood specimen preparation and adhesion strength measurement....	91
5.3. RESULTS AND DISCUSSION	92
5.3.1. Tensile strength.....	93
5.3.2. Water resistance of film	95
5.4. CONCLUSION.....	95
5.5. REFERENCES	96
Chapter 6 - CONCLUSION.....	104

List of Figures

Figure 3.1 Hypothesis of the reaction pathways between soy proteins and CSH at the covalent interface.....	44
Figure 3.2 DSC thermograms of MSP and fresh and aged MSP-CSH/20% APTES.	45
Figure 3.3 The degree of recovery of T_d and ΔH_d of MSP-CSH composites with different molar ratios of APTES.	46
Figure 3.4 The frequency dependence of the elastic modulus (G') of MSP and MSP-CSH composites with different molar ratios of APTES.	47
Figure 3.5 The complex viscosities of MSP and aged MSP-CSH composites with different molar ratios of APTES.	48
Figure 3.6 FT-IR spectra of (a) MSP and CSH/20% APTES and (b) fresh and aged MSP-CSH composites with different molar ratios of APTES for with spectral ranges from 1700 to 900 cm^{-1}	49
Figure 3.7 Enlarged spectral feature of peaks and the degree of peak shift at 1634 cm^{-1} (A) and at 1634 cm^{-1} (B) as insets.....	50
Figure 3.8 SEM images of MSP-CSH composites with different molar ratios of APTES (A) MSP, (B) MSP-CSH, (C) MSP-CSH/20% APTES and (D) MSP-CSH/40% APTES.	51
Figure 4.1 The effects of three variables on viscosity: Three levels (-1, 0, and +1) of (A) incubation times (X_2) are presented with trypsin concentrations (X_1), (B) trypsin concentrations (X_1) are presented with GA concentrations (X_3), and (C) GA concentrations (X_3) were presented with incubation times (X_2). The other variable was maintained at zero.	75
Figure 4.2 The molecular bands of reducing SDS-PAGE at 0.50wt% trypsin concentration. Lane (A): molecular weight standard; lane (B): control MSP; lane (C)-(F): MSP applied to 0.50 wt% trypsin with 1, 3, 6, and 12-h incubation times.	76
Figure 4.3 The effects of three variables on tacky force: Three levels (-1, 0, and +1) of (A) incubation times (X_2) are presented with trypsin concentrations (X_1), (B) trypsin concentrations (X_1) are presented with GA concentrations (X_3), and (C) GA concentrations (X_3) are presented with incubation time (X_2). The other variable was maintained at zero.	77

Figure 4.4 The effects of three variables on water resistance: Three levels (-1, 0, and +1) of (A) incubation times (X_2) are presented with trypsin concentrations (X_1), (B) trypsin concentrations (X_1) are presented with GA concentrations (X_3), and (C) GA concentrations (X_3) are presented with incubation times (X_2). The other variable was maintained at zero. 78

Figure 4.5 The regression model between viscosity and dry strength (a) and wet strength (b). .. 79

Figure 4.6 The regression model between tacky force and dry strength (a) and wet strength (b).80

Figure 4.7 The regression model between water resistance and dry strength (a) and wet strength (b)..... 81

Figure 5.1 The regression model between tensile strength (TB) and dry (a) and wet (b) shear adhesion strength. 99

Figure 5.2 The regression model between water resistance and dry (a) and wet (b) shear adhesion strength..... 100

List of Tables

Table 3.1 Sample information of organic CSH hybrids by varying the starting fraction of ATPES with molar ratio of 0, 20, and 40% based on TEOS.	52
Table 3.2 Summary of T_d and ΔT_d of MSP and MSP-CSH composites with different molar ratios of APTES.	53
Table 3.3 Shear adhesion strength and wood cohesive failure (WCF) of MSP-CSH composites with cherry wood.	54
Table 3.4 Shear adhesion strength and wood cohesive failure of MSP-CSH composites with yellow pine wood.	55
Table 4.1 Levels of parameter variables used in RSM design called CCD.	82
Table 4.2 Experimental design and the corresponding responses.	83
Table 4.3 Analysis of variance (ANOVA) for regression model for each response (A) viscosity, (B) tacky force, and (C) water resistance.	84
Table 4.4 Experiments of each response (A) viscosity, (B) tacky force, and (C) water resistance and corresponding shear adhesion strengths.	86
Table 5.1 The dry and wet shear adhesion strength of soy protein polymers with various concentrations of $\text{NH}_2\text{-PPG-NH}_2$	101
Table 5.2 Tensile strength (TB) and elongation at break (EB) of films from soy protein biopolymers with various concentrations of $\text{NH}_2\text{-PPG-NH}_2$	102
Table 5.3 Water resistance (%) of films from soy protein biopolymers with various concentrations of $\text{NH}_2\text{-PPG-NH}_2$	103

Acknowledgements

I would like to express my sincere gratitude and appreciation to my advisor Dr. Xiuzhi Susan Sun. She helps me complete the Ph.D. degree in Department of Grain Science and Industry with her constant guidance, valuable advice and patience with my mistakes and continuous encouragement. I would also like to thank Dr. Donghai Wang, Dr. Daniel Higgins, and Dr. Kyle Riding for being on my supervisory committee. I am very thankful for the friendship and support of my fellow graduate students and post-doctoral researchers in the Bio-materials and Technology Laboratory (BTL) and Department of Grain Science and Industry.

I would like to thank Dr. Praveen Vadlani for generously letting me use much lab equipment in his lab. Further thanks go to the staff in Department of Grain Science and Industry for their support.

I thank my family for their love, encouragement, and support throughout the years. I am also very thankful for all of my friends who have encouraged me and been there for me throughout my graduate years.

Chapter 1 - INTRODUCTION

1.1. GENERAL BACKGROUND

Fossil-based wood adhesives have been mainly used for plywood, particleboard, and the medium-density fiberboard in the construction industry (Sellers, 2001). Fossil fuels are relatively easy to convert into well-defined, uniform and specifically designed polymers. Because the synthetic polymers are made from a few monomers with similar functionality, they possess better mechanical properties than bio-based adhesives. They provide good resistance to heat, moisture, and decay and have dominated in the wood product market for structural and exterior wood products. Currently, the major adhesive resins derived from fossil fuel are phenol formaldehyde, urea formaldehyde, melamine formaldehyde and resorcinol formaldehyde (Koch et al., 1987; Sellers, 2001).

However, they can cause environmental, health and safety issues. They are non-biodegradable and have major potential to contaminate the environment. Furthermore, they can release formaldehyde, a potential human carcinogen capable of causing cancer and respiratory system damage as well as and more minor symptoms including headaches and eye irritation. In the United States, Congress enacted on July 7, 2010, the Toxic Substances Control Act to reduce the emissions of formaldehyde from composite wood products. The bill limited the amount of formaldehyde emissions allowed from these wood products to 0.09 parts per million (ppm), a standard companies had to meet by January 2013 (Open Congress 2010). On top of the environmental issues created by these products, their production adds to the depletion of already-falling crude oil reserves. The dilemma of the depleting petroleum reserves and increasing demand may escalate the price on the global market and could even cause political upheavals in already unstable parts of the world (Hirsch et al., 2005).

Such problems, combined with high petroleum prices and concerns about sustainability, have compelled industry to develop bio-based adhesives, in particular those made from soy proteins. Considerable work has been done to develop soy protein-based adhesives that possess adhesion performance comparable to petroleum-based products.

Soybeans are primarily an industrial crop with high oil and protein contents. Soy protein-based adhesives were first developed in 1923 from the meal ground into flour (Johnson, 1923). By then, soy protein has been researched as an adhesive for wood and paper, coating binders, and paints, and as emulsifiers in colloidal rubber products (Gardner, 2000; Lambuth, 2003; Markley, 1951; Myers, 1993). Researchers and industry have increasingly highlighted the renewability, biodegradability, low price, and modification properties of soy protein.

In order to produce soy protein-based adhesives with high adhesion performance and water resistance, many attempts have been made to modify the molecular structure or conformation through physical, chemical, or enzymatic agents (Chae et al., 1997; Hamada and Marshall, 1989; Hettiarachchy et al., 1995; Huang and Sun, 2000; Kalapathy et al., 1995; Kato, 1991; Lambuth, 1977; Mackay, 1998; Wu et al., 1998; Wu and Inglett, 1974; Zhong et al., 2001). In addition, crosslinking reactions among functional groups of soy protein have been confirmed to greatly improve the adhesion performance, especially the wet adhesion strength, by forming an entangled protein complex upon curing (Wang et al., 2007; Zhong and Sun, 2007). Soy protein can be converted to large and interwoven polymer chains during thermosetting, which contributes to firm attachments to the solid surfaces by adsorption and also prevents the penetration of water molecules into the interface of protein and wood. This crosslinking reaction can be done by co-polymerizing functional groups in unfolded soy protein alone or suitable crosslinking agents such as formaldehyde, phenol-formaldehyde, glutaraldehyde, and

poly(amidoamin)-epoxy resin in order to form water-stable or insoluble dried adhesives (Kumar et al., 2002; Wang et al., 2007; Zhong et al., 2007; Zhong and Sun, 2007).

In this work, inorganic calcium silicate hydrate derivative (CSH) was incorporated into soy protein polymeric matrix in order to prepare water-durable adhesives from soy protein. A crosslinking agent, 3-aminopropyltriethoxysilane (APTES) is a molecule carrying two different reactive groups on its silicone atom so that it can couple between organic soy protein and inorganic CSH phase. Soy protein-CSH composites with different concentrations of APTES were prepared and thermal, rheological, spectroscopic, and adhesion properties were studied with aging effect to understand interfacial mechanism between soy proteins and organic CSH hybrids.

Furthermore, this work has identified reliable indicators to predict shear adhesion strength of soy protein-based adhesives. When the modifiers are applied to soy protein to improve its adhesion properties, corresponding physicochemical properties are greatly affected. However, it has not yet been clearly understood about the physicochemical properties of soy protein-based adhesives and their relationship with shear adhesion performance. Little information has been available on how these changes in physicochemical properties can be used to predict and/or explain the adhesion performance. Industries are seeking time-efficient methods for both quality control and product development for soy protein-based adhesives. Such correlations would be useful to reduce long testing cycles and expenses. For this purpose, physical properties, viscosity, tacky force, and water solubility have been correlated with adhesion strength of enzymatically modified soy protein-based adhesives (ESP).

In addition, we studied the correlation between film strength and adhesion strength of soy protein. We assume that once a soy protein is converted into the film, the important mechanical properties of the film, such as tensile strength and water resistance of the films, may be related to

the adhesion properties of soy protein. The degree to which cohesion and crosslinking take place in the polymer network is critical to determining final mechanical properties of films and even plays an important role in the adhesion of soy protein. For this context, we hypothesized that film properties could represent the adhesion properties of soy protein. Therefore, mechanical properties including tensile strength and water resistance of film were chosen and studied the relationship with adhesion strength of soy protein.

1.2. OBJECTIVE

The objectives of this research were 1) to demonstrate the feasibility of inorganic CSH to prepare soy protein-based adhesives with better adhesion strength by incorporating a soy protein polymeric matrix and 2) to identify reliable indicators to predict shear adhesion properties of soy protein-based adhesives by building the relationship between physical and/or mechanical properties and adhesion properties of soy protein-based polymers.

The specific objectives were to:

1. Investigate the effect of CSH on soy protein with respect to different concentrations of the crosslinking agent (APTES) with aging time to understand interfacial mechanism between soy protein and CSH using thermal, spectroscopic, morphological, and adhesion properties.
2. Examine the correlation between physical properties such as viscosity, tackiness, and water resistance and adhesion performance of enzymatically modified soy protein (ESP) by a Response Surface Methodology (RSM) called a central composite design (CCD).
3. Study the relationship between film strength and adhesion strength of soy protein in terms of various concentrations of poly (propylene glycol) bis (2-aminopropyl ether) (molecular weight ~230, H₂N-PPG-NH₂) as a plasticizer.

1.3. REFERENCES

- Chae, H.J., In, M., Kim, M.H., 1997. Characteristic properties of enzymatically hydrolyzed soy proteins for the use in protein supplements, *Agricultural Chemistry and Biotechnology* 40, 404-408.
- Gardner, D.J., 2000. *Wood Handbook: Wood as an Engineering Material*. Reprinted from Forest Products Laboratory General Technical Report FPL-GTR-113. *Wood Fiber Sci.* 32, 134.
- Hamada, J.S., Marshall, W.E., 1989. Preparation and Functional-Properties of Enzymatically Deamidated Soy Proteins, *J. Food Sci.* 54, 598-&. doi: 10.1111/j.1365-2621.1989.tb04661.x.
- Hettiarachchy, N.S., Kalapathy, U., Myers, D.J., 1995. Alkali-modified soy protein with improved adhesive and hydrophobic properties, *Journal of the American Oil Chemists Society* 72, 1461-1464. doi: 10.1007/BF02577838.
- Hirsch, R.L., Bezdek, R., Wendling, R., 2005. Peaking of world oil production: impacts, migration, and risk management, .
- Huang, W., Sun, X., 2000. Adhesive properties of soy proteins modified by sodium dodecyl sulfate and sodium dodecylbenzene sulfonate, *Journal of the American Oil Chemists Society* 77, 705-708. doi: 10.1007/s11746-000-0113-6.
- Johnson, O., 1923. Adhesive formula and the product produced, US Patent 1,460,757.
- Kalapathy, U., Hettiarachchy, N., Myers, D., Hanna, M.A., 1995. Modification of Soy Proteins and their Adhesive Properties on Woods, *Journal of the American Oil Chemists Society* 72, 507-510. doi: 10.1007/BF02638849.
- Kato, A., 1991. Significance of Macromolecular Interaction and Stability in Functional-Properties of Food Proteins, *ACS Symp. Ser.* 454, 13-24.
- Koch, G.S., Klareich, F., Exstrum, B., 1987. Introduction and summary. In *Adhesives for the Composite Wood Panel Industry*. In: Anonymous , Park Ridge, NJ: Noyes data corporation, pp. 1.
- Kumar, R., Choudhary, V., Mishra, S., Varma, I.K., Mattiason, B., 2002a. Adhesives and plastics based on soy protein products, *Industrial Crops and Products* 16, 155-172. doi: 10.1016/S0926-6690(02)00007-9.
- Kumar, R., Choudhary, V., Mishra, S., Varma, I.K., Mattiason, B., 2002b. Adhesives and plastics based on soy protein products, *Industrial Crops and Products* 16, 155-172. doi: 10.1016/S0926-6690(02)00007-9.
- Lambuth, A.L., 2003. Protein adhesives for wood. *Handb. Adhes. Technol.* (2nd Ed. , Revis. Expanded) , 457-477.

Lambuth, A.L., 1977. Soybean glues. In: Skeist, I. (Ed.), Handbook of Adhesives. Van Nostrand Reinhold Co., New York, pp. 172-180.

Mackay, C.D., 1998. Good adhesive bonding starts with surface preparation, Adhes Age 41, 30-32.

Markley, K.S., 1951. Soybeans and Soybean Products. Vol. II. Interscience Publishers, Inc., New York.

Myers, D.J., 1993. Industrial applications for soy protein and potential for increased utilization. Cereal Foods World 38, 355-360.

Sellers, T., 2001. Wood adhesive innovations and applications in North America, For. Prod. J. 51, 12-22.

Wang, Y., Mo, X., Sun, X.S., Wang, D., 2007. Soy protein adhesion enhanced by glutaraldehyde crosslink, J Appl Polym Sci 104, 130-136. doi: 10.1002/app.24675.

Wu, W.U., Hettiarachchy, N.S., Qi, M., 1998. Hydrophobicity, solubility, and emulsifying properties of soy protein peptides prepared by papain modification and ultrafiltration, Journal of the American Oil Chemists Society 75, 845-850. doi: 10.1007/s11746-998-0235-0.

Wu, Y.V., Inglett, G.E., 1974. Denaturation of Plant Proteins Related to Functionality and Food Applications - Review, J. Food Sci. 39, 218-225. doi: 10.1111/j.1365-2621.1974.tb02861.x.

Zhong, Z.K., Sun, X.Z.S., Fang, X.H., Ratto, J.A., 2001. Adhesion strength of sodium dodecyl sulfate-modified soy protein to fiberboard, J. Adhes. Sci. Technol. 15, 1417-1427. doi: 10.1163/156856101753213277.

Zhong, Z., Sun, X.S., 2007. Plywood adhesives by blending soy protein polymer with phenol-formaldehyde resin, Journal of Biobased Materials and Bioenergy 1, 380-387. doi: 10.1166/jbmb.2007.014.

Zhong, Z., Sun, X.S., Wang, D., 2007. Isoelectric pH of polyamide-epichlorohydrin modified soy protein improved water resistance and adhesion properties, J Appl Polym Sci 103, 2261-2270. doi: 10.1002/app.25388.

Chapter 2 - LITERATURE REVIEW

2.1. STRUCTURE OF SOY PROTEIN

Like many other plant protein, soy protein is mainly a storage protein that provides amino acids during seed germination and protein synthesis. Soy protein can be categorized into water-soluble albumins and salt solution-soluble globulins. Most soy protein is globulin, containing about 25% acidic amino acids, 20% basic amino acids, and 20% hydrophobic amino acids. The main components of soy protein are glycinin (11S) and conglycinin (7S). Different soy protein classifications have also been characterized by their sedimentation constants (S stands for Svedberg Unit) (Thanh and Shibasaki, 1978). The numerical coefficient is the characteristic sedimentation constant in water at 20 °C. The content of 11S is around 52% and of 7S is 35%. The other minor fractions have been designated as 2S (8%) and 15S (5%). Two major fractions, known as 7S and 11S have been studied extensively.

7S protein comprises 20-30% of total soy protein with a molecular weight of 175KDa. It contains α , α' and β polypeptides, compactly folded together by hydrophobic forces and hydrogen bonding (Thanh and Shibasaki, 1978). Also, 11S protein, with a molecular weight 350KDa, makes up 30-50% of total soy protein and has six subunits. Each subunit has a generalized structure A-SS-B, where A and B represent acidic and basic polypeptides, respectively. Acidic and basic polypeptides are linked by a disulfide (SS) bond (Staswick et al., 1984). Generally, α , α' , and acidic polypeptides are regarded as hydrophilic while β and basic polypeptides are considered to be hydrophobic. The pH value of soy protein at the isoelectric point is approximately 4.5. For 7S, it is approximately 4.8, while 11S has a pI of approximately 5.8. The solubility of soy protein is minimized at its isoelectric point. The solubility of soy

protein in water is greatly affected by the pH. The pH dependence of solubility is widely used in the process of isolating soy protein.

Soy protein is a globular structure consisting of primary, secondary, tertiary, and quaternary structures of many polypeptide chains. The structure is stabilized by intermolecular interactions such as hydrophobic interaction, hydrogen bonding, electrostatic interaction, and disulfide bonding, with hydrophobic groups buried inside and hydrophilic groups exposed outside (Horton et al., 1996). The structures and three-dimensional conformations of globular soy proteins are vulnerable to environmental conditions such as pH, ionic strength and temperature. The resulting proteins with various surrounding conditions would provide different chemical and physical properties and reaction flexibility in order to manipulate the specific properties for applications.

2.2. SOY PROTEIN AS A WOOD ADHESIVE

2.2.1. Adhesive application to wood

Soy protein has the potential to produce adhesives with high gluing strength and water resistance. Once soy protein-based adhesives are prepared, they spread and wet over the wood surface for bond formation using spray, roller coating, doctor blade, and bead technologies (Frihart, 2013). After the adhesive is applied to the wood, open and closed assembly time are usually required depending on the specific bonding process. Those processes provide the time for adhesives to penetrate into the wood prior to bond formation, but the open assembly time usually depends on the evaporation of the solvent from the formulation. Optimization of open time is very important because appropriate flow is required for bonding to the substrate. Too much open time can cause the adhesives to dry out on the surface, leading to poor bonding strength. In the bonding process, pressure is used to bring two wood substrates together. For soy protein-based

adhesives, heat is usually used together with pressure. This process is called curing process in which soy protein becomes harder with crosslinking reactions (Sun, 2011).

Many factors can affect the wetting, penetrating, and bonding of the surface, like the relative surface energies of the adhesive and the substrate, viscosity, temperature of bonding, and pressure on the adhesive line. Wood is a particularly complex surface than that generally encountered in most adhesive applications. It is anisotropic because the cells are greatly elongated in the longitudinal direction, and the growth out from the center of the tree makes the radial properties different from the tangential properties. In addition, various types of wood have different characteristic between heartwood and sapwood, and between yellow pine wood and cherry wood. Besides, protein molecular structure, composition, modifiers, processing conditions of soy protein, and surface preparation methods of substrates are all important factors affecting the adhesion performance and applications.

2.2.2. Theories of adhesion

In order to design the soy protein-based adhesive, it is important to understand the adhesion mechanism between protein adhesives and wood substrates. Not a single theory can explain the adhesion mechanism between protein adhesives and substrates. Researchers in the past century have proposed several adhesion mechanisms, including mechanical interlocking, electron transfer, boundary layers and interfaces, adsorption, diffusion, and chemical bonding (Cheng, 2004; Sun, 2011).

In a mechanical interlocking, the adhesive provides strength through reaching into the pores of wood substrates. Protein adhesives spread and wet the surface, penetrate the fiber cells through a capillary path, then cure in place, acting like a mechanical anchor. Protein polymer has a certain molecule weight and distribution, which can contribute the degree of mechanical

interlocking. The smaller protein molecules can easily penetrate the capillary pores in the wood and cure to form continuous protein complexes with deep fibers as well as those larger protein molecules from the substrate surface. Also, the surface roughness is a critical factor dominating the mechanical interlocking. If the surface is too rough, cohesive wood failure occurs, and if the surface structure is too smooth, adhesive failure occurs. Therefore, wood surface structure, surface roughness, degree of crosslink, molecular weight and distribution, and entanglements among protein molecules contribute significantly to the degree of mechanical interlocking.

The other theory, adsorption theory, depends mainly upon any physical or electrostatic attraction between protein polymers and wood surface through hydrogen bonding and van der Waals forces. The weakest interaction is van der Waals force, the association of non-polar molecules. The other types of forces are generally related to polar groups. The weakest are the dipole-dipole interactions. Strongest of the interactions is the hydrogen bond formation. This type of bond is the interaction with polar compounds, including nitrogen, oxygen, and sulfur groups with attached hydrogens and carbonyl groups. Both interactions take place at the molecular level and require an intimate contact of the adhesive with wood substrate. The wood surface structure, protein structure and composition, surface wetting, contact angles and pressure should be major factors to influence adsorption theory.

Chemical bonding often can be formed with a covalent bond occurring at the interface between adhesives and substrate, the strongest interaction. Because the wood has hydroxyl groups in its three main components such as cellulose, hemicellulose, and lignin, and soy protein has many functional groups like hydroxyl group, carboxylic acid, and amine group, it is reasonable to assume that the covalent interaction could happen. However, this reaction may not occur unless under special reaction conditions due to the highly ordered globular structure of soy

protein. Therefore, the protein structure, functionality, and physical properties need to be altered by protein modification in order to form the covalent interaction between adhesives and substrates.

Based on the adhesion theories described above, mechanical interlocking, penetration, and attraction are the most important factors to determine the adhesion strength to cellulosic materials. Unfolded protein molecules can penetrate into wood surface cells through capillary paths and form entangled protein complexes as a mechanical anchor. The degree of penetration could be significantly influenced by unfolding soy protein structures, which could result in different protein molecular sizes, flowability, viscosity, and final adhesion strength. Furthermore, chemical and physical attraction is critical to enhancing adhesion performance at the interface. Denatured soy protein can expose many hydrophobic functional groups to the surface, which provides the enhancement of adhesion quality and hydrophobic interaction at the three-dimensional complex zone.

2.3. PERFORMANCE OF SOY PROTEIN ADHESIVES

Soy protein adhesives are one of the popular bio-based adhesives under investigation because of high adhesion strength, biodegradability, and renewability. The adhesion performance of soy protein is influenced by many parameters including the particle size, nature of surface, structure of protein, viscosity and pH, temperature, and pressure and time (Kumar et al., 2002; Lambuth, 1977).

2.3.1. PARTICLE SIZE

The particle size of the soybean flour used for adhesive processing has a significant effect on adhesion performance of soy protein. Fineness of the grind is often expressed in terms of

specific surface (cm^2/kg) rather than mesh size and the best adhesion strength was obtained using a specific surface area of 3000-6000 cm^2/g (Lambuth, 2001).

2.3.2. NATURE OF SURFACE AND SUBSTRATE

The nature of the bonded surface is critical to determining adhesion performance. When it comes to protein-based polymers, the bonding mechanism comprises a combination of mechanical interlocking and molecular attractive forces. The surface of wood is heterogeneous, anisotropic and varies by the type of wood. A rough surface structure generates a random micro 'finger joint' structure under pressure; on the other hand, a surface too smooth might have less micro random 'finger joint' effects, which might cause low gluing strength (Kumar et al., 2002). Qi et al studied the adhesion performance of soy protein with three different types of wood veneer: yellow poplar, maple, and cherry veneer (Qi et al., 2013). The shear adhesion strengths prepared from the same soy protein-based adhesives varied by wood type because of different degrees of porosity and surface roughness. Kalapathy et al observed highest strength with soft maple wood (280N) while it was lower with hard woods such as walnut (135N) and zero strengths with yellow pine (0N) and poplar (71N) soft woods (Kalapathy et al., 1995).

2.3.3. VISCOSITY

Viscosity is an important factor in determining the flow property and adhesion performance (Kumar et al., 2002; Lambuth, 1977; Sun, 2011). The soy protein with high viscosity can cause increased intermolecular interactions due to unfolded protein molecules, which generally hinder the strong adhesion between protein molecules and cellulosic wood materials. Thus, many researchers attempted to decrease viscosity for easy penetration and wetting of wood surface by treating with salts or reducing agents without adversely affecting the adhesion performance and water resistance. Ionic environments can weaken the electrostatic

interactions between protein molecules. When different concentrations of ionic salt, Na_2SO_4 , were added, an electrostatic shielding between the charged protein molecules was formed, weakening the electrostatic interaction between charged protein molecules and resulting in reduced viscosity of the soy protein-based adhesives (Kalapathy et al., 1996). Enzymatic treatments also provide decreased viscosity by cleaving soy protein polypeptides (Hettiarachchy et al., 1995). Furthermore, alkaline pH can disrupt intermolecular interactions, decrease viscosity, and subsequently improve the adhesion strength. However, viscosity decreased by extremely higher pH negatively affected the adhesive properties and shorter storage life. Therefore, a moderate pH and temperature combination of 10.0 and 50°C has been suggested for better mechanical performance (Hinterwaldner, 1997; Kalapathy et al., 1996).

2.3.4. PROCESSING PARAMETERS

The curing quality of soy protein-based adhesives can depend on curing conditions such as temperature, pressure, and thickness of plywood. Zhong et al investigated the adhesion properties of soy protein isolate (SPI) on fiber cardboard and effects of press conditions such as time, pressure, and temperature (Zhong et al., 2001). They found that the adhesion strength increased as press time (1-10 min), press pressure (0.4-4MPa), and/or press temperature (25- 100°C) increased. They also found that adhesion strength increased with increasing concentrations up to an optimum limit. The adhesion strength of SPI adhesives on the fiber cardboard was affected significantly by the ratio of SPI/water and reached a maximum value at 12:100(w/w). Soy protein-based adhesives in excessive concentrations had high viscosity, which has poor flowability and hard spreading, whereas too low concentrations of protein can easily penetrate into wood capillary pores and are not available on the surface for gluing.

2.4. SOY PROTEIN ADHESIVES AND MODIFICATION

Soy protein has a globular structure in its native state and is characterized by a highly ordered three-dimensional structure with hydrophobic groups buried inside and hydrophilic groups exposed outside in nature. This structure leads to limited contact area and insufficient functional groups interacting with wood substrates and lower the adhesion strength. It is inappropriate to transfer the concentration of stress from the interface to the soy protein when a force is applied to separate the adhesive bond (Norde and Favier, 1992; van der Leeden et al., 2000). Generally, a globular protein adsorbs as compact layers or rigid particles when attached to a solid substrate, resulting in poor stress transfer from the interface to the polymer bulk and consequently, poor bond strength. Furthermore, soy protein is hydrophilic nature, which could be a reason for low water resistance of soy protein-based adhesives. Various modification methods were investigated to degrade the soy globular structure and improve the soy protein adhesion strength and water resistance (Feeney, R E Whitaker, J R., 1977; Kalapathy et al., 1997; Kinsella, 1979).

2.4.1. DENATURATION AND CLEAVAGE OF SOY PROTEINS

The structure and three-dimensional conformation of globular soy proteins are denatured by environmental conditions such as pH, ionic strength and temperature. The resulting proteins with various surrounding conditions would provide different chemical and physical properties and reaction flexibility. Many methods used to denature proteins have been exploited including chaotropic agents like urea, guanidine hydrochloride (GH), sodium dodecyl sulphate (SDS) and sodium dodecyl benzene sulphonate (SDBS) (Huang and Sun, 2000a; Huang and Sun, 2000b) and salts or reducing agents like NaCl, Na₂SO₄, and NaHSO₃ (Kalapathy et al., 1996; Qi et al., 2012).

The effect of GH and urea of modified soy protein on adhesive properties was examined by Huang and Sun (Huang and Sun, 2000b). The modified soy proteins with treatment of 1 and 3M urea showed greater shear strengths than unmodified ones, while soy proteins modified by 0.5 and 1 M GH gave greater adhesion strengths than the unmodified protein. They indicated that the treatment of urea and GH results in partial denaturation of globular soy proteins leading to exposure hydrophobic amino acids and denatured secondary structures of globular soy proteins. This treatment enhance adhesion strength and water resistance as well. Moreover, the shear adhesion strength increases as the concentration of urea and GH increases. Proteins modified by 3 M urea or 1 M GH had higher content of secondary structure and more exposed hydrophobic amino acids compared to unmodified ones, which contributes to stronger adhesion with wood substrates.

Also, the effect of varying concentrations of SDS and SDBS on adhesion properties was evaluated by Huang et al (Huang and Sun, 2000a). Soy protein treated with 0.5 and 1% SDS or SDBS gave greater adhesion strength than unmodified soy protein. On the other hand, they found lower adhesion strength from modified soy protein with treatment of 3% SDS and SDBS (the highest concentration). The denaturation of protein is regarded as the method of change of its secondary, tertiary and quaternary structure. Detergents such SDS and SDBD can produce a cooperative conformation change in proteins at a low concentration. Thus, 3% SDS and SDBS can make soy protein with a greater unfolding degree, which is undesirable for adhesion properties. Therefore, a modification method for soy protein should be optimized to accomplish the best adhesion.

The effects of salts like NaCl, Na₂SO₄ and reducing agents like NaHSO₃ on soy protein have been studied by many researchers. Environments made ionic by salts weaken the

electrostatic interaction among protein molecules by electrostatic shielding. The effects of ionic strength on the functional properties of soy proteins, such as emulsification, foaming, water binding, and gelation have been reported by Kinsella et al (Kella, Navin Kumar D. Kang, Yeung Kinsella, John Kella, Navin, 1988; Kinsella, 1979; Klemaszewski and Kinsella, 1991). Viscosity and adhesion properties decreased with increasing concentrations of salts. At 0.1M concentration of NaCl, Na₂SO₄, and Na₂SO₃ reduced viscosity of soy protein with no significant adverse effect on adhesion strength and water resistance (Kalapathy et al., 1996).

Reducing agents, such as sulphites, can cleave the inter- and intra-disulphide bonds in protein molecules. Cleavage of disulfide bonds by reducing agents leads to an increase in surface hydrophobicity, foaming capacity, foam solubility (Kalapathy et al., 1997; Kawamura et al., 1985; Kim and Kinsella, 1986) and adhesion performance (Qi et al., 2012). Qi and Sun et al developed a new viscous cohesive soy protein adhesive system modified by NaHSO₃ with a high solid content of up to 38 %, good flowability, long shelf life, and good water resistance comparable to formaldehyde-based adhesives.

2.4.2. ENZYMATIC MODIFICATION

Enzymatic modification has been used to degrade the soy globular structure. The advantages of enzyme modification include high reaction rates, mild conditions, and specificity. Proteases such as pepsin, trypsin, and papain hydrolyze the specific peptide bonds and modify the protein structure. Modified soy protein isolate with papain was reported to affect hydrophobicity, solubility, and emulsifying properties (Wu et al., 1998). Trypsin-modified SPI (TSPI) or soybean flour exhibited much higher adhesive strength on soft maple, compared with that of unmodified SPI (Kalapathy et al., 1995). Furthermore, TSPI showed improved hydrophobicity, which was due to the exposure of hydrophobic functional groups by limited

hydrolysis. Papain and urease modified soy protein isolate (SPI) showed better adhesive strength compared to unmodified SPI adhesives on rubber wood, while chymotrypsin modified SPI showed zero adhesive strength. All enzymatically modified adhesives showed lower viscosity when compared to unmodified SPI adhesives (Kumar et al., 2004a; Kumar et al., 2004b).

2.4.3. CROSSLINKING

Crosslinking of protein involves joining the two molecular components by a covalent bond achieved through the crosslinking agent. A compact protein complex would be formed and induce more entanglements and crosslinking during thermal setting, which would maintain their structure better than the unmodified adhesive after water soaking. Various chemicals have been used to increase the degree of crosslinking density and molecular weight. Rogers et al used 1,3-dichloro-2-propanol to crosslink soy protein through the reaction among the functional groups, and yielded enhanced adhesive performance (Rogers et al., 2004). In addition, an example of polyamide-epichlorohydrin (PAE) showed the improvement of adhesion strength and reversible crosslinking reaction between PAE and soy protein. Epoxies are active crosslinking agents for alkaline soy glues and improve the adhesive strength and durability. An approach to exploit silanation is to increase the interfacial interaction between soy polymeric matrix and glass fiber via a coupling silane agent (Liang and Wang, 1999). A diamine silane such as 3-(2-aminoethyl)-aminopropyl trimethoxysilane (AAPS) was chosen as the coupling agent in order to promote adhesion between soy proteins and glass fiber. During the reaction, the amino functional group in AAPS reacts with the amino acid in side chains of soy proteins and AAPS and soy protein can be linked via a covalent interaction. Also, Wang et al reported that the wet strength of soy protein was improved by 115% at optimal concentration of glutaraldehyde (20mM) (Wang et al., 2007). Efforts of crosslinking soy protein-based adhesive with formaldehyde or its derivatives have

been reported. Liu and Li developed modified soy protein adhesives using two-step modification (Liu and Li, 2007). Soy protein isolate (SPI) was first modified by maleic anhydride (MA) to form MA-grafted SPI (MPSI), then polyethylenimine (PEI) was used to modify MSPI. The optimal formula of the modified SPI was made from 20% PEI and 80% MSPI, which gave a dry strength 6.8 MPa and boiling strength of 1.5 MPa.

2.4.4. NANO TECHNOLOGY

Many researchers have attempted to improve the performance of soy protein-based adhesives with nano-scale modification. Soy protein/CaCO₃ hybrids as wood glue showed stable wet adhesion strength more than 6 MPa because of the compact rivets, interlocking structure and ion crosslinking reaction induced by calcium, carbonate and hydroxyl ions in the soy protein (Liu et al., 2010). In addition, montmorillonite (MMT) has attracted great academic interest because of its high aspect ratio of silicate nanolayer and its high surface area (Zhang et al., 2013). The water resistance of soy protein-based adhesive greatly improved due to the chemical crosslinking by nano-modification of soy protein by intercalated or exfoliated MMT. Depending on the MMT content, highly exfoliated and intercalated structure were made in SPI/MMT nanocomposites, which contribute to higher adhesion strength.

2.5. REFERENCES

- Cheng, E., 2004. Adhesion mechanism of soybean protein adhesives with cellulosic materials. 109.
- Feeney, R E Whitaker, J R., 1977. Food proteins. Improvement through chemical and enzymatic modification. Food Proteins 160, viii-312pp.
- Frihart, C.R., 2013. Wood adhesion and adhesives. Handb. Wood Chem. Wood Compos. (2nd Ed.), 255-319. doi: 10.1201/b12487-13.
- Hettiarachchy, N.S., Kalapathy, U., Myers, D.J., 1995. Alkali-modified soy protein with improved adhesive and hydrophobic properties, Journal of the American Oil Chemists Society 72, 1461-1464. doi: 10.1007/BF02577838.

- Hinterwaldner, R., 1997. Plant proteins as resources for innovations in backbone binders. *Coating* 30, 323-325.
- Horton, H.R., Moran, L.A., Ochs, R.S., Rawn, J.D., Scrimgeour, L.G., 1996. Protein: Three-Dimensional structure and function. In: Anonymous *Principles of Biochemistry*, Upper Saddle River, NJ, pp. 79-117.
- Huang, W.N., Sun, X.Z., 2000a. Adhesive properties of soy proteins modified by sodium dodecyl sulfate and sodium dodecylbenzene sulfonate, *Journal of the American Oil Chemists Society* 77, 705-708. doi: 10.1007/s11746-000-0113-6.
- Huang, W.N., Sun, X.Z., 2000b. Adhesive properties of soy proteins modified by urea and guanidine hydrochloride, *Journal of the American Oil Chemists Society* 77, 101-104. doi: 10.1007/s11746-000-0016-6.
- Kalapathy, U., Hettiarachchy, N., Myers, D., Hanna, M.A., 1995. Modification of Soy Proteins and their Adhesive Properties on Woods, *Journal of the American Oil Chemists Society* 72, 507-510. doi: 10.1007/BF02638849.
- Kalapathy, U., Hettiarachchy, N.S., Myers, D., Rhee, K.C., 1996. Alkali-modified soy proteins: Effect of salts and disulfide bond cleavage on adhesion and viscosity, *Journal of the American Oil Chemists Society* 73, 1063-1066. doi: 10.1007/BF02523417.
- Kalapathy, U., Hettiarachchy, N.S., Rhee, K.C., 1997. Effect of dyeing methods on molecular properties and functionalities of disulfide bond-cleaved soy proteins, *Journal of the American Oil Chemists Society* 74, 195-199. doi: 10.1007/s11746-997-0123-z.
- Kawamura, Y., Matsumura, Y., Matoba, T., Yonezawa, D., Kito, M., 1985. Selective Reduction of Interpolypeptide and Intrapolypeptide Disulfide Bonds of Wheat Glutenin from Defatted Flour, *Cereal Chem.* 62, 279-283.
- Kella, Navin Kumar D. Kang, Yeung Kinsella, John Kella, Navin, 1988. Effect of oxidative sulfitolysis of disulfide bonds of bovine serum albumin on its structural properties: A physicochemical study, *J. Protein Chem.* 7, 535-548. doi: 10.1007/BF01024872.
- Kim, S.H., Kinsella, J.E., 1986. Effects of Reduction with Dithiothreitol on some Molecular-Properties of Soy Glycinin, *J. Agric. Food Chem.* 34, 623-627. doi: 10.1021/jf00070a009.
- Kinsella, J.E., 1979. Functional-Properties of Soy Proteins, *Journal of the American Oil Chemists Society* 56, 242-258. doi: 10.1007/BF02671468.
- Klemaszewski, J.L., Kinsella, J.E., 1991. Sulfitolysis of Whey Proteins - Effects on Emulsion Properties, *J. Agric. Food Chem.* 39, 1033-1036. doi: 10.1021/jf00006a005.
- Kumar, R., Choudhary, V., Mishra, S., Varma, I.K., 2004a. Enzymatically modified soy protein - Part 1. Thermal behaviour, *Journal of Thermal Analysis and Calorimetry* 75, 727-738. doi: 10.1023/B:JTAN.0000027169.19897.30.

- Kumar, R., Choudhary, V., Mishra, S., Varma, I.K., 2004b. Enzymatically-modified soy protein part 2: adhesion behaviour, *J. Adhes. Sci. Technol.* 18, 261-273. doi: 10.1163/156856104772759458.
- Kumar, R., Choudhary, V., Mishra, S., Varma, I.K., Mattiason, B., 2002. Adhesives and plastics based on soy protein products, *Industrial Crops and Products* 16, 155-172. doi: 10.1016/S0926-6690(02)00007-9.
- Lambuth, A., 2001. Soybean, blood, and casein glues. *Coat. Technol. Handb. (2nd Ed.)*, 519-531.
- Lambuth, A.L., 1977. Soybean glues. In: Skeist, I. (Ed.), *Handbook of Adhesives*. Van Nostrand Reinhold Co., New York, pp. 172-180.
- Liang, F., Wang, Y., 1999. Effects of silane coupling agents on the interface of soy protein and glass fiber. *PROCEEDINGS- AMERICAN SOCIETY FOR COMPOSITES American Society for Composites Technical conference; 14th, American Society for Composites 14th*, 511-520.
- Liu, D., Chen, H., Chang, P.R., Wu, Q., Li, K., Guan, L., 2010. Biomimetic soy protein nanocomposites with calcium carbonate crystalline arrays for use as wood adhesive, *Bioresour. Technol.* 101, 6235-6241. doi: 10.1016/j.biortech.2010.02.107.
- Liu, Y., Li, K., 2007. Development and characterization of adhesives from soy protein for bonding wood, *Int J Adhes Adhes* 27, 59-67. doi: 10.1016/j.ijadhadh.2005.12.004.
- Norde, W., Favier, J.P., 1992. Structure of Adsorbed and Desorbed Proteins, *Colloids and Surfaces* 64, 87-93. doi: 10.1016/0166-6622(92)80164-W.
- Qi, G., Li, N., Wang, D., Sun, X.S., 2013. Physicochemical properties of soy protein adhesives modified by 2-octen-1-ylsuccinic anhydride, *Industrial Crops and Products* 46, 165-172. doi: 10.1016/j.indcrop.2013.01.024.
- Qi, G., Li, N., Wang, D., Sun, X.S., 2012. Physicochemical Properties of Soy Protein Adhesives Obtained by In Situ Sodium Bisulfite Modification During Acid Precipitation. *J. Am. Oil Chem. Soc.* 89, 301-312. doi: 10.1007/s11746-011-1909-6.
- Rogers, J., Geng, X.L., Li, K.C., 2004. Soy-based adhesives with 1,3-dichloro-2-propanol as a curing agent, *Wood Fiber Sci.* 36, 186-194.
- Staswick, P.E., Hermodson, M.A., Nielsen, N.C., 1984. Identification of the Cystines which Link the Acidic and Basic Components of the Glycinin Subunits, *J. Biol. Chem.* 259, 3431-3435.
- Sun, X.S., 2011. Soy Protein Polymers and Adhesion Properties, *Journal of Biobased Materials and Bioenergy* 5, 409-432. doi: 10.1166/jbmb.2011.1183.
- Thanh, V.H., Shibasaki, K., 1978. Major Proteins of Soybean Seeds - Subunit Structure of Beta-Conglycinin, *J. Agric. Food Chem.* 26, 692-695.

van der Leeden, M., Rutten, A., Frens, G., 2000. How to develop globular proteins into adhesives, *J. Biotechnol.* 79, 211-221. doi: 10.1016/S0168-1656(00)00238-8.

Wang, Y., Mo, X., Sun, X.S., Wang, D., 2007. Soy protein adhesion enhanced by glutaraldehyde crosslink, *J Appl Polym Sci* 104, 130-136. doi: 10.1002/app.24675.

Wu, W.U., Hettiarachchy, N.S., Qi, M., 1998. Hydrophobicity, solubility, and emulsifying properties of soy protein peptides prepared by papain modification and ultrafiltration, *Journal of the American Oil Chemists Society* 75, 845-850. doi: 10.1007/s11746-998-0235-0.

Zhang, Y., Zhu, W., Lu, Y., Gao, Z., Gu, J., 2013. Water-Resistant Soybean Adhesive for Wood Binder Employing Combinations of Caustic Degradation, Nano-Modification, and Chemical Crosslinking, *Bioresources* 8, 1283-1291.

Zhong, Z.K., Sun, X.S., Fang, X.H., Ratto, J.A., 2001. Adhesion properties of soy protein with fiber cardboard, *Journal of the American Oil Chemists Society* 78, 37-41. doi: 10.1007/s11746-001-0216-0.

Chapter 3 - ADHESION PROPERTIES OF SOY PROTEIN CROSSLINKED WITH ORGANIC CALCIUM SILICATE HYDRATE HYBRID¹

3.1. ABSTRACT

The objective of this work was to investigate if inorganic calcium silicate hydrate (CSH) hybrids could improve soy protein adhesion properties. 3-aminopropyltriethoxysilane (APTES) was used as a crosslinking agent to make covalent linkage between organic soy protein and inorganic CSH phases. Soy protein-calcium silicate hydrate (MSP-CSH) composites with different mole ratio of APTES were prepared and the effect of crosslinking reaction on physicochemical properties such as thermal, rheological, spectroscopic, and morphological and adhesion properties were studied with physical aging effect. With aging effect, the denaturation temperature (T_d) and enthalpies (ΔH_d) of each fraction of soy protein increased in DSC thermograms, representing higher thermal stability and the viscoelasticity of the composites also increased. In addition, the covalent interaction between soy protein and CSH was confirmed by peak maxima shift in spectroscopic measurement and the roughly coated surface was observed in SEM images. Dry and wet adhesion strength of the MSP-CSH composites was higher than the control MSP alone.

3.2. INTRODUCTION

Soy protein consists of two major storage proteins, β -conglycinin (7S) and glycinin (11S), which contribute to the physicochemical properties of soy proteins (Peng et al., 1984). 7S

¹ Results have been published. M. Kim & X. Sun. 2014. Adhesion properties of soy protein crosslinked with organic calcium silicate hydrate hybrids, J. Appl. Polym. Sci.131(7) DOI: 10.1002/app.40693 (reuse by permission of John Wiley and Sons)

protein comprises 20–30% of total soy protein with a molecular weight of 175KDa. It contains α , α' , and β polypeptides that are compactly folded together by hydrophobic forces and hydrogen bonding (Thanh and Shibasaki, 1978). 11S protein, with a molecular weight 350KDa, makes up 30–50% of total soy protein and has six subunits. Each subunit has a generalized structure of A-SS-B, where A and B represent acidic and basic polypeptides, respectively, linked by a disulfide (SS) bond (Staswick et al., 1984). Generally, α , α' , and acidic polypeptides are regarded as hydrophilic, whereas β and basic polypeptides are considered to be more hydrophobic. Inherent differences in structure and molecular properties of each component of soy protein make them possess different properties such as solubility, thermal properties, and adhesion performance (Chae et al., 1997; Hamada and Marshall, 1989; Hettiarachchy et al., 1995; Huang and Sun, 2000a; Kalapathy et al., 1995; Kato, 1991; Lambuth, 1977; Mackay, 1998; Markley, 1951; Wu et al., 1998; Zhong and Sun, 2001).

Polymeric materials, especially those obtained from renewable resources such as natural fibers, have attracted increasing attention during the last few years due to environmental concerns (Singha and Thakur, 2010a; Singha and Thakur, 2010b; Singha and Thakur, 2010c; Singha and Thakur, 2009; Thakur et al., 2010a; Thakur et al., 2010b). Particularly, limited petroleum resources and the pollution caused by formaldehyde-based adhesives have spurred many efforts to develop bio-based adhesives with good adhesion properties that can compete with synthetic petroleum-based adhesives. Among them, soy protein-based adhesives have attracted considerable attention as bio-based adhesives since 1930s. Hydrophilic/hydrophobic and charged polypeptide fractions in soy protein can be manipulated to modify surface reactivity and accessibility, which enables soy protein to be applied in the adhesive application. Efforts to improve adhesion properties of soy protein-based adhesives have included using denaturants,

reducing agents, and crosslinking agents as well as enzyme hydrolysis (Hettiarachchy et al., 1995; Huang and Sun, 2000b; Kalapathy et al., 1996; Kumar et al., 2004; Li et al., 2004; Liang and Wang, 1999; Otaigbe, 1998). However, the low water resistance of soy protein based adhesives still limits their extensive applications (Frihart, 2010; van der Leeden et al., 2000; Wescott, J M Frihart, C R Traska, A E., 2006).

Calcium silicate hydrates (CSH) are the main hydrated phases in cement paste and can be simply synthesized by preparing a mixture of popular silica precursor, tetraethoxysilane (TEOS) and calcium chloride solutions as the starting materials, which procedure has been established by Suzuki (Suzuki and Sinn, 1993). The structure of the prepared inorganic CSH consists of condensed silicate tetrahedra sharing oxygen atoms with a central, calcium hydroxide-like CaO_2 sheet (Taylor, 1986). CSH is a main component that contributes to the mechanical strength of cement and a loosely organized binding phase with an associated internal network of micro-sized pores (Kalapathy et al., 1995; Lin et al., 2010; Liu and Chang, 2009a; Yip and Van Deventer, 2003). Due to its nanocrystalline structure with high specific surface area (Liu and Chang, 2009b; Mojumdar and Raki, 2005) and bioactivity, it has been a potential to be applied for drug delivery and biomedical applications (Lin et al., 2010; Liu and Chang, 2009a). Minet et al. then introduced the small organic moieties into inorganic CSH phase by using a mixture of two silica precursors, 3-aminopropyltriethoxysilane (APTES) and TEOS that was named organic CSH hybrid (Minet et al., 2006). They achieved the successful graft of small aminopropyl molecules to the interlayer domain of inorganic CSH without disrupting their structural integrity, which contribute to reinforced mechanical properties of cement. Their novel approach can provide us with another possibility to fabricate polymer-CSH composite *via* covalent bridges.

This report focuses on the synthesis and characterization of soy protein–based CSH composites that possess desirable properties for adhesives. We hypothesize that the specific incorporation of CSH into continuous soy polymeric phases may be achieved by forming covalent bridges between functional groups of soy protein and aminopropyl groups from organic CSH hybrids. This may improve interfacial adhesion strength by accomplishing the inclusion of small inorganic crystallites, the formation of covalent interface, and the reduction of water-sensitive functional groups. To promote the reaction between aminopropyl group of CSH and soy protein, soy protein must be unfolded to expose its functional groups. Considerable attempts have been made to unfold soy proteins (Wescott and Frihart, 2004; Yang et al., 2006), but they have not been able to overcome the disadvantages such as high viscosity, low concentration of soy protein, and low water resistance (Qi, 2011; van der Leeden et al., 2000). Our preliminary studies successfully exploited a new viscous modified soy protein based adhesive by sodium bisulfate (MSP) with high solid content of 38%, good flowability, long shelf life, and good water resistance (Qi et al., 2012; Qi et al., 2013). We strongly believe that this partially unfolded MSP would have advantages over conventional soy protein isolate (SPI), soy flour (SF), and soy concentrate with a native state for adhesive applications. In this work, MSP was used as a base polymer to prepare modified soy protein-CSH (MSP-CSH) composites and the influence of different synthesis parameters on thermal, spectroscopic and mechanical properties of the composite was studied. Especially, we focus on the study of the interfacial crosslinking effect of aminopropyl silane (APTES) on functional properties of MSP-CSH composite.

3.2.1. Reaction mechanism hypothesis

The proposed interfacial mechanism governing this experiment is illustrated in Figure 3.1. Initially, the two silicate precursors APTES and TEOS can be hydrolyzed under acidic

conditions, leading to silanol formation in the synthesis of organic CSH hybrids. The silanols from the reaction interact with each other to undergo polycondensation, making very stable siloxane bonds of organic CSH hybrids. During *in-situ* sol-gel polymerization, aminopropyl organic groups of APTES can be incorporated with silicate chains with less than 40% molar ratio, confirming CSH structural integrity (Minet et al., 2006). These hybrid materials obtained by the sol-gel method maintain a lamellar structure constituted by an inorganic calcium silicate layer with organic groups confined in the interlayer as shown in the reaction 2 of Figure 3.1 (Minet et al., 2006; Suzuki and Sinn, 1993). APTES is a molecule that carries two different reactive groups on its silicon atom and as shown in reaction 3 of Figure 3.1, we assumed that MSP and organic CSH hybrid can be grafted through covalent bridges of APTES. When preparing MSP-CSH composites, aminopropyl group of APTES could react with side chains such as carboxylic acid and hydroxyl groups of soy protein (Liang and Wang, 1999) and simultaneously, couple with CSH phases. Upon curing, MSP-CSH composites could form a stable and interconnected structure at the interface. In summary, the introduction of such small crystallite CSH in soy protein would contribute to improved interfacial adhesion through the formation of covalent bridges between soy protein molecules and CSH. Furthermore, we expected to achieve lower surface energy as well as a hydrophobic effect in the presence of non-polar alkyl groups at the interface, which would result in improved wet shear adhesion. This chemistry strategy has been previously demonstrated by other researchers using other polymers (Liang and Wang, 1999; Otaigbe and Adams, 1997; Otaigbe, 1998). This report is the first attempt to examine the potential of inorganic CSH to improve the adhesion properties of soy protein *via* covalent linkages. To verify this hypothesis, the physicochemical and adhesive properties of MSP-CSH composites with the different synthesis parameter were studied.

3.3. EXPERIMENTAL PROCEDURES

3.3.1. MSP sample preparation

MSP was extracted from soy flour slurry modified with sodium bisulfite using the acid precipitation method described by Qi et al (Qi et al., 2012; Qi et al., 2013). Defatted soy protein flour was dispersed in water at pH 9.5 using 2N NaOH. The NaHSO₃ (6g/L) was added to the soy protein slurry and stirred for 2 hours. The pH of the slurry was then adjusted to pH 5.4 with 2N HCl to remove carbohydrates by centrifugation at 12000 g. Then, the pH of the supernatant was adjusted to 4.8 with 2N HCl and centrifuged at 8000 g.

3.3.2. Synthesis of hybrid organic CSH and adhesive preparation

Organic CSH hybrids were prepared following the sol–gel synthesis method by Minet (Minet et al., 2006). Base solution was prepared by dissolving 0.46 g of CaCl₂ in 0.1 M HCl (1.35 cm³) and ethanol (6.9 cm³). The mole percentage of APTES relative to the total source of silicon (APTES + TEOS) was varied from 0, 20, and 40%. Different moles of APTES and TEOS were added to the base solution to prepare organic CSH hybrids (Table 3.1). The pure inorganic material (0% APTES, 100% TEOS) is pure CSH as shown in Table 3.1. As APTES increased, the mixture solution rapidly became opaque due to the rapid gelation of silica precursors. At CSH/40% APTES, the mixture solution immediately became cloudy and opaque. The prepared organic CSH hybrids (5 wt% of total weight basis) were thoroughly blended with MSP to fabricate the composites for adhesives. The last column of the Table 3.1 includes the sample information of the composites prepared.

3.3.3. Differential scanning calorimetry (DSC)

The thermal denaturation properties of soy proteins were assessed with a differential scanning calorimeter (DSC) (DSC7, Perkin-Elmer, Norwalk, CT) calibrated with indium and

zinc. Wet samples of MSP-CSH composites were weighed (15mg) and hermetically sealed in a large-volume stainless pan. Each sample was held at 30 °C for 1 min, then scanned from 20 to 170 °C at a heating rate of 10 °C/min. Peak temperatures (T_d) and denaturation enthalpies (ΔH_d) were calculated from thermograms.

3.3.4. Dynamic viscoelastic measurement

A Bohlin CVOR 150 rheometer (Malvern Instruments, Southborough, MA) was used to characterize the viscoelastic properties of MSP-CSH composites. A parallel plate head was used with 20-mm plate diameter and a 500- μ m gap. The measurements were performed in a strain-controlled mode wherein the amplitude of shear strain was 0.01%, and the frequency range was from 0.01 to 25 Hz. The testing temperature was 25 °C. A thin layer of silicon oil was spread over the circumference of the sample to prevent dehydration of the samples during test. The elastic modulus (G') and complex viscosity (η) were continuously recorded, and all measurements were triplicated and averaged.

3.3.5. FT-IR spectroscopy

Fourier transform infrared (FT-IR) spectra were collected in the region of 4000-650 cm^{-1} with a Perkin-Elmer Spotlight 100 FTIR spectrometer (Waltham, MA). All samples for IR spectroscopic measurement were freeze-dried then ground into powder. Then the samples were made into a disk under the constant force of 30 units. Spectra of the attenuated total reflection (ATR) mode were collected with 128 scans at a resolution of 4 cm^{-1} .

3.3.6. Scanning Electron Microscopy

A Hitachi S-3500 N (Hitachi Science System, Ibaraki, Japan) SEM was used to observe the microstructure of cured MSP-CSH composites. The grounded powder of cured MSP-CSH composite were affixed to an aluminum stub with two-sided tape and coated with an alloy of

60% gold and 40% palladium with a sputter coater (Desk II Sputter/Etch Unit, Moorestown, NJ, USA). The SEM images of the composites were performed with operation conditions at an accelerating voltage of 5kV.

3.3.7. Two ply plywood specimen preparation

Cherry wood veneers with dimensions of $50 \times 127 \times 5$ mm were preconditioned in a chamber (Electro-Tech Systems, Inc., Glenside, PA) for 7 day at 23 °C and 50% relative humidity. The adhesives were brushed onto one end of a piece of cherry wood with dimensions of 127×20 mm (length \times width) until the entire area was completely wet. Two brushed wood pieces were assembled immediately and conditioned for 10 min at room temperature. Then the assembled wood specimens were pressed with a hot press (Model 3890 Auto M; Carver, Inc., Wabash, IN) at 1.4 MPa and 170 °C for 10 min.

3.3.7. Three ply plywood specimen preparation

Southern yellow pine veneer with dimension of $300 \times 300 \times 3.5$ mm were preconditioned in the 27 °C and 30% relative humidity chamber for 7 day prior to the panel assemble. The adhesive was applied to the bottom and top of the center ply only by a brush with spread rate 20–22 g/ft², on a wet weight basis. Veneers were oriented in the typical layup, in which the grain of the middle panel is perpendicular to the grain of the top and bottom panels. The assembled three ply veneers were conditioned for 10 min at room temperature, and then hot pressed at 150 psi (1.03 MPa) and 170 °C for 10 min.

3.3.8. Shear strength measurement

For two ply plywood samples, the assembled wood samples were cooled, conditioned at 23 °C and 50% relative humidity for 48 h, and cut into 5 pieces with dimensions of 80×20 mm (glued area of 20×20 mm). The cut wood specimens were conditioned for another 2 days before

measurements were taken. Wood specimens were tested with an Instron Tester (Model 4465, Canton, MA) according to ASTM Standard Method D2339-98 (ASTM, 2002c) at a crosshead speed of 1.6 mm/min. Shear adhesion strength at maximum load was recorded; reported values are the average of four specimen measurements. Water resistance of the wood assemblies was measured following ASTM Standard Methods D1183-96 (ASTM, 2002d) and D1151-00 (ASTM, 2002a). Six preconditioned specimens were soaked in tap water at 23 °C for 48 h, and wet strength was tested immediately after soaking.

For three ply plywood samples, the bonded wood samples were conditioned at 23°C and 50% relative humidity for 48 h before cutting. From each panel, 15 specimens (6 for dry strength and 9 for wet strength) with dimensions of 82.6 × 25.4 mm were obtained according to ASTM Standard Method D 906-98 (ASTM, 2002b). The cut specimens were conditioned for 48 h, and tested with the same Instron tester at a crosshead speed of 1.0 mm/min. Dry shear adhesion strength at maximum load was recorded; reported values are the average of six specimen measurements. Water resistance of three ply plywood samples was evaluated in terms of wet shear strength. Nine preconditioned specimens (82.6 × 25.4 mm) were soaked in water at 23 °C for 24 h, and wet strength was tested immediately after soaking.

3.4. RESULTS AND DISCUSSION

3.4.1. Thermal Properties

The organic CSH hybrid was synthesized by *in-situ* sol gel polymerization in which small silicone oxide molecules are converted to an integrated network of polymers and the resulting structure changes with aging, producing strengthening, stiffening, or shrinkage of the network. Particularly, the polymerization and solidification of CSH network structure is known to contribute to the mechanical strength of the cement paste after aging (Lin et al., 2010; Peterson et

al., 2006). For this reason, comparing fresh and aged composites to determine aging effect is critical to observe the interfacial interaction and detailed crosslinking mechanism between soy proteins and CSH. Therefore, aged composites were prepared to store the fresh samples in a plastic container with a lid for 7 days. The DSC thermograms of both fresh and aging composites were collected (Figure 3.2); data are summarized in Table 3.2.

DSC provides valuable information on unfolding the quaternary, tertiary, and secondary structures of soy protein and subsequent interaction between soy protein and CSH *via* a crosslinking function of aminopropyl silane (APTES). As shown in Figure 3.2, MSP has two endothermic transition peaks: One is at 79.97 °C from 7S and 97.25 °C from 11S for the denaturation peak temperature (T_d) with total enthalpy (ΔH_d) of 5.62 J/g. When MSP-CSH/20% APTES was prepared, the T_d and ΔH_d of the fresh composite decreased, however, they became higher in aged composites with aging effect as shown in Figure 3.2. Table 3.2 summarizes the T_d of 7S and 11S and total ΔH_d in composites with different molar ratios of APTES. The T_d and ΔH_d of aged composites was higher than for the corresponding fresh ones, representing higher thermal stability. As shown in Table 3.2, the recoveries of T_d and ΔH_d in the MSP-CSH with APTES was significant when APTES was applied as a crosslinking agent, on the other hand, the recovery in MSP-CSH was trivial when the pure CSH (0% APTES, 100% TEOS) was applied. Less thermal stability in the fresh composites means that the three-dimensional structure of 7S and 11S was affected by the organic CSH hybrid polymerization process. The MSP tends to be additionally unfolded by the byproducts (e.g., ethanol) of the sol-gel reactions during hydrolysis of the organic CSH hybrid. Generally, the organic solvent, such as methanol or ethanol, can denature globular soy proteins by disrupting hydrogen bonds (FUKUSHIM.D, 1969). The ethanol produced in the hydrolysis of silicate precursors can break the intra-or intermolecular

interactions within the soy proteins and disrupt the hydrogen bonds, resulting in lower denaturation temperatures for both 7S and 11S in the fresh composites. Moreover, the effect of calcium ionic strength was another possibility to disrupt the three-dimensional structure of protein, resulting in more extensive unfolding of soy protein structure with less thermal stability (Babajimopoulos et al., 1983). However, with aging, T_d and ΔH_d of 7S and 11S changed in the aged composites during the interaction between soy protein polymers and CSH *via* the crosslinking function of APTES. Figure 3 presents the degree of recovery of T_d and ΔH_d in MSP-CSH composites with different molar ratios of APTES. They were calculated by subtracting the T_d and ΔH_d of fresh composites from those of aged ones. As shown in Figure 3.3, the aged SP-CSH/20% APTES had the largest degree of recovery in T_d and ΔH_d but displayed no increase as the molar ratio of APTES increased further. APTES acts as a crosslinking agent and the unfolded soy proteins could be re-assembled through covalent bridges at the interface between soy protein and CSH. With an increasing molar ratio of APTES in the composite, APTES contributed to more crosslinking or grafted reaction between soy polymeric matrix and CSH, showing the higher T_d and ΔH_d . The coupling effect of APTES seemed to level off in the composites, however, when APTES was higher than 20%, which might be due to a random aggregation of silicate precursors in the preparation of organic CSH hybrids. In general, all parameters for sol-gel chemistry significantly affect the gelation time, reaction rate of hydrolysis, and polycondensation and geometry of final silica materials (Brinker and Scherer, 1985). The molar ratio of the two silica precursors varies in this work and consequently affects the gelation time and rate of aggregation. When CSH/40% APTES was prepared, silica precursors immediately started to aggregate, which could mean losses of opportunities for covalent bridges with soy proteins due to such a rapid gelation process. Additionally, the recovery of T_d and ΔH_d was

insignificant in MSP-CSH without using a crosslinking agent, confirming that APTES functions as a crosslinking agent between two very different polymer materials. Yet, it still means that unfolded soy proteins also facilitate re-association with non-covalent interaction based on the small recovery in the aged MSP-CSH (with 0% APTES).

3.4.2. Dynamic Viscoelastic Properties

Upon the *in-situ* polymerization of organic CSH hybrids, a three-dimensional network was formed in the MSP-CSH composites by a crosslinking process. According to thermal properties of MSP-CSH composites, MSP tended to re-assemble with covalent and non-covalent interactions in the aged composites, which is expected to possess better adhesion strength.

Dynamic rheological measurement was used to study viscoelastic properties of polymers and was carried out at a small strain within the linear viscoelastic region; the modulus curve was monitored as a function of time and frequency. The elastic modulus of fresh and aged composites is shown in Figure 3.4. By comparing the elastic modulus of fresh and aged composites, the viscoelastic properties of the MSP-CSH composites changed with aging. Aged composites had higher elastic moduli than fresh ones. The highest elastic modulus was observed in the aged MSP-CSH/20% APTES composite, rather decreased in MSP-CSH/40% APTES. MSP-CSH without addition of APTES had almost similar elastic modulus in spite of aging effect. This phenomenon was similar with interpretation of thermal properties. As described earlier, unfolded protein originating from ethanol lead to rearrangement of the protein polymeric matrix and CSH via crosslinking functions, and it is apparent that the grafting silane improves the viscoelastic properties of the MSP-CSH composites. Based on the increase in viscoelastic properties of MSP-CSH composites with aging, we concluded that the crosslinking process of aminopropyl silane occurred between soy proteins and CSH does the rearrangement of protein-protein complex,

which lead to the change of rheological properties. Complex viscosities of all aged composites decreased as the frequency increased (Figure 3.5), revealing a shear thinning behavior. Similarly, the MSP-CSH/20% APTES showed the highest viscosities because of strong intramolecular and intermolecular interactions due to the grafting process of aminopropyl silane. The specific covalent interactions occurring between protein macromolecular chains and organic CSH hybrids resulted in an entangled and interconnected three-dimensional structure in the chemical grafting reaction process.

3.4.3. FT-IR Spectroscopic properties

FT-IR spectroscopy was used to identify the conformation change of soy proteins caused by inorganic calcium derivatives and provides supportive evidence for the covalent bonds at the interface between soy proteins and CSH *via* the crosslinking process of APTES. Figure 3.6 (a) shows the IR spectra of MSP and CSH/20% APTES. The spectrum of MSP shows the main absorption bands of peptide linkage in soy proteins. The peak near 1633 cm^{-1} is the amide I band, which resulted from the C=O stretching vibrations of the peptide bond. Similarly, the peaks near 1518 cm^{-1} (N-H bending vibration/C-N stretching vibration) and 1230 cm^{-1} (C-N stretching vibration/N-H bending vibration) are called the amide II band and amide III band, respectively (Schmidt et al., 2005). The peak near 1392 cm^{-1} resulted from protein side-chain COO^- . Furthermore, the stretching C-NH₂ of side-chain primary amines appeared at 1446 cm^{-1} , and weaker bands related to C-N stretching and bending vibrations of protein backbone and amino acid residues were located at 1057 cm^{-1} .

The spectroscopic samples of CSH/20% APTES were prepared by completing the gelation process at ambient temperature, evaporating all solvent, and then freeze-drying. The spectral region between 1700 and 860 cm^{-1} has several bands whose intensities are mainly due to

APTES: δ (NH_2) at 1472 cm^{-1} and δ_A (CH_3) at 1426 cm^{-1} due to CH_3 and CH_2 bending and stretching of APTES (Pena-Alonso et al., 2007). A strong band of O-H stretching vibration is at 1630 cm^{-1} due to the absorption of atmospheric moisture. The most intensive spectral region is between 1200 and 900 cm^{-1} . The C-N stretching of APTES amino groups is shown at 1200 cm^{-1} . Si-O-C asymmetric stretching occurs at 1094 cm^{-1} , and Si-O-Si symmetric stretching occurs at 1027 cm^{-1} (Kamnev et al., 2002; Pena-Alonso et al., 2007). As the molar ratio of APTES varied from 40% to 0%, the ratio of two peaks at 1094 cm^{-1} to 1027 cm^{-1} decreased (data not shown).

The spectral range from 1750 to 860 cm^{-1} of both fresh and aged MSP-CSH composites with 0, 20, and 40% APTES are shown in the Figure 3.6 (b). All fundamental structural absorption peaks of MSP still appeared in the spectra of all composites. The strong amide I and II bands appeared in all composites and other spectral features were similar to MSP, except for the spectral range from 1200 to 1000 cm^{-1} . The bands from this range were mostly from Si-O-Si bonds of CSH. In the fresh composites, two bands relating to silicone oxide appeared at 1160 and 1112 cm^{-1} ; these bands were shifted compared with those at 1094 and 1027 cm^{-1} of CSH/20% APTES (Figure 3.6(a)). This shift indicates that CSH interact with MSP to create *in-situ* polymerization, and these two peaks were integrated and merged into one broad band with weak intensity, with aging effects as shown in Figure 3.6(b).

Because the aminopropyl group of APTES mostly overlaps with soy proteins in IR spectral features, a slight change in peak ratio or shift can provide an important clue to explain the crosslinking mechanism at the interface between protein polymers and CSH. Two important peak shifts occurred in the spectral features at 1634 cm^{-1} and 1441 cm^{-1} . Figure 3.7 (a) presents the amide I band at 1634 cm^{-1} and the inset shows the degree of the peak shift. The peak shift was calculated by subtracting peak maxima of IR spectra of aged composites from those of fresh

ones; they were all blue shifted toward shorter wavelength and higher energy. The degree of the peak shift was the most significant in the aged MSP-CSH/20% APTES, as shown in the inset of Figure 3.7 (a). As described earlier, this peak was a strong typical amide I resulting mainly from C=O stretching. The shift of this peak indicates that possible intra-hydrogen bonding was involved between protein polymers and CSH (Liang and Wang, 1999; Qi and Sun, 2011). Soy protein contains many functional groups, including carboxylic (-COOH) and hydroxyl (-OH) acids, which have potential to react with the aminopropyl (-NH₂(CH₂)₃-) of APTES. Another interesting point is the peak shift of the adsorption bands at 1441cm⁻¹ with C-NH₂ stretching. All composites demonstrated a blue shift with aging, as depicted in Figure 3.7 (b). Peak maxima were blue shifted with aging effect and the largest shift was observed in aged MSP-CSH/20% APTES. Changes to peak maxima in the aged composites indicate that the crosslinking of APTES occurred at the interface of soy proteins and CSH. The NH₂ of APTES reacted with side chains of soy protein, which was confirmed by the peak shift at C=O stretching at 1634 cm⁻¹ and NH₂ stretching at 1441 cm⁻¹. Such a reaction of aminopropyl groups of the silicate precursor with side chains of proteins has been observed by IR spectroscopy performed by other researchers (Liang and Wang, 1999).

3.4.5. Morphological Properties

The microstructures of MSP-CSH composites are presented in Figure 3.8. Pure MSP showed irregular particles with different sizes and smooth surfaces as shown in Figure 3.8 (A). As APTES concentration increased from 0 to 40%, the protein particle surface became more coarse and fluctuant, exhibiting a rough appearance (Figure 3.8 (B)-(D)). Pure inorganic CSH is a silica aggregate particle with sizes ranging from approximately 80 to 300 nm confirmed by transmission electron microscopy. However, the particle surface had big bumps and a little

rougher surface in MSP-CSH as shown in Figure 3.8 (B). In addition, the roughness became increased as the mole ratio of APTES was increased in Figure 3.8 (C) and (D), meaning silica aggregates from inorganic CSH coated the protein surface. As explained previously, MSP is partially unfolded protein and its functional groups can react with APTES coupled to inorganic CSH, displaying reacted rough coatings.

3.4.6. Shear Adhesion Strength

The dry and wet shear adhesion strength of MSP and MSP-CSH composites were evaluated with two types of wood substrates, cherry wood (Table 3.3) and southern yellow pine (Table 3.4). The dry and wet adhesion strengths of all composites with cherry wood were improved compared with MSP as summarized in Table 3.3. The MSP-CSH/20% APTES has the highest adhesion strength (2.73 MPa for dry and 2.44 MPa for wet strength) and wood cohesive failure (WCF). The crosslinking effect was the most significant in the MSP-CSH/20% APTES, which formed a covalent interface with improved cohesion and adhesion in the MSP-CSH/20% APTES.

Table 3.4 summarizes the shear adhesion strength results of all composites with southern yellow pine. The dry strength increased with the increased molar ratio of APTES from 0.92 to 1.19 MPa, but WCF was highest for the MSP-CSH/20% APTES then decreased for the MSP-CSH/40% APTES. Highest WCF showed the fiber pulled out from the glued wood surface at 20% APTES mole ratio could be grafted onto some soy protein functional groups, such as COOH and OH, through aminopropyl silane coupling, which could be beneficial to the protein adhesion strength. On the other hand, wet shear adhesion strength of all composites improved significantly compared with MSP. The MSP-CSH/20% APTES showed the most improvement in wet adhesion strength and WCF. Through the reaction between soy protein and CSH to form

stable covalent bridges, water-sensitive functional groups were removed and this helps to increase water resistance of the composites.

3.5. CONCLUSION

This work was the first demonstration of the potential of inorganic CSH to improve the adhesion strength of soy protein-based composites. The partially unfolded soy protein was reacted with aminopropyl groups of APTES, which was incorporated into inorganic CSH phases. APTES helped to form a crosslinked interface between soy protein and CSH, which was confirmed by changes in thermal, rheological, spectroscopic, and morphological properties with aging effect. More entangled and interwoven polymeric structure based on the crosslinked interface could help attachment to the solid surface, which consequently leads to the improvement of bonding strength compared to unmodified soy protein-based adhesives. This could be a reason of great resistance of MSP-CSH composites to the wood substrates sliding past one another, preventing detachment. This finding may have other possible applications in the field of plastic, packaging, or other disposable manufacturing products.

3.6. REFERENCES

ASTM, 2002a. **Standard Practice for Effect of Moisture and Temperature on Adhesive Bonds**. Annual Book of ASTM Standards. ASTM International, West Conshohocken, PA, pp. 67-69.

ASTM, 2002b. **Standard Test Method for Strength Properties of Adhesives in Plywood Type Construction in Shear by Tension Loading**. Annual Book of ASTM Standards. ASTM International, West Conshohocken, PA, pp. 1-4.

ASTM, 2002c. **Standard Test Method for Strength Properties of Adhesives in Two-Ply Wood Construction in Shear by Tension Loading**. Annual Book of ASTM Standards. ASTM International, West Conshohocken, PA, pp. 158-160.

ASTM, 2002d. **Standard Test Methods for Resistance of Adhesives to Cyclic Laboratory Aging Conditions**. Annual Book of ASTM Standards. ASTM International, West Conshohocken, PA, pp. 70-73.

Babajimopoulos, M., Damodaran, S., Rizvi, S.S.H., Kinsella, J.E., 1983. Effects of various Anions on the Rheological and Gelling Behavior of Soy Proteins - Thermodynamic Observations, *J. Agric. Food Chem.* 31, 1270-1275. doi: 10.1021/jf00120a032.

Brinker, C.J., Scherer, G.W., 1985. Sol-]Gel-]Glass .1. Gelation and Gel Structure, *J. Non Cryst. Solids* 70, 301-322. doi: 10.1016/0022-3093(85)90103-6.

Chae, H.J., In, M., Kim, M.H., 1997. Characteristic properties of enzymatically hydrolyzed soy proteins for the use in protein supplements, *Agricultural Chemistry and Biotechnology* 40, 404-408.

Frihart, C.R., 2010. Soy protein adhesives, *McGraw Hill Yearbook of Science and Technology* 2010 , 354.

FUKUSHIM.D, 1969. ENZYMATIC HYDROLYSIS OF ALCOHOL-DENATURED SOYBEAN PROTEINS, *Cereal Chem.* 46, 405-&.

Hamada, J.S., Marshall, W.E., 1989. Preparation and Functional-Properties of Enzymatically Deamidated Soy Proteins, *J. Food Sci.* 54, 598-&. doi: 10.1111/j.1365-2621.1989.tb04661.x.

Hettiarachchy, N.S., Kalapathy, U., Myers, D.J., 1995. Alkali-modified soy protein with improved adhesive and hydrophobic properties, *Journal of the American Oil Chemists Society* 72, 1461-1464. doi: 10.1007/BF02577838.

Huang, W.N., Sun, X.Z., 2000a. Adhesive properties of soy proteins modified by sodium dodecyl sulfate and sodium dodecylbenzene sulfonate, *Journal of the American Oil Chemists Society* 77, 705-708. doi: 10.1007/s11746-000-0113-6.

Huang, W.N., Sun, X.Z., 2000b. Adhesive properties of soy proteins modified by urea and guanidine hydrochloride, *Journal of the American Oil Chemists Society* 77, 101-104. doi: 10.1007/s11746-000-0016-6.

Kalapathy, U., Hettiarachchy, N., Myers, D., Hanna, M.A., 1995. Modification of Soy Proteins and their Adhesive Properties on Woods, *Journal of the American Oil Chemists Society* 72, 507-510. doi: 10.1007/BF02638849.

Kalapathy, U., Hettiarachchy, N.S., Myers, D., Rhee, K.C., 1996. Alkali-modified soy proteins: Effect of salts and disulfide bond cleavage on adhesion and viscosity, *Journal of the American Oil Chemists Society* 73, 1063-1066. doi: 10.1007/BF02523417.

Kamnev, A.A., Dykman, L.A., Tarantilis, P.A., Polissiou, M.G., 2002. Surface-enhanced Fourier transform infrared spectroscopy of protein A conjugated with colloidal gold. *Met. Ions Biol. Med.* 7, 104-107.

Kato, A., 1991. Significance of Macromolecular Interaction and Stability in Functional-Properties of Food Proteins, *ACS Symp. Ser.* 454, 13-24.

Kumar, R., Choudhary, V., Mishra, S., Varma, I.K., 2004. Enzymatically modified soy protein - Part 1. Thermal behaviour, *Journal of Thermal Analysis and Calorimetry* 75, 727-738. doi: 10.1023/B:JTAN.0000027169.19897.30.

Lambuth, A.L., 1977. Soybean glues. In: Skeist, I. (Ed.), *Handbook of Adhesives*. Van Nostrand Reinhold Co., New York, pp. 172-180.

Li, K., Peshkova, S., Geng, X., 2004. Investigation of soy protein-Kymene((R)) adhesive systems for wood composites, *J. Am. Oil Chem. Soc.* 81, 487-491. doi: 10.1007/s11746-004-0928-1.

Liang, F., Wang, Y., 1999. Effects of silane coupling agents on the interface of soy protein and glass fiber. *PROCEEDINGS- AMERICAN SOCIETY FOR COMPOSITES American Society for Composites Technical conference; 14th, American Society for Composites 14th*, 511-520.

Lin, Q., Lan, X., Li, Y., Ni, Y., Lu, C., Chen, Y., Xu, Z., 2010. Preparation and characterization of novel alkali-activated nano silica cements for biomedical application, *Journal of Biomedical Materials Research Part B-Applied Biomaterials* 95B, 347-356. doi: 10.1002/jbm.b.31722.

Liu, W., Chang, J., 2009a. In vitro evaluation of gentamicin release from a bioactive tricalcium silicate bone cement, *Materials Science & Engineering C-Materials for Biological Applications* 29, 2486-2492. doi: 10.1016/j.msec.2009.07.015.

Liu, W., Chang, J., 2009b. In vitro evaluation of gentamicin release from a bioactive tricalcium silicate bone cement, *Materials Science & Engineering C-Materials for Biological Applications* 29, 2486-2492. doi: 10.1016/j.msec.2009.07.015.

Mackay, C.D., 1998. Good adhesive bonding starts with surface preparation, *Adhes Age* 41, 30-32.

Markley, K.S., 1951. *Soybeans and Soybean Products*. Vol. II. Interscience Publishers, Inc., New York.

Minet, J., Abramson, S., Bresson, B., Franceschini, A., Van Damme, H., Lequeux, N., 2006. Organic calcium silicate hydrate hybrids: a new approach to cement based nanocomposites, *Journal of Materials Chemistry* 16, 1379-1383. doi: 10.1039/b515947d.

Mojumdar, S., Raki, L., 2005. Preparation and properties of calcium silicate hydrate-poly(vinyl alcohol) nanocomposite materials, *J. Therm. Anal. Calorim.* 82, 89-95. doi: 10.1007/s10973-005-0846-8.

Otaigbe, J.U., Adams, D.O., 1997. Bioabsorbable soy protein plastic composites: Effect of polyphosphate fillers on water absorption and mechanical properties, *J. Environ. Polymer Degradation* 5, 199-208.

Otaigbe, J., 1998. Controlling the water absorbency of agricultural biopolymers, *Plast. Eng.* 54, 37-+.

Pena-Alonso, R., Rubio, F., Rubio, J., Oteo, J.L., 2007. Study of the hydrolysis and condensation of gamma-aminopropyltriethoxysilane by FT-IR spectroscopy, *J. Mater. Sci.* 42, 595-603. doi: 10.1007/s10853-006-1138-9.

Peng, I.C., Quass, D.W., Dayton, W.R., Allen, C.E., 1984. The Physicochemical and Functional-Properties of Soybean 11s Globulin - a Review, *Cereal Chem.* 61, 480-490.

Peterson, V.K., Neumann, D.A., Livingston, R.A., 2006. Effect of NaOH on the kinetics of tricalcium silicate hydration: A quasielastic neutron scattering study, *Chemical Physics Letters* 419, 16-20. doi: 10.1016/j.cplett.2005.11.032.

Qi, G.S., Xiuzhi, 2011. Soy Protein Adhesive Blends with Synthetic Latex on Wood Veneer, *J. Am. Oil Chem. Soc.* 88, 271-281. doi: 10.1007/s11746-010-1666-y.

Qi, G., Li, N., Wang, D., Sun, X.S., 2013. Physicochemical properties of soy protein adhesives modified by 2-octen-1-ylsuccinic anhydride, *Industrial Crops and Products* 46, 165-172. doi: 10.1016/j.indcrop.2013.01.024.

Qi, G., Li, N., Wang, D., Sun, X.S., 2012. Physicochemical Properties of Soy Protein Adhesives Obtained by In Situ Sodium Bisulfite Modification During Acid Precipitation. *J. Am. Oil Chem. Soc.* 89, 301-312. doi: 10.1007/s11746-011-1909-6.

Qi, G., Sun, X.S., 2011. Soy Protein Adhesive Blends with Synthetic Latex on Wood Veneer, *Journal of the American Oil Chemists Society* 88, 271-281. doi: 10.1007/s11746-010-1666-y.

Schmidt, V., Giacomelli, C., Soldi, V., 2005. Thermal stability of films formed by soy protein isolate-sodium dodecyl sulfate, *Polym. Degrad. Stab.* 87, 25-31. doi: 10.1016/j.polymdegradstab.2004.07.003.

Singha, A.S., Thakur, V.K., 2010a. Mechanical, Morphological, and Thermal Characterization of Compression-Molded Polymer Biocomposites, *International Journal of Polymer Analysis and Characterization* 15, 87-97. doi: 10.1080/10236660903474506.

Singha, A.S., Thakur, V.K., 2010b. Synthesis, Characterization and Study of Pine Needles Reinforced Polymer Matrix Based Composites, *J Reinf Plast Compos* 29, 700-709. doi: 10.1177/0731684408100354.

Singha, A.S., Thakur, V.K., 2010c. Synthesis and Characterization of Short *Grewia optiva* Fiber-Based Polymer Composites, *Polymer Composites* 31, 459-470. doi: 10.1002/pc.20825.

Singha, A.S., Thakur, V.K., 2009. Study of Mechanical Properties of Urea-Formaldehyde Thermosets Reinforced by Pine Needle Powder, *Bioresources* 4, 292-308.

Staswick, P.E., Hermodson, M.A., Nielsen, N.C., 1984. Identification of the Cystines which Link the Acidic and Basic Components of the Glycinin Subunits, *J. Biol. Chem.* 259, 3431-3435.

Suzuki, S., Sinn, E., 1993. The 1.4 nm tobermorite-like calcium silicate hydrate prepared at room temperature from tetrahydroxysilane and calcium chloride solutions. *J. Mater. Sci. Lett.* 12, 542-544.

Taylor, H.F.W., 1986. Proposed Structure for Calcium Silicate Hydrate Gel, *J Am Ceram Soc* 69, 464-467. doi: 10.1111/j.1151-2916.1986.tb07446.x.

Thakur, V.K., Singha, A.S., Kaur, I., Nagarajarao, R.P., Yang Liping, 2010a. SILANE FUNCTIONALIZATION OF Saccharum Cilliare FIBERS: THERMAL, MORPHOLOGICAL, AND PHYSICOCHEMICAL STUDY, *International Journal of Polymer Analysis and Characterization* 15, 397-414. doi: 10.1080/1023666X.2010.510106.

Thakur, V.K., Singha, A.S., Mehta, I.K., 2010b. Renewable Resource-Based Green Polymer Composites: Analysis and Characterization, *International Journal of Polymer Analysis and Characterization* 15, 137-146. doi: 10.1080/10236660903582233.

Thanh, V.H., Shibasaki, K., 1978. Major Proteins of Soybean Seeds - Subunit Structure of Beta-Conglycinin, *J. Agric. Food Chem.* 26, 692-695.

van der Leeden, M., Rutten, A., Frens, G., 2000. How to develop globular proteins into adhesives, *J. Biotechnol.* 79, 211-221. doi: 10.1016/S0168-1656(00)00238-8.

Wescott, J M Frihart, C R Traska, A E., 2006. High-soy-containing water-durable adhesives, *J. Adhes. Sci. Technol.* 20, 859-873. doi: 10.1163/156856106777638734.

Wescott, J.M., Frihart, C.R., 2004. Competitive soybean flour/phenol-formaldehyde adhesives for oriented strandboard. *Int. Wood Compos. Mater. Symp. Proc.* 38th, 199-206.

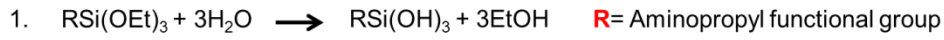
Wu, W.U., Hettiarachchy, N.S., Qi, M., 1998. Hydrophobicity, solubility, and emulsifying properties of soy protein peptides prepared by papain modification and ultrafiltration, *Journal of the American Oil Chemists Society* 75, 845-850. doi: 10.1007/s11746-998-0235-0.

Yang, I., Kuo, M., Myers, D.J., 2006. Bond Quality of Soy-based Phenolic Adhesives in Southern Pine Plywood, *Journal of the American Oil Chemists Society* 73, 231-237.

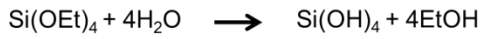
Yip, C.K., Van Deventer, J.S.J., 2003. Microanalysis of calcium silicate hydrate gel formed within a geopolymeric binder, *J. Mater. Sci.* 38, 3851-3860. doi: 10.1023/A:1025904905176.

Zhong, Z.K., Sun, X.Z.S., 2001. Properties of soy protein isolate/polycaprolactone blends compatibilized by methylene diphenyl diisocyanate, *Polymer* 42, 6961-6969. doi: 10.1016/S0032-3861(01)00118-5.

Figure 3.1 Hypothesis of the reaction pathways between soy proteins and CSH at the covalent interface.

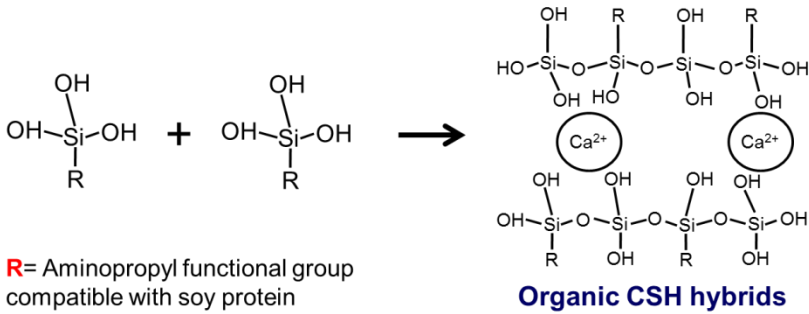


APTES



TEOS

2.



3.

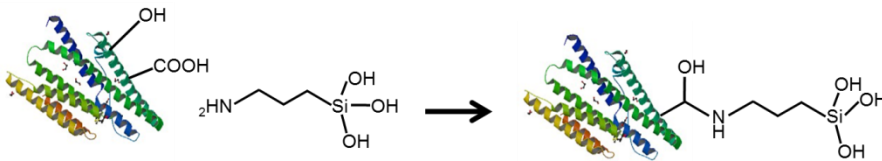


Figure 3.2 DSC thermograms of MSP and fresh and aged MSP-CSH/20% APTES.

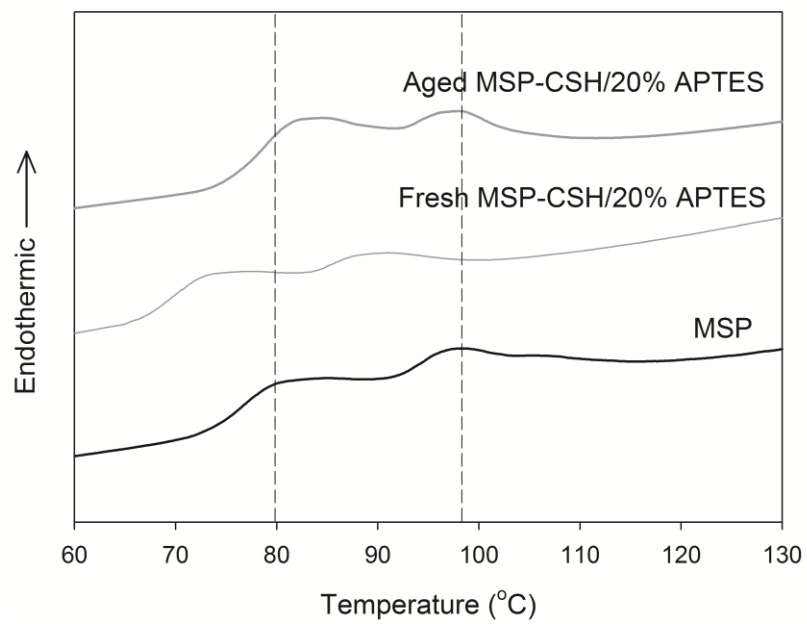


Figure 3.3 The degree of recovery of T_d and ΔH_d of MSP-CSH composites with different molar ratios of APTES.

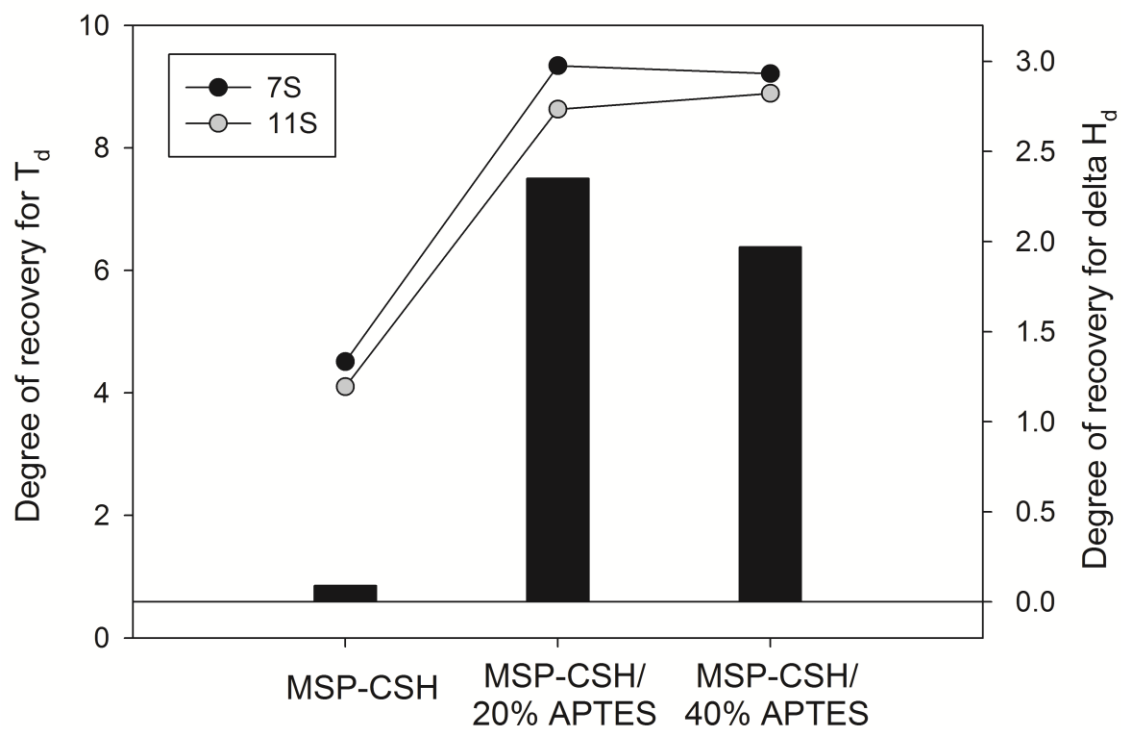


Figure 3.4 The frequency dependence of the elastic modulus (G') of MSP and MSP-CSH composites with different molar ratios of APTES.

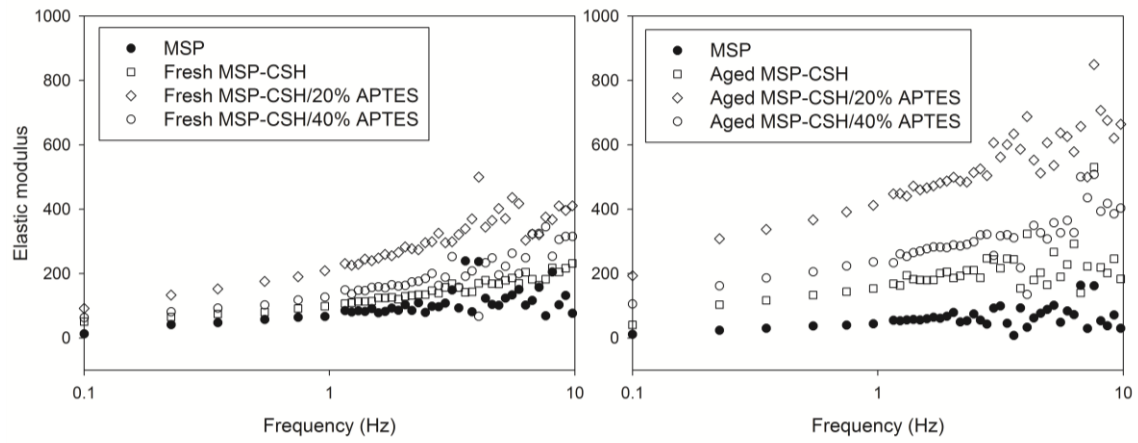


Figure 3.5 The complex viscosities of MSP and aged MSP-CSH composites with different molar ratios of APTES.

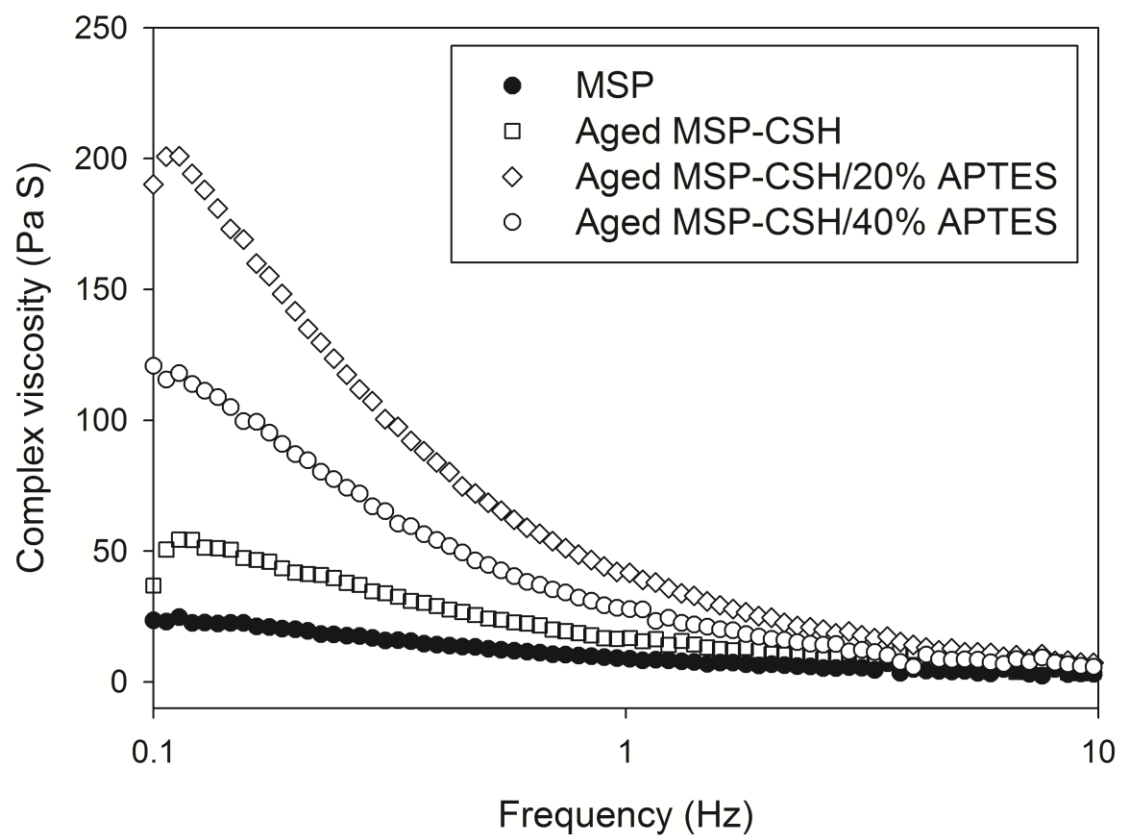


Figure 3.6 FT-IR spectra of (a) MSP and CSH/20% APTES and (b) fresh and aged MSP-CSH composites with different molar ratios of APTES for with spectral ranges from 1700 to 900 cm^{-1} .

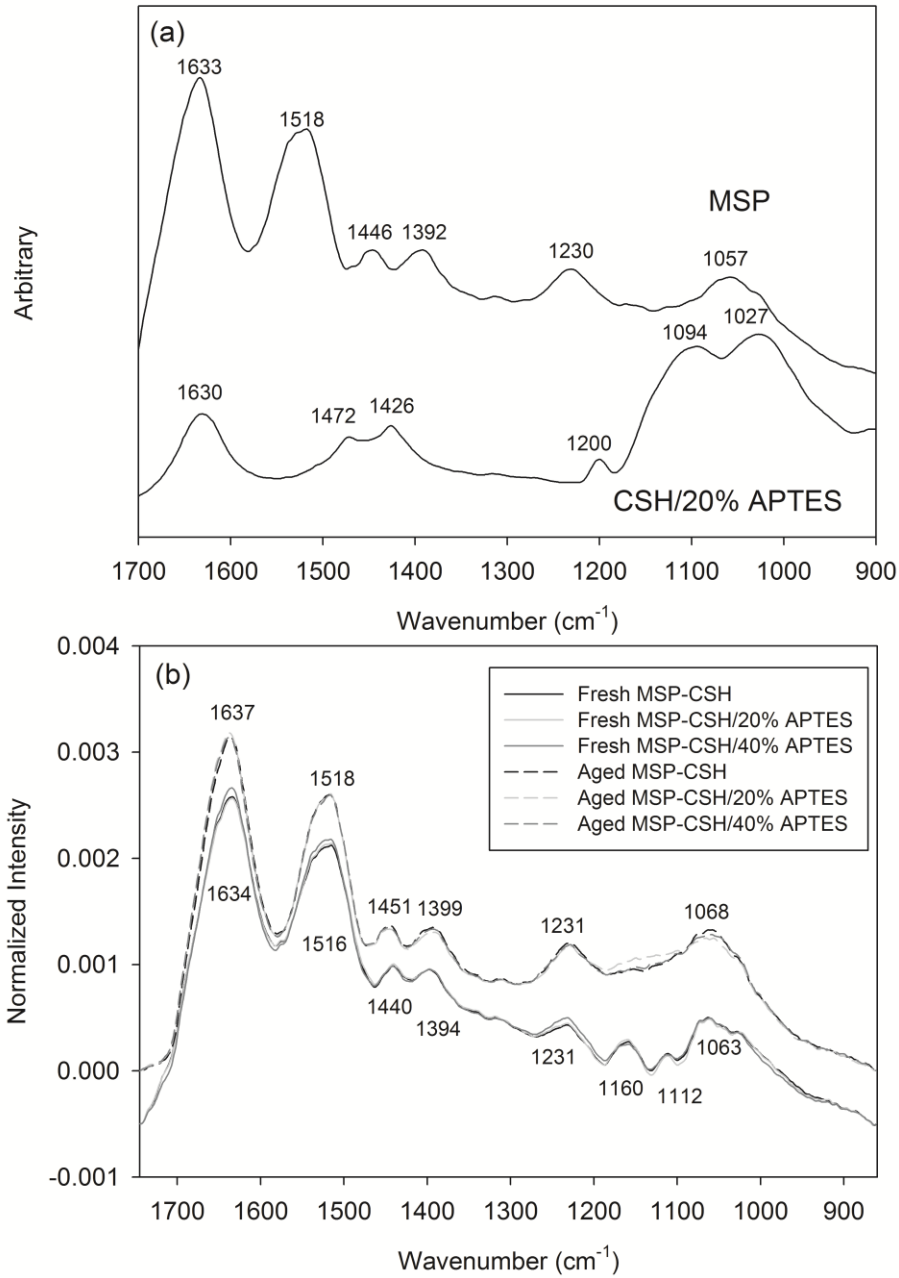


Figure 3.7 Enlarged spectral feature of peaks and the degree of peak shift at 1634 cm⁻¹(A) and at 1634 cm⁻¹(B) as insets.

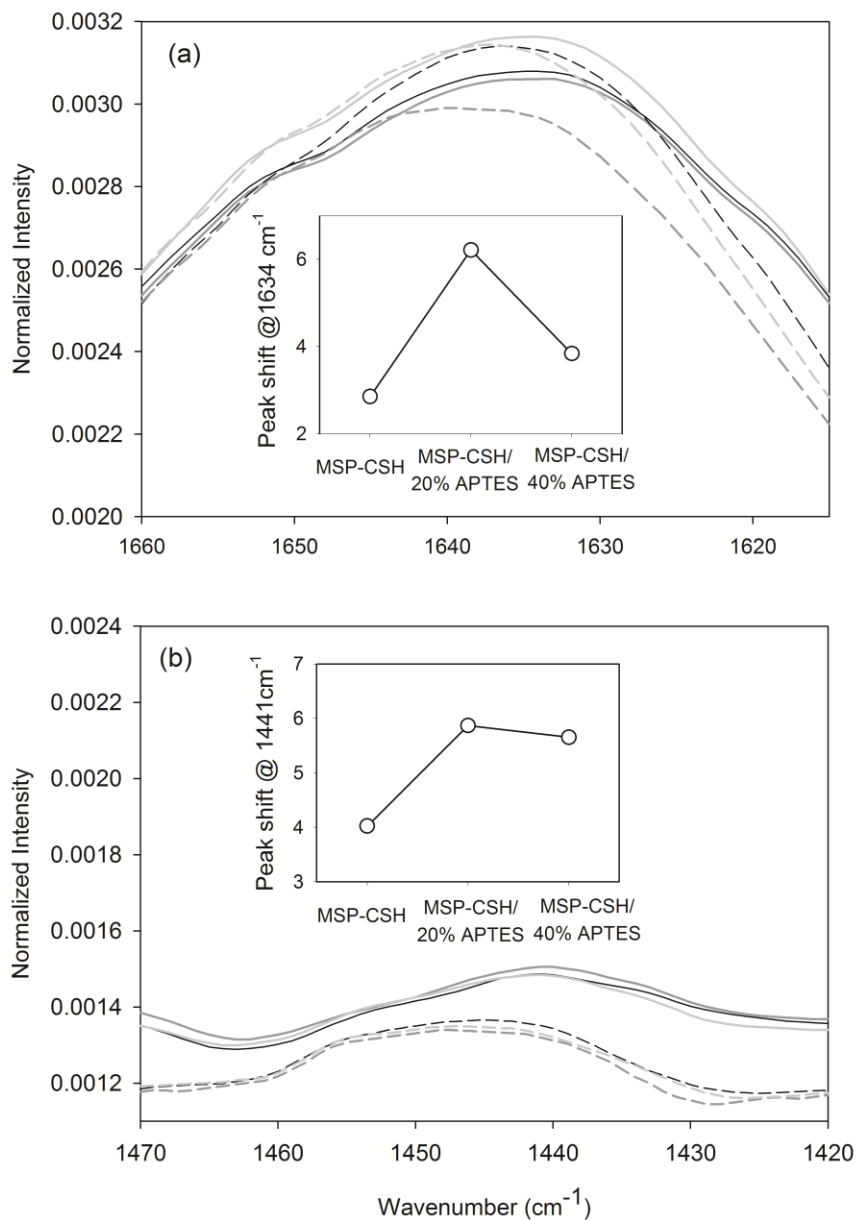


Figure 3.8 SEM images of MSP-CSH composites with different molar ratios of APTES (A) MSP, (B) MSP-CSH, (C) MSP-CSH/20% APTES and (D) MSP-CSH/40% APTES.

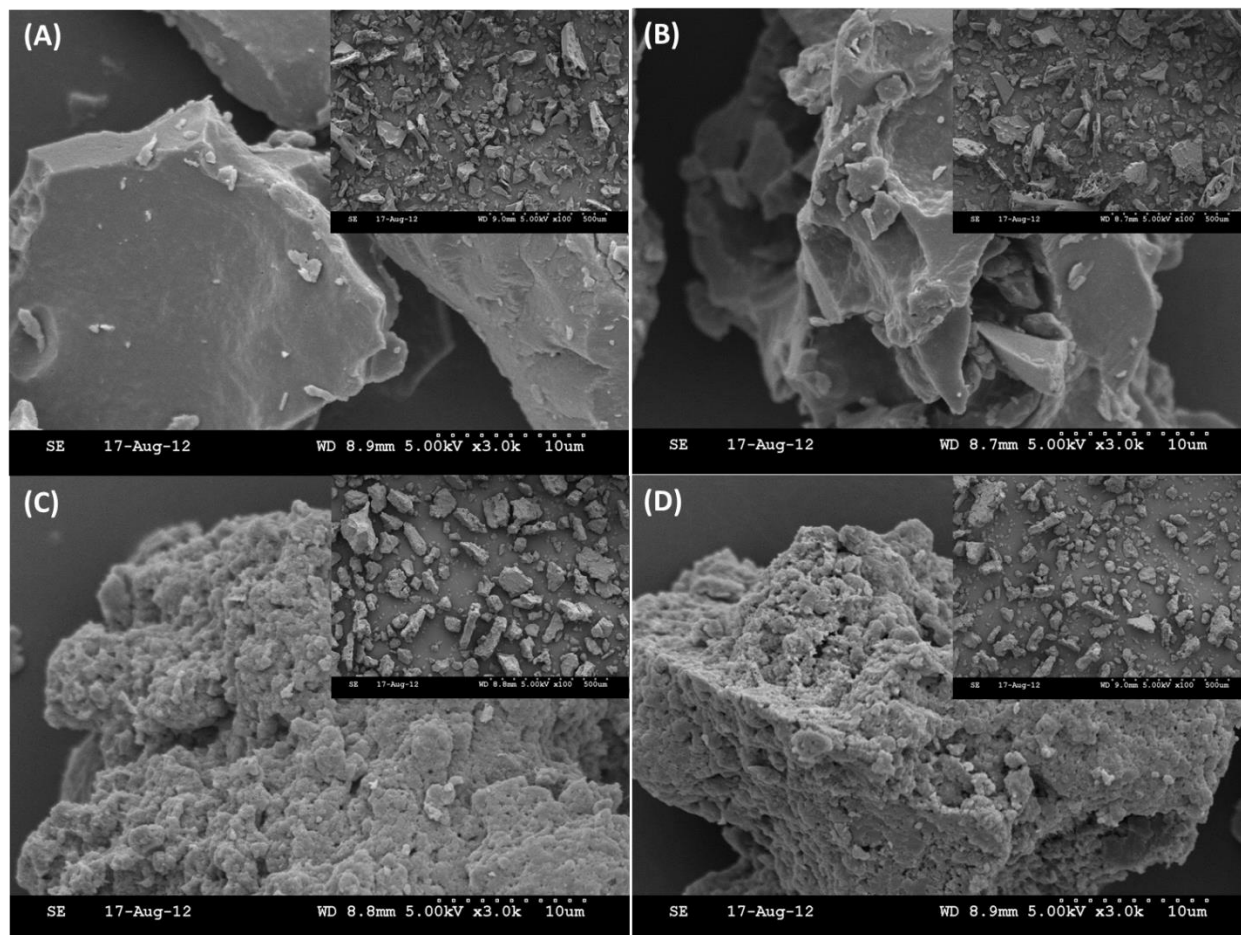


Table 3.1 Sample information of organic CSH hybrids by varying the starting fraction of ATPES with molar ratio of 0, 20, and 40% based on TEOS.

<i>In-situ</i> organic CSH hybrid synthesis				
Sample name	Molar ratio of APTES to TEOS	Molar concentration of APTES	Molar concentration of TEOS	Composite Name
CSH	0.0:1.0	0.000	0.606	MSP-CSH
CSH/20% APTES	0.2:0.8	0.121	0.485	MSP-CSH/20% APTES
CSH/40% APTES	0.4:0.6	0.242	0.364	MSP-CSH/40% APTES

Table 3.2 Summary of T_d and ΔT_d of MSP and MSP-CSH composites with different molar ratios of APTES.

MSP/CSH Composites		T_d (°C)		Total (ΔH_d) (J/g)
		7S	11S	
MSP		79.97	97.25	5.62
MSP-CSH	Fresh	73.01	89.64	5.49
	Aged	77.52	93.74	5.58
MSP-CSH/20% APTES	Fresh	73.21	89.97	5.45
	Aged	82.55	98.60	7.80
MSP-CSH/40% APTES	Fresh	72.82	90.10	5.17
	Aged	82.03	98.99	7.14

Table 3.3 Shear adhesion strength and wood cohesive failure (WCF) of MSP-CSH composites with cherry wood.

Samples	Dry strength	WCF (%)	Wet strength	WCF (%)
	(MPa)		(MPa)	
MSP	2.19 ± 0.22	41.67	1.99 ± 0.39	15.83
MSP-CSH	2.28 ± 0.29	51.67	2.22 ± 0.23	11.67
MSP-CSH/20% APTES	2.72 ± 0.21	60.00	2.76 ± 0.05	23.33
MSP-CSH/40% APTES	2.54 ± 0.25	73.33	2.48 ± 0.13	11.67

Table 3.4 Shear adhesion strength and wood cohesive failure of MSP-CSH composites with yellow pine wood.

Samples	Dry strength (MPa)	WCF (%)	Wet strength (MPa)	WCF (%)
MSP	0.92 ± 0.18	11.25	0.10 ± 0.06	2.86
MSP-CSH	0.86 ± 0.23	18.13	0.47 ± 0.11	18.57
MSP-CSH/20% APTES	1.08 ± 0.18	56.25	0.63 ± 0.20	30.00
MSP-CSH/40% APTES	1.19 ± 0.27	15.63	0.43 ± 0.10	14.00

Chapter 4 - CORRELATION BETWEEN PHYSICAL PROPERTIES AND SHEAR ADHESION STRENGTH OF ENZYMATICALLY MODIFIED SOY PROTEIN-BASED ADHESIVES²

4.1. ABSTRACT

Soy protein has long been used as a wood adhesive and has gained increasing attention as an alternative to formaldehyde-based adhesives. Despite much research, the physicochemical properties of soy protein-based adhesives and their relationship with shear adhesion performance remains unclear. When modifiers are applied to enhance the adhesion properties of soy protein, physicochemical properties such as thermal, spectroscopic, and rheological properties are significantly affected. Little information is available about how these changes in physicochemical properties can be used to predict and/or explain adhesion performance; consequently, it is necessary to establish the correlation between physical properties and adhesion performance. In this work, three important physical properties of viscosity, tackiness, and water solubility were selected to correlate with the shear adhesion strength of soy protein-based adhesives.

To accomplish this objective, response surface methodology (RSM), called a central composite design (CCD), was used with three independent variables from enzymatically modified soy protein-based adhesives (ESP): trypsin concentration (X_1), incubation time (X_2), and glutaraldehyde (GA) concentration (X_3). Three response variables were viscosity (Y_1), tacky force (Y_2), and water resistance (Y_3). These responses were all greatly affected by three independent variables, with significance at the 95% confidence level. The responses then were

² Results were submitted and under review. J. Am. Oil Chem. Soc.

correlated with the shear adhesion properties of ESP. The regression models between the three responses and their shear adhesion strengths were preliminarily identified and demonstrate the potential to establish reliable and fast screening methods to predict the adhesion performance of soy protein-based adhesives.

4.2. INTRODUCTION

Soy proteins have shown strong potential as wood adhesives, and much research has been dedicated to improving the adhesion performance of soy protein-based adhesives. High adhesive strength, water resistance, and low viscosity are the basic requirements for wood glue. To meet these requirements, adhesive strength and water resistance have been improved to modify soy protein-based adhesives using denaturation reagents, reducing agents, crosslinking agents, and enzyme hydrolysis (Hettiarachchy et al., 1995; Huang and Sun, 2000; Kato, 1991; Lambuth, 1977; Mackay, 1998; Markley, 1951; Wu and Inglett, 1974). Application of modifiers to enhance the adhesion properties of soy protein should greatly affect the resulting physicochemical properties, such as thermal, spectroscopic, and rheological properties. Many works have shown improvement in adhesion strength and changes in physiochemical properties to support this conclusion. Industries are seeking time-efficient methods for both quality control and screening in soy protein-based adhesive product development; however, research has not determined the correlation between physicochemical properties and shear adhesion performance, and knowing such correlations would help reduce long testing cycle and expenses.

The objective of this study was to investigate the physical properties of soy protein-based adhesives that can explain and predict adhesion performance and their relationship with shear adhesion strength. Viscosity, tackiness, and water solubility were measured to correlate the shear adhesion strength of soy protein-based adhesives. Viscosity is one of the most critical factors that

affects the flow property and penetration of soy protein molecules through wood materials, which could directly influence adhesion strength. Tackiness could represent the degree of mechanical interlocking between soy protein molecules and another metal substrate and could be an indirect indicator of adhesion performance. Water solubility important to the water resistance of soy protein-based adhesives and could be obtained by measuring the solubility of soy protein molecules in water. These three properties were used to establish reliable and representative methodologies to correlate with adhesion strength. Our preliminary studies successfully accomplished a new viscous modified soy protein-based adhesive (MSP) using NaHSO_3 with a high solid content of 38%, good flowability, long shelf life, and good water resistance (Qi et al., 2012; Sun et al., 2006). In this work, MSP was used as a base polymer for further treatment to prepare enzymatically modified soy protein-based adhesives (ESP) with three independent variables (X_1 : trypsin concentration, X_2 : incubation time, and X_3 : glutaraldehyde (GA) concentration as a crosslinker,) using response surface methodology (RSM) called a central composite design (CCD). A series of treatments was applied to MSP, and the important physical properties of viscosity (Y_1), tacky force (Y_2), and water resistance (Y_3) were measured and investigated the relationship with shear adhesion strength.

4.3. EXPERIMENTAL PROCEDURES

4.3.1. Materials

Defatted soy flour with a protein dispersion index of 90 was provided by Cargill (Cedar Rapids, IA). Trypsin was purchased from MP biochemical (Santa Ana, CA), and GA was purchased from Fisher Scientific (Hampton, NH). Cherry wood samples with dimensions of 50 mm (width) \times 127 mm (length) \times 5 mm (thickness) were obtained from Veneer One (Oceanside, NY). Orientation of the wood grain was perpendicular to the length of the wood samples.

4.2.2. Experimental design

Three variables, trypsin concentration (X_1), incubation time (X_2), and GA concentration (X_3), were chosen as parameter variables, and the corresponding viscosity (Y_1), tacky force (Y_2), and water resistance (Y_3) were the responses. The ranges of each variable were selected based on preliminary experiments and the coded and un-coded variables were summarized in Table 4.1.

A standard RSM design called central composite design (CCD) was applied to study the effects and interactions of the parameter variables (X_1 , X_2 , and X_3) on the responses (Y_1 , Y_2 , and Y_3). A set of 20 experiments, including eight factorial experiments, six star points, and six center points, were carried out. The distance of the star points from the center point is given by $\alpha=2^{n/4}$, where n is the number of factors (for three factors, $\alpha=2^{3/4}=1.682$). The system behavior is described by a second-order polynomial regression model carried out using Design Expert software (Trial version 9.0.0, Stat-Made Easy, Minneapolis, MN) and given by:

$$Y = \alpha_0 + \sum \alpha_i X_i + \sum \alpha_{ii} X_{i2} + \sum \alpha_{ij} X_i X_j + \epsilon \quad (1)$$

where Y is the response variable; α_0 is a constant; α_i , α_{ij} , and α_{ii} are the linear, quadratic and interactive coefficients, respectively; X_i and X_j are the levels of the parameter variables, and ϵ is the random error. The responses obtained from the experimental design were subjected to multiple non-linear regressions using Design Expert. The quality of the fit of the polynomial model equation was evaluated by the coefficient of determination (R^2) and adequate precision (AP) and standard deviation (SD). The significance of the regression coefficient was determined using an F-test and p-value.

4.2.3. MSP and ESP sample preparation

MSP was extracted from soy flour slurry modified with sodium bisulfate using the acid precipitation method described by Qi et al (Qi et al., 2012; Qi et al., 2013). Defatted soy protein flour was dispersed in water (1:16 ratio) at pH 9.5 using 3N NaOH. The NaHSO₃ (6g/L) was added to the soy protein slurry and stirred for 2 h. The pH of the slurry was then adjusted to pH 5.4 with 2N HCl to remove carbohydrates by centrifugation at 12,000 g. Then, the pH of the supernatant was adjusted to 4.8 with 2N HCl and centrifuged at 8000 g. The precipitate, MSP, was collected. As noted in Table 4.2, a variation of treatments was applied to MSP to prepare ESP. A specific amount of trypsin was added to the MSP, and the mixture was incubated at ambient temperature for corresponding incubation time while gently stirring. Immediately after the enzyme reaction had taken place, the trypsin was inactivated by heating at 90 °C for 3 min (Kalapathy et al., 1995). Then, the corresponding GA concentration was added to ESP and stirred thoroughly for complete mixing.

4.2.4. Physicochemical properties measurement

4.2.4.1. Viscosity Measurement

A Bohlin CVOR 150 rheometer (Malvern Instruments, Southborough, MA) was used to measure viscosity of ESP. A parallel plate head with 20-mm plate diameter and a 500-um gap was used. The measurements were performed with the single shear rate of 40 s⁻¹. The testing temperature was 25 °C. A thin layer of silicon oil was spread around the circumference of the sample to prevent dehydration. Viscosities were recorded for 120 sec, and all measurements were triplicated and averaged.

4.2.4.2. Tacky force

The standard test method for a loop tack test for pressure-sensitive adhesives (ASTM D 6195-03) was followed to measure the tackiness of ESP. This test method involved a loop of ESP applied on papers (LaserJet printing paper, Hewlett-Packard, Palo Alto, CA) to be brought into controlled contact with a 1 in.² stainless steel surface. To ensure that the same amount of ESP was applied to the paper, a brass mold was built with a square hole (25.4 × 25.4 × 0.25 mm) in the middle of the rectangular brass plate (60.0 × 40.0 × 0.25 mm). The sample amount was controlled by the thickness of the mold. The mold was placed on the middle of the paper (1 × 7 in.), the sample was placed inside the hole of the mold, and excess sample was removed by scraping a stainless steel stick across the surface of the brass mold. The paper with samples was bent form a teardrop-shaped loop with the sample surface facing out. The ends of the loop were fastened into the upper grips of the tensile tester (Imada tensile tester, DS2-11, Northbrook, IL). Moving the tensile tester down meant the specimen loop completely covered the 1 in.² area of the stainless steel portion of the test fixture. After waiting for 30 sec (dwell time), the maximum force required to remove the specimen loop from the stainless steel was recorded. All measurements were triplicated.

4.2.4.3. Water resistance

Water solubility of ESP was determined by measuring the protein loss after soaking the cured soy protein film in water. The adhesive samples were spread on a glass slide using a spatula to make a thin film, and the specimen was cured in an oven at 100 °C for 1 h. The specimen was soaked in water (tap water, temperature 21 °C) for 30 min to observe the loss or dissolution of the cured protein film. The wet specimens were dried in the oven at 100 °C for 1 h. Water resistance (%) was calculated based on the weight difference of protein film before and

after soaking using equation (2); lower water solubility means higher water resistance of cured protein film.

$$\text{Water resistance(\%)} = \left[\frac{(W_b - W_a)}{W_b} \right] \times 100 \quad (2)$$

where W_b and W_a are weights of sample before and after water soaking, respectively.

4.2.5. Mechanical plywood properties

4.2.5.1. Two ply plywood specimen preparation

Cherry wood veneers with dimensions of $50 \times 127 \times 5$ mm were preconditioned in a chamber (Electro-Tech Systems, Inc., Glenside, PA) for 7 days at 23 °C and 50% relative humidity. The adhesives were brushed onto one end of a piece of cherry wood with dimensions of 127×20 mm (length \times width) until the entire area was completely wet. Two brushed wood pieces were assembled immediately and conditioned for 10 min at room temperature. Then the assembled wood specimens were pressed with a hot press (Model 3890 Auto M; Carver, Inc., Wabash, IN) at 1.4 MPa and 170 °C for 10 min.

4.2.5.2. Shear strength measurement

For two-ply plywood samples, the assembled wood samples were cooled, conditioned at 23 °C and 50% relative humidity for 48 h, and cut into 5 pieces with dimensions of 80×20 mm (glued area of 20×20 mm). The cut wood specimens were conditioned for another 2 days before measurements were taken. Wood specimens were tested with an Instron Tester (Model 4465, Canton, MA) according to ASTM Standard Method D2339-98 (ASTM, 2002b) at a crosshead speed of 1.6 mm/min. Shear adhesion strength at maximum load was recorded; reported values are the average of four specimen measurements. Water resistance of the wood assemblies was measured following ASTM Standard Methods D1183-96 (ASTM, 2002c) and D1151-00 (ASTM,

2002a). Six preconditioned specimens were soaked in tap water at 23 °C for 48 h, and wet strength was tested immediately after soaking.

4.4. RESULTS AND DISCUSSION

Adhesion between soy protein and wood is attributed to a combination of three mechanisms: mechanical interlocking, physical interaction, and covalent chemical bonding (Skeist, 1962). When applied to wood, protein adhesives spread, wet, and penetrate the wood surface, forming mechanical interlocking, physical interaction, and covalent bonding upon thermal curing to achieve a strong bond. Soy protein is composed of an array of polypeptides with different molecular sizes and could be partially cleaved or degraded by trypsin, which specifically hydrolyses carbonyl bonds formed by basic amino acids such as lysine and arginine (Shutov et al., 1991). In this work, trypsin was used to degrade the soy protein into smaller molecular size and expose more hydrophobic groups to the surface (Hettiarachchy et al., 1995; Kalapathy et al., 1996). GA was subsequently applied as a crosslinking agent to rebuild or reconstruct the structure of soy protein by increasing crosslinking density with large and interwoven polymers. To navigate the effect of each variable (X_1 , X_2 , and X_3) on three important responses (Y_1 , Y_2 , and Y_3) of ESP, CCD was employed to build a regression model between the preparation variables to the three responses of ESP; results obtained from the experiments are listed in Table 4.2.

4.3.1. Model fitting

For viscosity (Y_1), a quadratic model suggested by Design Expert software was selected. The coefficients of the parameter variables (X_1 , X_2 , and X_3) for the viscosity (Y_1) can be expressed by the following second-order polynomial equation in terms of coded values:

$$Y = 0.12 - 1.445 \times 10^{-3}X_1 - 9.247 \times 10^{-3}X_2 - 7.338 \times 10^{-3}X_3 + 0.031X_1X_2 + 4.219 \times 10^{-3}X_1X_3 + 0.012X_3 + 0.011X_1^2 + 9.289 \times 10^{-3}X_2^2 + 2.293 \times 10^{-3}X_3^2 \quad (3)$$

A positive or negative coefficient indicates a synergistic and antagonistic effect, respectively.

The coefficient of the model for viscosity was estimated using the multiple regression analysis technique included in RSM. Adequate precision (AP) represents the signal-to-noise ratio, where a ratio greater than four is desirable. For Eq. (3), the R^2 , AP, and standard deviation (SD) were 0.840, 9.183, and 0.016, respectively. These indicate that 84.0% of the total variation in viscosity is attributed to the experimental variables. The adequacy of the models was further justified through an analysis of variance (ANOVA). Results from the ANOVA for the quadratic model for viscosity are listed in Table 4.3 (A). Corresponding variables are more significant at greater F- and smaller p-values. As shown in Table 4.3 (A), F-value of 5.84 and p-value of 0.0054 (less than 0.0500) of the model suggests that model terms are significant. Also, X_1X_2 and X_1^2 affected the viscosity significantly, whereas the X_2 , X_3 , X_1X_3 , and X_2X_3 were all insignificant to the response.

For tacky force (Y_2), a quadratic model suggested by Design Expert software was selected. The second-order polynomial equation of the parameter variables (X_1 , X_2 , and X_3) for the tacky force (Y_2) can be expressed by the following in terms of coded values:

$$Y = 0.65 - 0.036X_1 + 2.411 \times 10^{-3}X_2 + 0.14X_3 + 0.055X_1X_2 - 0.11X_1X_3 + 0.045X_2X_3 + 0.10X_1^2 + 0.048X_2^2 + 0.080X_3^2 \quad (4)$$

For the tacky force model, the R^2 , AP, and SD were 0.740, 5.647, and 0.16, respectively. As the results from ANOVA analysis summarize in Table 4.3 (B), an F-value of 3.16 and a p-value less than 0.0500 indicate that model terms are significant. In this case, X_3 and X_1^2 are significant model terms.

In addition, a quadratic model was built for water resistance (Y_3) based on the second-order polynomial equation of the parameter variables (X_1 , X_2 , and X_3):

$$Y = 4.24 + 0.58X_1 + 1.43X_2 + 0.83X_3 - 0.33X_1X_2 - 0.074X_1X_3 - 1.00X_2X_3 - 0.34X_1^2 + 1.72X_2^2 - 0.32X_3^2 \quad (5)$$

For the water resistance model, the R^2 , AP, and SD were 0.746, 7.325, and 1.25, respectively. The model F-value of 3.26 and p-value less than 0.0500 mean that model terms are significant; in particular, X_2 and X_2^2 are affected significantly by water resistance of ESP. The regression models of three responses (Y_1 , Y_2 , and Y_3) were greatly affected by three variable parameters (X_1 , X_2 , and X_3), resulting from high R^2 . Despite the complexity of the system to be tested, three variables successfully reflected the three responses based on statistical explanation.

4.3.2. Interpretation of response surface model

To further investigate the effects of the three variables on the responses, the relationship between the variable parameters and responses is shown in Figures 4.1, 4.3, and 4.4. To simplify the effects of variables on responses, three levels (-1, 0, and +1) of one variable are presented with another variable while maintaining the other variable at zero.

The effects of trypsin concentration (X_1) and incubation time (X_2) on viscosity (Y_1) are shown in Figure 4.1(A). Viscosities seem to increase with increased trypsin concentration (X_1) at the early stage of hydrolysis ($X_2 = 3.23$ h); however, at 6.50 h of incubation time (X_2), viscosities increased up to trypsin concentration (X_1) of 1.30 wt% but started to decrease with higher trypsin concentration (X_1), and viscosities seemed to decrease with concentrations of whole trypsin (X_1) after 9.77 h of incubation time (X_2). In general, reduced viscosity can provide evidence of proteolytic hydrolysis by confirming weaker intermolecular interaction and smaller polypeptide chains. The increased viscosities at a low concentration of trypsin (X_1) and with short incubation

time (X_2) did not agree with previous findings, and we assume that this might explain the hydrolysis mechanism of trypsin on MSP.

For further investigation, reducing SDS-PAGE was performed to study the effects of low trypsin concentration and short incubation time on MSP hydrolysis, as shown in Figure 4.2. For this purpose, only qualitative analysis of SDS-PAGE was performed. At low trypsin concentration (0.50 wt%), some molecular bands became darker and thicker after 6 h of incubation (Lane D) but became gradually lighter and disappeared after 12 h of incubation (Lane E and F). We believe this might be strongly related to the trypsin activity, depending on hydrolysis conditions. The physical morphology of MSP as a starting protein polymer is highly viscoelastic, which initially might block enzymes from accessing and/or digesting the surface of the soy protein at low concentration, causing lower enzyme activity. Furthermore, the reaction conditions of MSP were pH 4.6 and ambient temperature, which were away from the optimum conditions for trypsin activity of pH 8 and 37 °C (Barkia et al., 2010; Sipos and Merkel, 1970). Adverse reaction conditions and low enzyme concentrations might cause low trypsin activity during the early stages of incubation. We assume that increased surface area of soy protein due to enzyme hydrolysis might lead to intermolecular interactions at certain solid contents, thus increasing viscosity. Trypsin concentration (X_1) above 1.30 wt% concentrations could start to hydrolyze soy protein in the early stages of incubation, providing reduced viscosity due to low molecular weight and cleaved molecular bands; however, the detailed hydrolysis mechanism needs to be investigated.

Viscosities increased as GA concentration (X_3) increased at all trypsin concentrations (X_1), as shown in Figure 4.1(B). The effects of GA concentration (X_3) and incubation time (X_2) on viscosity are shown in Figure 4.1(C). With different GA concentrations (X_3), viscosities

tended to increase up to 9.77 h of incubation time (X_2), then decrease. Increased viscosities could be explained by the hydrolysis mechanism of trypsin on MSP as mentioned earlier. At long incubation times ($X_2 > 9.77$ h), however, viscosities decreased with GA concentration (X_3). GA generally increases the crosslinking density of protein polymeric matrix, and subsequently viscosity, but enzymatic degradation would lower viscosity. The crosslinking function of GA marginally affects viscosity, which could be advantageous for adhesives in wetting and spreading on the wood surface.

The relationship of each variable to tacky force (Y_2) is presented in Figure 4.3. Tacky force decreased at low trypsin concentration (X_1) but increased gradually at higher trypsin concentrations (X_1) as shown in Figure 4.3(A). With higher trypsin concentration (X_1) and longer incubation time (X_2), cleaved soy proteins could expose many functional groups and contribute to increased cohesion and adhesion at the interface between paper and the aluminum substrate.

Tacky force increased with GA concentration (X_3) as shown in Figure 4.3(B). Additional protein functional groups could interact with GA to form the entangled structure at the interface, leading to enhanced tacky force. Furthermore, GA concentration (X_3) was significant, and incubation time (X_2) had only a minor effect on tacky force as shown in Figure 4.3(C). Because tacky force indicates the ability of an adhesive to adhere to the substrate, it is highly dependent on the polymer chains and extent of crosslinking (Pang et al., 2013). The enzymatic modification and subsequent crosslinking construction of the protein structure led to loosed polymers, then to increased crosslinking density with the help of GA. This two-step process could reflect the tacky force, which is further expected to correlate with the shear adhesion performance.

The last response, water resistance (Y_3), was presented in Figure 4. Water resistance increased with incubation time (X_2) and trypsin concentration (X_1), as illustrated in Figure 4.4(A). Also, as trypsin concentration (X_1) increased, we found slightly higher water resistance. As incubation time (X_2) and trypsin concentration (X_1) increased, hydrolyzed soy protein would have more functional groups available to form a higher degree of entanglement, which could contribute to better water resistance. As shown in Figure 4.4(B), water resistance improved with increased trypsin concentration (X_1) and GA concentration (X_3); furthermore, Figure 4.4(C) shows that water resistance seemed to decrease at the beginning of hydrolysis but started to increase after 9.77 h of incubation time (X_2). This result occurred because of the complex hydrolysis mechanism of trypsin on MSP as mentioned above.

4.3.3. Relationship between three responses and shear adhesion properties

Based on the response value (low, medium, and high), nine experimental treatments of each response from Table 4.3 were selected for adhesion strength measurement. Correlations between each response (i.e. viscosity, tacky force, and water resistance) and adhesion strength were then established using a linear regression model (Table 4.4); the coefficients of determination (R^2) are presented in Figures 4.5 - 4.7.

4.3.3.1. Viscosity

Viscosity can be dramatically affected by protein structure. For soy protein-based adhesives, viscosity is a result of intermolecular interactions, such as electrostatic interaction and disulfide bonding among protein molecules. Because viscosity, or flow property, governs the penetration and wetting of soy protein through the wood material, it could directly affect adhesion strength (Cheng and Sun, 2006; Scheikl and Dunky, 1998). To achieve strong adhesion,

an appropriate penetration depth into wood cells or capillary pores is necessary to form a strong bond to the adherend.

The linear regression between viscosity and dry shear adhesion strength had an R^2 value of 0.7678 (as indicated in by filled circles in Figure 4.5), which suggests that viscosity has a remarkable effect on dry strength. Adhesion decreased as viscosity increased up to 10.5 Pa S. As explained in the previous section, viscosity was significantly affected by trypsin concentration (X_1^2) and the interaction between trypsin concentration and incubation time (X_1X_2). Enzymatic hydrolysis causes a reduction in molecular size and intermolecular interactions, resulting in lower viscosity, which could play an important role in wettability and penetration of protein molecules to an appropriate depth in the wood surface. For adhesives with higher viscosities, molecular attractions among protein molecules would be stronger, which would result in a shallower penetration due to the greater restriction caused by molecular attraction. On the other hand, adhesives with moderate viscosity from progressive proteolytic hydrolysis could penetrate deeper than those with a higher viscosity and eventually develop a much stronger three-dimensional zone at the interface. Upon curing, the soy protein molecules were entangled and cured in this three-dimensional zone, contributing to mechanical interlocking.

To determine the optimum viscosity range for processing parameters, the ESP with low viscosity were prepared with higher trypsin concentrations (3%) and longer incubation times (12, 24, 48, and 72 h). The viscosities (3.486, 2.865, 2.249, and 2.127 Pa S respectively) were decreased due to prolonged hydrolysis time as presented with empty circles in Figure 4.5(a) and had a R^2 of 0.8847 using linear regression. The overall R^2 value was also calculated using all viscosities with cubic nonlinear regression and presented in Figure 4.5(a). The dry strength seemed consistent with the viscosity range from 2.80 to 6.10 Pa S, which can lead to fairly stable

and good adhesion performance with wood substrates. On the other hand, the linear regression model between viscosity and wet strength was very low, with a R^2 value of 0.0011, as shown in Figure 4.5(b). Crosslinking agents play an important role in the formation of interwoven and entangled structure, which could be used as water barrier to improve the wet adhesion of soy protein (Cheng, 2004; Frihart, 2010; Sun, 2011). Because GA increases the crosslinking density in this soy protein system, it would be more related to wet adhesion strength, but viscosity was statistically reflected by the interaction between trypsin concentration and incubation time (X_1X_2) and the trypsin concentration (X_1^2) rather than GA concentration (X_3). Therefore, GA may not significantly affect viscosity compared with trypsin concentration (X_1) and incubation time (X_2).

4.3.2.2. Tacky force

The bonding mechanism involves comprehensive understanding of simultaneous cohesion (the internal strength among protein molecules) and adhesion (the tendency of the protein molecule to stick to a wood surface) (Sowa et al., 2014). The loop tack test could be an easy way to evaluate the cohesion and adhesion properties of polymer adhesives, particularly pressure-sensitive adhesives. Although this method is generally limited to bonding strength at the interface, in this study it is used as a simple method to predict the adhesion strength of soy protein-based adhesives. The thickness of protein-based adhesives on paper was thin enough to be cured on an aluminum substrate surface with a short dwelling time (30 sec), and we could expect similar adhesion and cohesion between protein molecules and wood materials. Paper is a cellulosic material like wood. The bonding mechanism, including wetting, penetration, and mechanical interlocking, could occur at the interface between paper and an aluminum substrate surface.

As presented in Figure 4.6, the linear regression model between tack force and dry and wet strength was built with R^2 values of 0.3660 and 0.7082, respectively. Tacky force is positively related to wet strength based on R^2 values. The tacky force was significantly affected by GA concentration (X_3), as confirmed by ANOVA analysis in Table 4.3(C). As discussed earlier, GA would play an important role in determining the wet strength by building an entangled structure as a water barrier. Accordingly, the tacky force could be an indicator to explain wet strength. Soy protein is a thermosetting polymer and becomes harder with crosslinking reactions at elevated temperatures. Curing conditions in this loop tack test differed in temperature and pressure from wood tests, which might lead to different adhesion phenomena of protein molecules between paper and aluminum substrate; however, the loop tack test can be used as a good predictor of adhesion strength based on results of the high correlation between tacky force and dry/wet strength.

4.3.3.3. Water resistance

Upon curing at high temperatures, soy protein could make an entangled three-dimensional zone between protein molecules and glass surface. Measuring the protein solubility into water of the cured protein film allows water resistance to be used to predict wet adhesion strength. Wet adhesion performance is an important property to determine the resistance to moisture of the soy protein-based adhesive, which will help expand its applications in the wood product market for structural and exterior wood products. As shown in Figure 4.7, dry and wet strength were well correlated to the water resistance of thin protein film, with R^2 values of 0.5257 and 0.6930, respectively. This method of determining water resistance can be used to predict wet adhesion strength.

4.4. CONCLUSION

This work has shown the potential to correlate important physical properties and shear adhesion strengths of protein-based adhesives. Viscosity was successfully reflected by parameter variables and showed the good correlation with dry shear strength. Tacky force was a good indicator of wet shear adhesion strength, which was significantly reflected by cohesion and adhesion phenomena between the paper and aluminum substrates. Water resistance can be used to predict wet adhesion strength based on its good relationship with wet adhesion strength. The crosslinking degree plays an important role in developing entangled three-dimensional zones, which can be used as a water barrier then as a predictor of wet adhesion strength. This work preliminarily identified the most significant physical property that can explain and predict the shear adhesion strength of an enzymatically modified soy protein-based adhesive system, but the results need to be further confirmed by another protein modification system in order to give generic conclusion.

4.5. REFERENCES

- ASTM, 2002a. **Standard Practice for Effect of Moisture and Temperature on Adhesive Bonds**. Annual Book of ASTM Standards. ASTM International, West Conshohocken, PA, pp. 67-69.
- ASTM, 2002b. **Standard Test Method for Strength Properties of Adhesives in Two-Ply Wood Construction in Shear by Tension Loading**. Annual Book of ASTM Standards. ASTM International, West Conshohocken, PA, pp. 158-160.
- ASTM, 2002c. **Standard Test Methods for Resistance of Adhesives to Cyclic Laboratory Aging Conditions**. Annual Book of ASTM Standards. ASTM International, West Conshohocken, PA, pp. 70-73.
- Barkia, A., Bougatef, A., Nasri, R., Fetoui, E., Balti, R., Nasri, M., 2010. Trypsin from the viscera of Bogue (Boops boops): isolation and characterisation, *Fish Physiol. Biochem.* 36, 893-902. doi: 10.1007/s10695-009-9365-z.
- Cheng, E., 2004. Adhesion mechanism of soybean protein adhesives with cellulosic materials. , 109.

Cheng, E., Sun, X., 2006. Effects of wood-surface roughness, adhesive viscosity and processing pressure on adhesion strength of protein adhesive, *J. Adhes. Sci. Technol.* 20, 997-1017. doi: 10.1163/156856106777657779.

Frihart, C.R., 2010. Soy protein adhesives, *McGraw Hill Yearbook of Science and Technology* 2010 , 354.

Hettiarachchy, N.S., Kalapathy, U., Myers, D.J., 1995. Alkali-modified soy protein with improved adhesive and hydrophobic properties, *Journal of the American Oil Chemists Society* 72, 1461-1464. doi: 10.1007/BF02577838.

Huang, W., Sun, X., 2000. Adhesive properties of soy proteins modified by sodium dodecyl sulfate and sodium dodecylbenzene sulfonate, *Journal of the American Oil Chemists Society* 77, 705-708. doi: 10.1007/s11746-000-0113-6.

Kalapathy, U., Hettiarachchy, N., Myers, D., Hanna, M.A., 1995. Modification of Soy Proteins and their Adhesive Properties on Woods, *Journal of the American Oil Chemists Society* 72, 507-510. doi: 10.1007/BF02638849.

Kalapathy, U., Hettiarachchy, N.S., Myers, D., Rhee, K.C., 1996. Alkali-modified soy proteins: Effect of salts and disulfide bond cleavage on adhesion and viscosity, *Journal of the American Oil Chemists Society* 73, 1063-1066. doi: 10.1007/BF02523417.

Kato, A., 1991. Significance of Macromolecular Interaction and Stability in Functional-Properties of Food Proteins, *ACS Symp. Ser.* 454, 13-24.

Lambuth, A.L., 1977. Soybean glues. In: Skeist, I. (Ed.), *Handbook of Adhesives*. Van Nostrand Reinhold Co., New York, pp. 172-180.

Mackay, C.D., 1998. Good adhesive bonding starts with surface preparation, *Adhes Age* 41, 30-32.

Markley, K.S., 1951. *Soybeans and Soybean Products*. Vol. II. Interscience Publishers, Inc., New York.

Pang, B., Ryu, C., Kim, H., 2013. Improvement in wettability of pressure-sensitive adhesive on silicon wafer using crosslinking agent with siloxane groups, *J Appl Polym Sci* 129, 276-281. doi: 10.1002/app.38737.

Qi, G., Li, N., Wang, D., Sun, X.S., 2013. Physicochemical properties of soy protein adhesives modified by 2-octen-1-ylsuccinic anhydride, *Industrial Crops and Products* 46, 165-172. doi: 10.1016/j.indcrop.2013.01.024.

Qi, G., Li, N., Wang, D., Sun, X.S., 2012. Physicochemical Properties of Soy Protein Adhesives Obtained by In Situ Sodium Bisulfite Modification During Acid Precipitation. *J. Am. Oil Chem. Soc.* 89, 301-312. doi: 10.1007/s11746-011-1909-6.

Scheikl, M., Dunky, M., 1998. Measurement of dynamic and static contact angles on wood for the determination of its surface tension and the penetration of liquids into the wood surface, *Holzforschung* 52, 89-94. doi: 10.1515/hfsg.1998.52.1.89.

Shutov, A.D., Pineda, J., Senyuk, V.I., Reva, V.A., Vaintraub, I.A., 1991. Action of Trypsin on Glycinin - Mixed-Type Proteolysis and its Kinetics - Molecular Mass of Glycinin-T, *European Journal of Biochemistry* 199, 539-543. doi: 10.1111/j.1432-1033.1991.tb16152.x.

Sipos, T., Merkel, J.R., 1970. An Effect of Calcium Ions on Activity, Heat Stability, and Structure of Trypsin, *Biochemistry (N. Y.)* 9, 2766-&. doi: 10.1021/bi00816a003.

Skeist, I., 1962. *Handbook of Adhesives*.

Sowa, D., Czech, Z., Byczynski, L., 2014. Peel adhesion of acrylic pressure-sensitive adhesives on selected substrates versus their surface energies, *Int J Adhes Adhes* 49, 38-43. doi: 10.1016/j.ijadhadh.2013.12.013.

Sun, X.S., 2011. Soy Protein Polymers and Adhesion Properties, *Journal of Biobased Materials and Bioenergy* 5, 409-432. doi: 10.1166/jbmb.2011.1183.

Sun, X., Zhu, L., Wang, D., 2006. Surface active and interactive soy protein polymers and making hydrophobic clusters and complexes of soybean globular proteins. *PCT Int. Appl.* 2006-US15943; 2005-674176P, 101.

Wu, Y.V., Inglett, G.E., 1974. Denaturation of Plant Proteins Related to Functionality and Food Applications - Review, *J. Food Sci.* 39, 218-225. doi: 10.1111/j.1365-2621.1974.tb02861.x.

Figure 4.1 The effects of three variables on viscosity: Three levels (-1, 0, and +1) of (A) incubation times (X_2) are presented with trypsin concentrations (X_1), (B) trypsin concentrations (X_1) are presented with GA concentrations (X_3), and (C) GA concentrations (X_3) were presented with incubation times (X_2). The other variable was maintained at zero.

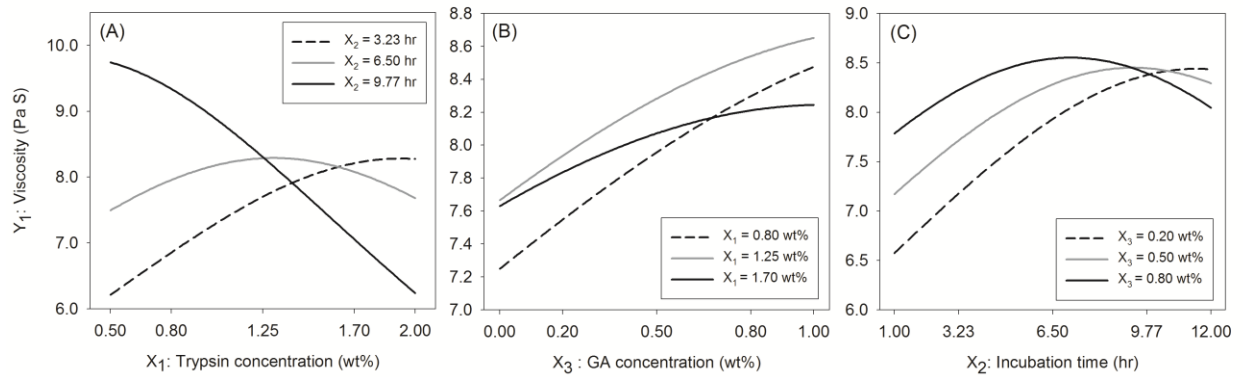


Figure 4.2 The molecular bands of reducing SDS-PAGE at 0.50wt% trypsin concentration. Lane (A): molecular weight standard; lane (B): control MSP; lane (C)-(F): MSP applied to 0.50 wt% trypsin with 1, 3, 6, and 12-h incubation times.

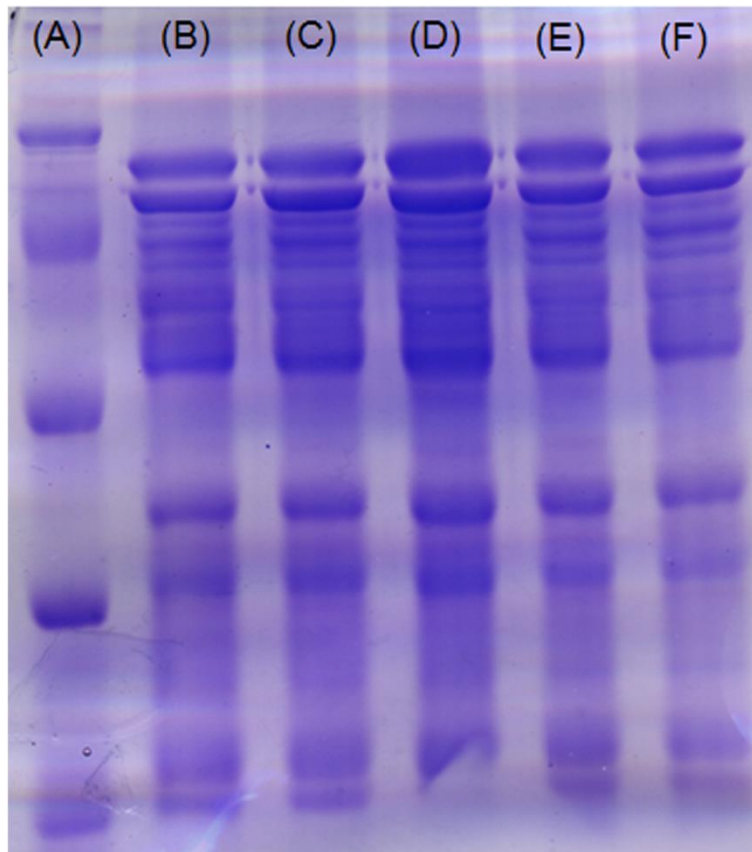


Figure 4.3 The effects of three variables on tacky force: Three levels (-1, 0, and +1) of (A) incubation times (X_2) are presented with trypsin concentrations (X_1), (B) trypsin concentrations (X_1) are presented with GA concentrations (X_3), and (C) GA concentrations (X_3) are presented with incubation time (X_2). The other variable was maintained at zero.

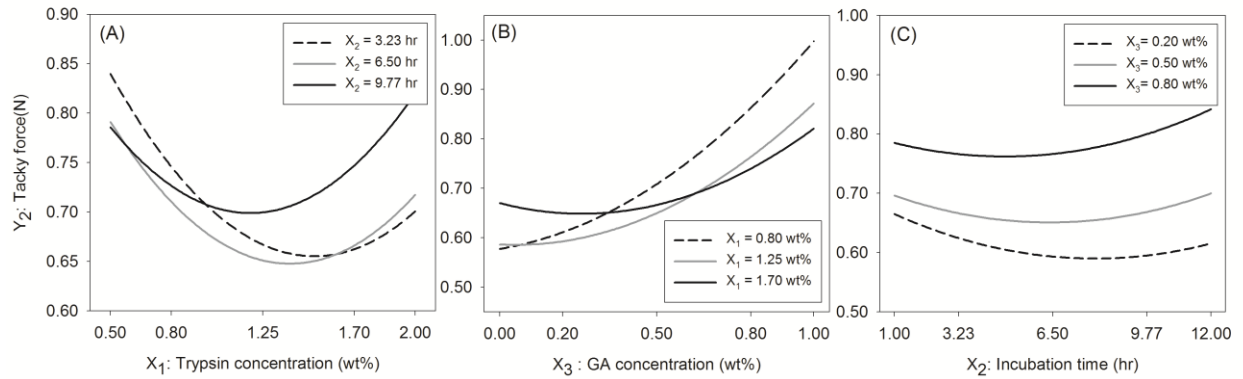


Figure 4.4 The effects of three variables on water resistance: Three levels (-1, 0, and +1) of (A) incubation times (X_2) are presented with trypsin concentrations (X_1), (B) trypsin concentrations (X_1) are presented with GA concentrations (X_3), and (C) GA concentrations (X_3) are presented with incubation times (X_2). The other variable was maintained at zero.

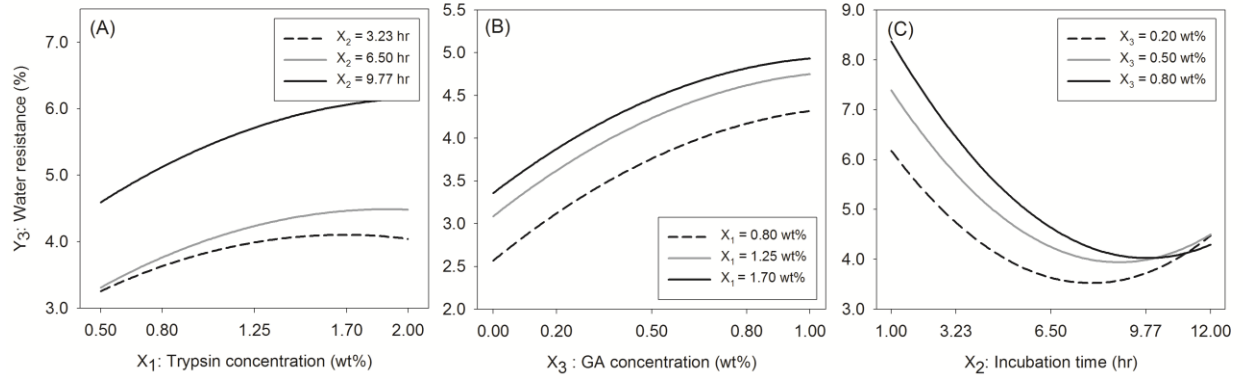


Figure 4.5 The regression model between viscosity and dry strength (a) and wet strength (b).

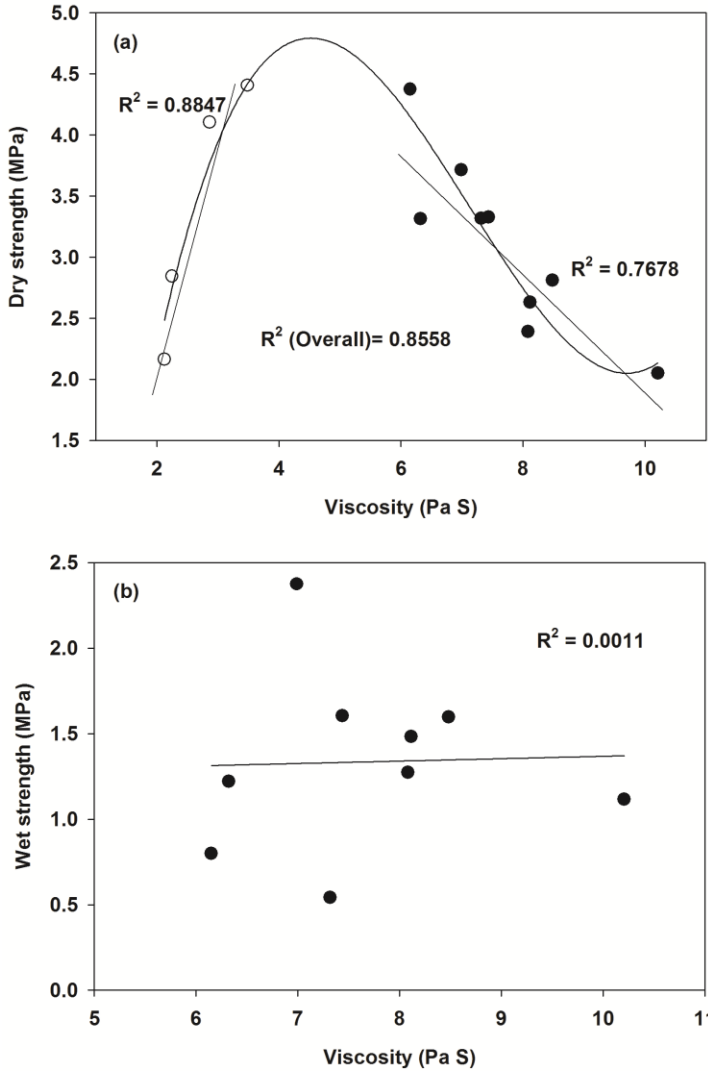


Figure 4.6 The regression model between tacky force and dry strength (a) and wet strength (b).

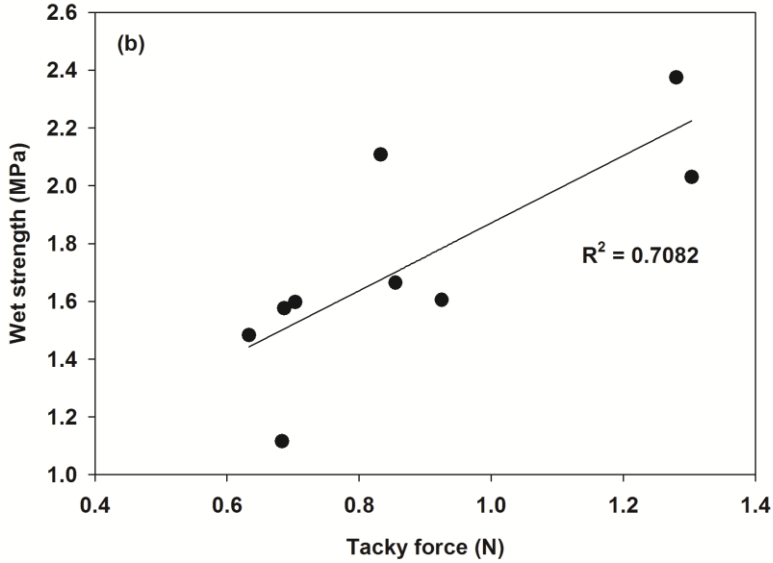
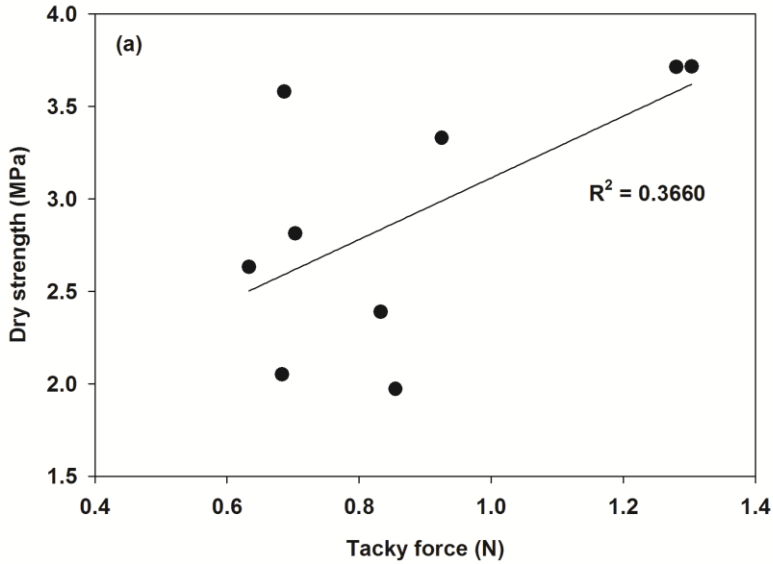


Figure 4.7 The regression model between water resistance and dry strength (a) and wet strength (b).

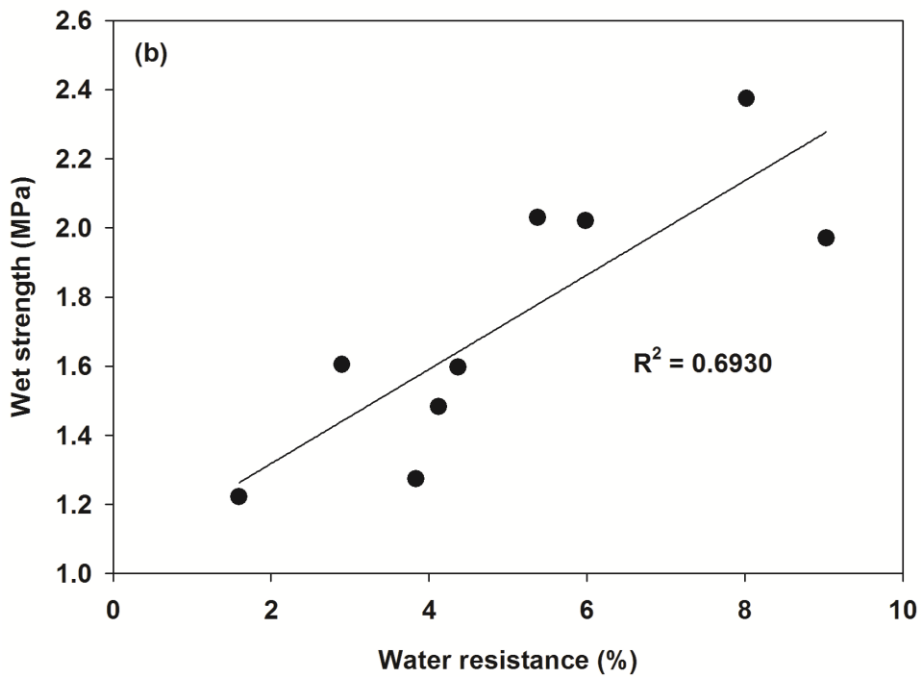
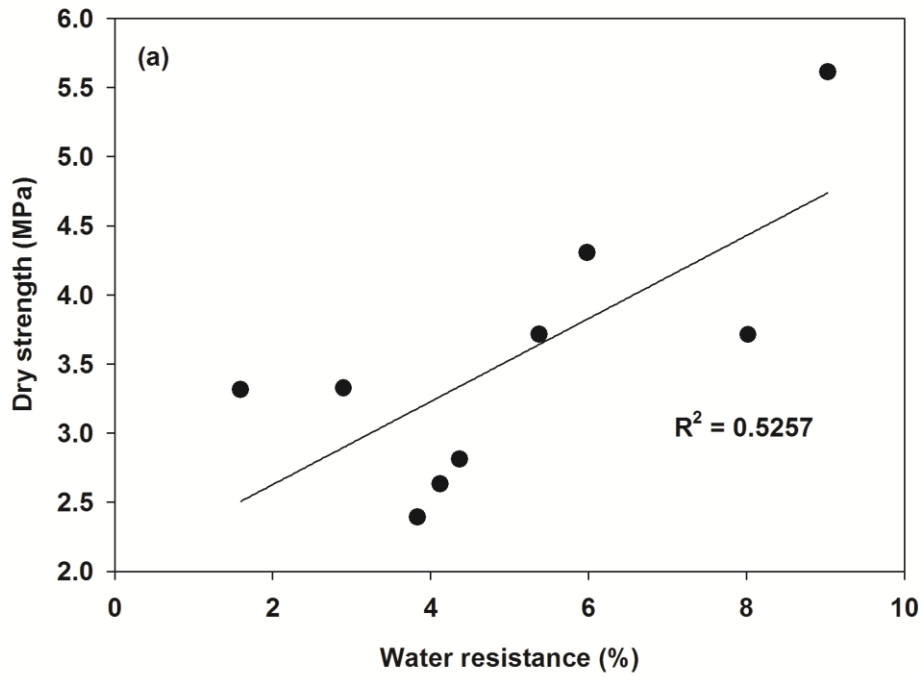


Table 4.1 Levels of parameter variables used in RSM design called CCD.

Coded and un-coded variables	Levels				
Coded variables (Z_i)	-1.682	-1	0	1	1.682
Trypsin concentration (X_1 , wt%)	0.50	0.80	1.25	1.70	2.00
Incubation time (X_2 , hr)	1.00	3.23	6.50	9.77	12.00
GA concentration (X_3 , wt%)	0.00	0.20	0.50	0.80	1.00

Table 4.2 Experimental design and the corresponding responses.

Run number	Trypsin concentration (X ₁ , wt%)	Incubation time (X ₂ , hr)	GA concentration (X ₃ , wt%)	Viscosity (Y ₁ , Pa S)	Tacky force (Y ₂ , N)	Water resistance (Y ₃ , %)
1	-1.682	0	0	6.32±0.14	0.90±0.07	1.60±0.44
2	0	0	0	8.11±0.35	0.63±0.05	4.12±0.02
3	1	-1	1	9.36±0.44	0.78±0.13	9.03±0.41
4	1	1	1	6.56±0.17	1.18±0.20	5.01±0.50
5	0	0	0	8.30±0.42	0.67±0.13	5.98±0.38
6	0	0	0	8.28±0.44	0.52±0.25	3.10±0.22
7	0	0	0	8.48±0.43	0.70±0.05	4.37±0.36
8	-1	1	-1	10.21±0.19	0.68±0.07	3.87±0.38
9	-1	-1	1	6.99±0.22	1.28±0.23	8.02±0.67
10	0	0	0	9.10±0.06	0.61±0.10	2.79±0.19
11	0	0	-1.682	7.32±0.27	0.66±0.18	4.04±0.29
12	-1	-1	-1	4.48±0.47	0.69±0.04	2.58±0.32
13	0	-1.682	0	5.78±0.18	0.83±0.24	13.47±0.47
14	-1	1	1	8.86±0.32	1.30±0.06	5.38±0.72
15	0	0	0	7.05±0.10	0.81±0.09	5.05±0.22
16	1	1	-1	5.99±0.34	0.86±0.24	3.86±0.41
17	1	-1	-1	8.08±0.15	0.79±0.10	3.83±0.51
18	0	0	1.682	7.44±0.11	0.96±0.12	2.90±0.24
19	0	1.682	0	7.27±0.11	0.57±0.08	5.01±0.57
20	1.682	0	0	6.15±0.20	0.82±0.05	5.21±0.21

Table 4.3 Analysis of variance (ANOVA) for regression model for each response (A) viscosity, (B) tacky force, and (C) water resistance.

(A) Viscosity	Sum squares	of	Df	Mean square	F-value	p-value
Model	0.013		9	1.496E-003	5.84	0.0054
X ₁	2.850E-005		1	2.850E-005	0.11	0.7455
X ₂	1.168E-003		1	1.168E-003	4.56	0.0584
X ₃	7.354E-004		1	7.354E-004	2.87	0.1209
X ₁ X ₂	7.456E-003		1	7.456E-003	29.13	0.0003
X ₁ X ₃	1.424E-004		1	1.424E-004	0.56	0.4729
X ₂ X ₃	1.184E-003		1	1.184E-003	4.63	0.0570
X ₁ ²	1.770E-003		1	1.770E-003	6.91	0.0252
X ₂ ²	1.241E-003		1	1.241E-003	4.85	0.0523
X ₃ ²	7.580E-005		1	7.580E-005	0.30	0.5982
Residual	2.559E-003		10	2.559E-004		
Lack of fit	1.999E-003		5	3.998E-004	5.84	0.0946
Pure Error	5.605E-004		5	1.121E-004		
Correlation total	0.016		19			

(B) Tacky force	Sum squares	of	Df	Mean square	F-value	p-value
Model	0.69		9	0.076	3.16	0.0435
X ₁	0.017		1	0.017	0.72	0.4153
X ₂	7.937E-005		1	7.937E-005	3.290E-003	0.9554
X ₃	0.29		1	0.29	11.83	0.0063
X ₁ X ₂	0.024		1	0.024	1.00	0.3402
X ₁ X ₃	0.10		1	0.10	4.23	0.0668
X ₂ X ₃	0.016		1	0.016	0.66	0.4358
X ₁ ²	0.16		1	0.16	6.52	0.0287
X ₂ ²	0.033		1	0.033	1.36	0.2703
X ₃ ²	0.092		1	0.092	3.82	0.0790
Residual	0.24		10	0.024		
Lack of fit	0.19		5	0.038	3.92	0.0801
Pure Error	0.049		5	9.812E-003		
Correlation total	0.93		19			

(C) Water resistance	Sum squares	of	Df	Mean square	F-value	p-value
Model	100.37		9	11.15	3.26	0.0398
X ₁	4.65		1	4.65	1.36	0.2708
X ₂	28.03		1	28.03	8.19	0.0169
X ₃	9.47		1	9.47	2.77	0.1272
X ₁ X ₂	0.87		1	0.87	0.25	0.6256
X ₁ X ₃	0.044		1	0.044	0.013	0.9119
X ₂ X ₃	7.94		1	7.94	2.32	0.1588

X_1^2	1.71	1	1.71	0.50	0.4963
X_2^2	42.62	1	42.62	12.46	0.0055
X_3^2	1.48	1	1.48	0.43	0.5251
Residual	34.22	10	3.42		
Lack of fit	27.09	5	5.42	3.80	0.0844
Pure Error	7.12	5	1.42		
Correlation total	134.59	19			

Table 4.4 Experiments of each response (A) viscosity, (B) tacky force, and (C) water resistance and corresponding shear adhesion strengths.

(A)

Run number	Trypsin concentration (X ₁ , wt%)	Incubation time (X ₂ , hr)	Glutaraldehyde concentration (X ₃ , wt%)	Viscosity (Y ₁ , Pa S)	Dry strength (MPa)	Wet strength (MPa)
1	0.50	6.50	0.50	6.32±0.14	3.31±0.37	1.22±0.39
2	1.25	6.50	0.50	8.11±0.35	2.63±0.03	1.48±0.40
7	1.25	6.50	0.50	8.48±0.43	2.81±0.26	1.60±0.40
8	0.80	9.77	0.20	10.21±0.19	2.05±0.26	1.12±0.24
9	0.80	3.23	0.80	6.99±0.22	3.71±0.28	2.38±0.33
11	1.25	6.50	0.00	7.32±0.18	3.32±0.25	0.54±0.37
17	1.70	3.23	0.20	8.08±0.10	2.39±0.29	1.27±0.28
18	1.25	6.50	1.00	7.44±0.11	3.33±0.41	1.61±0.13
20	2.00	6.50	0.50	6.15±0.20	4.37±0.19	0.80±0.28

(B)

Run number	Trypsin concentration (X ₁ , wt%)	Incubation time (X ₂ , hr)	Glutaraldehyde concentration (X ₃ , wt%)	Tacky force (Y ₂ , %)	Dry strength (MPa)	Wet strength (MPa)
8	0.80	9.77	0.20	0.68±0.07	2.05±0.26	1.12±0.24
9	0.80	2.32	0.80	1.28±0.23	3.71±0.28	2.38±0.33
13	1.25	1.00	0.50	0.83±0.24	2.39±0.27	2.11±0.29
12	0.80	3.23	0.20	0.69±0.04	3.58±0.19	1.58±0.20
2	1.25	6.50	0.50	0.63±0.05	2.63±0.03	1.48±0.40
18	1.25	6.50	1.00	0.96±0.12	3.33±0.41	1.61±0.13
7	1.25	6.50	0.50	0.70±0.05	2.81±0.26	1.60±0.40
14	0.80	9.77	0.80	1.30±0.06	3.71±0.04	2.03±0.25
16	1.70	9.77	0.20	0.86±0.24	1.97±0.30	1.66±0.38

(C)

Run number	Trypsin concentration (X ₁ , wt%)	Incubation time (X ₂ , hr)	Glutaraldehyde concentration (X ₃ , wt%)	Water resistance (Y ₃ , %)	Dry strength (MPa)	Wet strength (MPa)
1	0.50	6.50	0.50	1.60±0.44	3.31±0.37	1.22±0.39
3	1.70	3.23	0.80	9.03±0.81	5.61±0.05	1.97±0.38
5	1.25	6.50	0.50	5.98±0.38	4.30±0.37	2.02±0.15
9	0.80	3.23	0.80	8.02±0.97	3.71±0.28	2.38±0.33
17	1.70	3.23	0.20	3.83±0.51	2.39±0.29	1.27±0.28
2	1.25	6.50	0.50	4.12±0.02	2.63±0.03	1.48±0.40
18	1.25	6.50	1.00	2.90±0.24	3.33±0.41	1.61±0.13
7	1.25	6.50	0.50	4.37±0.86	2.81±0.26	1.60±0.40
14	0.80	9.77	0.80	5.38±0.72	3.71±0.04	2.03±0.25

Chapter 5 - CORRELATION BETWEEN FILM STRENGTH AND ADHESION STRENGTH OF SOY PROTEIN

5.1. ABSTRACT

This work studied the correlation between film and adhesion strength of soy protein. Because cohesion among protein molecules plays an important role in both film and adhesion mechanisms, we hypothesized that the film strength might be a reliable indicator to predict the adhesion strength of soy protein. Soy protein isolate (SPI) solutions were prepared with different concentration of plasticizer (poly (propylene glycol) bis (2-aminopropyl ether) ($H_2N-PPG-NH_2$)) loaded and measured the mechanical properties of the film and adhesion properties. The results revealed the low correlation between film and adhesion strength of the soy protein system in the presence of the plasticizer. This result may come from different curing parameters for film and adhesive applications. Soy protein is a kind of thermosetting polymer and the molecular structure of soy protein, presence of plasticizer, and curing parameters all significantly affect the curing behavior as well as mechanical properties of final materials. Thus, we believe that the same curing conditions for film and adhesive applications are required to obtain the correlation of film and adhesion strength of soy protein. Besides, water resistance of the film has a solid correlation with dry and wet adhesion strength and can be used to predict the adhesion strength of the soy protein system of this work.

5.2. INTRODUCTION

Soy protein-based adhesives have shown great potential as wood adhesives and much effort has been made to prepare soy protein-based adhesives in order to replace petroleum-based adhesives (Kumar et al., 2002; Sun, 2011). As a wood adhesive, soy protein should meet basic

requirements such as high adhesive strength, water resistance and low viscosity. Many researchers have attempted to modify soy protein-based adhesives using denaturation reagents, reducing agents, crosslinking agents and enzyme hydrolysis to improve adhesion performance (Chae et al., 1997; Hamada and Marshall, 1989; Hettiarachchy et al., 1995; Huang and Sun, 2000; Kalapathy et al., 1995; Kato, 1991; Lambuth, 1977; Wu et al., 1998; Wu and Inglett, 1974; Zhong et al., 2001). In order to evaluate the adhesion performance of soy protein-based adhesives, it is widely accepted to follow national standards to ensure the comparative shear adhesion strengths of adhesives in plywood-type construction. These standard methods are required for long testing cycles and expenses. If we could predict or screen the adhesion strength with simple and reliable methods instead of those national standard methods, it could help reduce time and expenses for related industrial fields.

This work attempted to find reliable parameters or predictors that represent the adhesion performance of soy protein. We assume that once soy protein is converted into the film, the important mechanical properties of the film may be related to adhesion properties of soy protein. Cohesion or crosslinking degree in the soy protein polymer network is critical to influence mechanical properties of films and even plays an important role in adhesion with wood substrates. For this context, we hypothesized that film strength could represent the adhesion strength of soy protein. The film preparation usually takes shorter time and less expense compared to wood adhesion testing and this would benefit related industrial fields. Therefore, important mechanical properties of the films including tensile strength and water resistance were chosen and their relationship with adhesion strength of soy protein was studied.

The film prepared from soy protein alone is fragile and brittle because of internal bonds and interactions among protein chains (Sothornvit and Krochta, 2000). Generally, it is necessary

to add plasticizers to reduce interactions among protein chains in order to improve their processibility and the mechanical properties of the final material. Plasticizers increase chain mobility and reduce brittleness by decreasing interactions between proteins and replacing them with protein-plasticizer interactions (Adeodato Vieira et al., 2011). Various plasticizers include polyols, such as sorbitol, glycerol, polythethylene glycol (PEG), and glucose for this purpose (Hernandez-Izquierdo and Krochta, 2008). Among these plasticizers, glycerol is one of the most widely used in protein processing and soy protein plasticized with glycerol has favorable processing properties with good final properties (Jagadish et al., 2010; Soares and Soldi, 2010; Yan et al., 2012; Zhang et al., 2011). Our preliminary study identified a new plasticizer, poly (propylene glycol) bis (2-aminopropyl ether) (molecular weight ~230, H₂N-PPG-NH₂) for soy protein. It can be used as a plasticizer for soy protein to overcome the brittleness and improve the flexibility and toughness. Diamine group at the end could provide opportunities with more polarity and solubility to affect hydrogen bonding ability with soy protein and subsequently influence the plasticizing effect. Also, it is a hydrophobic polymer, which is also expected to increase the water resistance of soy protein. In this work, soy protein isolate (SPI) solutions were prepared with different concentrations of NH₂-PPG-NH₂ and resulting solutions were used for film and adhesive application. We measured mechanical properties (tensile strength and water resistance of the films) and adhesion properties of soy protein and studied the correlation between them.

5.2. EXPERIMENTAL PROCEDURES

5.2.1. Materials and SPI separation

Defatted soy flour with a protein dispersion index (PDI) of 90 was provided from Cargill (Cedar Rapids, IA, USA). Lithium perchlorate (LiClO₄) and poly (propylene glycol) bis (2-

aminopropyl ether) (Average $M_n \sim 230$, $\text{NH}_2\text{-PPG-NH}_2$) were purchased from Sigma Aldrich (St. Louis, MO, USA). Plywood ($50 \times 127 \times 5$ mm) was produced from cherry veneer supplied by Veneer One (Oceanside, NY, USA).

5.2.2. SPI Separation and soy protein based biopolymer preparation.

The SPI was extracted from the defatted soy flour by isoelectric point precipitation at pH 4.2 (Kinsella, 1979; Wolf, 1970). The precipitate was freeze-dried and then milled into powder. The freeze-dried SPI had an averaged protein content of 93% (dry basis). SPI dispersions were prepared by magnetically stirring 6g SPI in 100ml LiClO_4 solution (0.6 mol/L) and the pH was adjusted to 10.0 with 3M sodium hydroxide solution. Then, the solution was sonicated with high power for 30 minutes. The resulting dispersions were used to dissolve the $\text{NH}_2\text{-PEG-NH}_2$ powder with different concentration (0, 1, 5, 10, 20, 30, and 40 % based on dry weight of SPI) and the mixture was magnetically agitated again to assure complete dissolution of the $\text{NH}_2\text{-PEG-NH}_2$.

5.2.3. Preparation of soy protein-based films

The resulting solutions were casted-onto a teflon coated-cavity mold (1 in. \times 6 in.). The cavity mold is 700 μm deep and the prepared protein solution was poured into the cavity. The film thickness was controlled by casting the same volume solution (5.0 mL). The casting was dried at 70 °C for 24 hour. The finished intact films were peeled off the plates. All film samples were preconditioned at 23 °C and 50% relative humidity for 48 h prior to test in accordance with ASTM D882-12.

5.2.4. Characterization of physical and mechanical properties of the film

5.2.4.1. Tensile strength and Elongation at Break of the film

Tensile strength (TS, MPa; maximum stress on the cross-section of film in the tensile test) and breaking elongation (EB, %; percentage of elongation at breakage to the original length of film in the tensile test) were tested using an tensile tester (TT-1100, ChemInstruments, Fairfield, OH, USA) at a cross-head speed of 2.0 in./min according to ASTM D882-12. The initial grip separation was set at 4 in. The prepared films were 1 in. wide and 6 in. long and the average thickness of those was 0.23±0.01 mm. All samples were conditioned at at 23 °C and 50% relative humidity for 48 h prior to test in accordance with ASTM D882-12. The values were reported as the average of six measurements.

5.2.4.2. Water resistance of the film

A simple method to measure water resistance of the film was established in this work. Water resistance of the film was measured by comparing the weights before and after water soaking of cured soy protein film. A small piece of soy protein film (1 in. × 1 in.) was soaked in water (tap water, temperature 21 °C) for 30 minutes in order to observe the loss or dissolution of cured protein film into water. The wet specimens were put into the oven at a temperature of 70 °C for 24 hour for complete the drying of water. Water resistance (%) was calculated based on the difference of weight of protein film before and after water soaking with the equation (1). The lower the water solubility means the higher the water resistance of cured protein film.

$$\text{Water resistance(\%)} = \left[\frac{(W_b - W_a)}{W_b} \right] \times 100 \quad (1)$$

where W_b and W_a are weight of sample before and after water soaking, respectively.

5.2.4.3. Two ply plywood specimen preparation and adhesion strength measurement

Cherry wood veneers with dimensions of 50 × 127 × 5 mm were preconditioned in a chamber (Electro-Tech Systems, Inc., Glenside, PA) for 7 day at 23 °C and 50% relative humidity. The adhesive samples were the same SPI solution as prepared for the films. The wood

specimen was prepared by following the procedures established in our lab (Sun and Bian, 1999). The protein solution (600mg) was placed on each side of a piece of wood and spread uniformly with a brush onto one end of a piece of cherry wood with dimensions of 127 × 20 mm (length × width) until the entire area was completely wet. Two wood pieces were allowed to rest at room temperature for 15 minutes and were then assembled and pressed together using a Hot Press (Model 3890 Auto M; Carver, Inc., Wabash, IN) at 1.4 MPa and 170 °C for 10 min.

For two-ply plywood samples, the assembled wood samples were cooled, conditioned at 23 °C and 50% relative humidity for 48 hours, and cut into 5 pieces with dimensions of 80 × 20 mm (glued area of 20 × 20 mm). The cut wood specimens were conditioned for another 2 days before measurements were taken. Wood specimens were tested with an Instron Tester (Model 4465, Canton, MA) according to ASTM Standard Method D2339-98 at a crosshead speed of 1.6 mm/min. Shear adhesion strength at maximum load was recorded; reported values are the average of four specimen measurements. Water resistance of the wood assemblies was measured following ASTM Standard Methods D1183-03 and D1151-00. Six preconditioned specimens were soaked in tap water at 23 °C for 48 hours, and wet strength was tested immediately after water soaking.

5.3. RESULTS AND DISCUSSION

This work focused on the correlation between mechanical properties of films and adhesion properties of soy protein in terms of concentrations of the plasticizer. The detailed plasticizing mechanism and effect of NH₂-PPG-NH₂ on soy protein was not investigated in this study and will be studied in the future. The dry and wet adhesion strength of soy protein were measured with increasing concentration of NH₂-PPG-NH₂ on soy protein and summarized in Table 5.1. The dry strengths and wet strengths were gradually higher with increasing

concentrations of NH₂-PPG-NH₂. We believe that the plasticizing effect of NH₂-PPG-NH₂ would also help to improve the adhesion properties of soy protein. The incorporation of the plasticizer could reduce protein chain-to-chain interaction and induce conformation changes in soy globular structure. The plasticizing effect is due to the ability of plasticizer molecules to position them within the three-dimensional protein network, increasing the free-volume and facilitating the mobility of the polymer chains (Wihodo and Moraru, 2013). Strong internal interactions stabilizing three-dimensional structures of soy globular protein generally hinder the interaction with wood substrate, causing low adhesion strength. Therefore, disrupted intermolecular interactions among protein chains could present more opportunities to interact with cellulosic wood materials containing many hydroxyl groups. The adhesion strengths presented in Table 5.1 were used to build the linear regression model of mechanical properties of the film from soy protein.

5.3.1. Tensile strength

Table 5.2 summarizes the tensile strength (TS) and elongation at break (EB) with increasing concentrations of the plasticizer. TS greatly increased with the addition of the plasticizer and tended to increase up to 20% NH₂-PPG-NH₂ before starting to decrease. EB gradually increased with higher concentrations of the plasticizer and sharply improved with incorporation of 30% and 40% NH₂-PPG-NH₂. We believe that too much use of the plasticizer might adversely influence the TB. Generally, appropriate usages of plasticizer could lead to sufficient workability and processibility. Many researchers already pointed out that excessive usage of plasticizer caused the decrease the mechanical properties of soy protein-based film such as TB and water vapor permeability (Song et al., 2011; Wihodo and Moraru, 2013). As mentioned earlier, the plasticizer could alter the structure of soy protein by changing the type and

number of intermolecular interactions like electrostatic, hydrophobic, and hydrogen bonding. This structural change might negatively influence hydrogen bonding ability in presence of too much use of plasticizer.

Subsequently, a linear regression model between TB and adhesion strengths was built for correlation. The relationship between TB and dry/wet adhesion strength was low with R^2 values of 0.0018 and 0.2268, respectively as shown in Figure 5.1. This result is not agreement of our hypothesis and might be a reason of the different curing behavior of soy protein of film and adhesion mechanism. Adhesion mechanism of soy protein with wood substrates happened at different processing conditions from those for film formation and this would contribute to big different characteristics on cohesion and adhesion of each film and adhesive application.

Soy protein becomes harder from crosslinking reactions, which is called the curing process. Upon curing, the thermosetting soy protein adhesive undergoes irreversible chemical and physical changes, converting to the interwoven and entangled structure. Two main external factors, heat and pressure, significantly influence the curing behavior of soy protein (Sun, 2011). Soy protein adhesives were cured at 170 °C and 1.4 MPa, while soy protein films were cured at 70°C and no pressure. The major differences in these curing parameters could lead to different degree of crosslinking in soy protein polymeric matrix and divergent characteristic of final soy protein materials. Mo et al found that such curing processes are temperature-dependent, affecting final curing quality such as curing speed, tensile strength, and microstructure, of soy protein polymers (Mo et al., 1999). For example, the soy protein plastics takes about 10 min to reach maximum curing strength at a molding temperature of $\leq 120^\circ\text{C}$, whereas at 150°C , the curing process takes about 3 min. Therefore, soy protein with different curing parameters may have different phase transition behavior upon curing, which consequently could make it difficult to

correlate the film strength and adhesion strength from the same soy protein. We assume that high temperature could lead to unfolding and aggregation, revealing association/dissociation behaviors, which is particularly advantageous for bonding mechanisms with wood substrates.

5.3.2. Water resistance of film

Table 5.3 summarizes the water resistance of films from soy protein with increasing concentrations of the plasticizer. Water resistance tended to increase with the addition of the plasticizer. Regarding soy protein-based materials, low water resistance is one of the limitations because of the hydrophilic nature of soy protein. The plasticizer used in this work is a type of hydrophobic polymer and the more concentration of plasticizer loaded on soy protein could lead to improved water resistance properties.

Furthermore, a linear regression model between water resistance and adhesion strengths was built to study correlation. The relationship between water resistance and dry/wet adhesion strength had R^2 values of 0.8249 and 0.7205, respectively, as shown in Figure 5.2. With similar conclusion from previous chapter, the water resistance of the film can be used to predict the dry and wet shear adhesion strength of soy protein system in this work.

5.4. CONCLUSION

This work attempted to correlate the film strength and shear adhesion strength of soy protein. The results revealed that film strength in the presence of the plasticizer, $\text{NH}_2\text{-PPG-NH}_2$, was not correlated with the adhesion strength of soy protein. We believe that the different curing conditions (temperature and pressure) of soy protein might lead to different curing behavior and structural changes. This could contribute to cohesion and adhesion of specific soy protein application in a different ways. In order to achieve the relationship of film and adhesion strength,

similar or comparative curing conditions should be applied. However, water resistance of film was positively correlated with adhesion strength of soy protein.

5.5. REFERENCES

- Adeodato Vieira, M.G., da Silva, M.A., dos Santos, L.O., Beppu, M.M., 2011. Natural-based plasticizers and biopolymer films: A review, *European Polymer Journal* 47, 254-263. doi: 10.1016/j.eurpolymj.2010.12.011.
- Chae, H.J., In, M., Kim, M.H., 1997. Characteristic properties of enzymatically hydrolyzed soy proteins for the use in protein supplements, *Agricultural Chemistry and Biotechnology* 40, 404-408.
- Hamada, J.S., Marshall, W.E., 1989. Preparation and Functional-Properties of Enzymatically Deamidated Soy Proteins, *J. Food Sci.* 54, 598-&. doi: 10.1111/j.1365-2621.1989.tb04661.x.
- Hernandez-Izquierdo, V.M., Krochta, J.M., 2008. Thermoplastic processing of proteins for film formation - A review, *J. Food Sci.* 73, R30-R39. doi: 10.1111/j.1750-3841.2007.00636.x.
- Hettiarachchy, N.S., Kalapathy, U., Myers, D.J., 1995. Alkali-modified soy protein with improved adhesive and hydrophobic properties, *Journal of the American Oil Chemists Society* 72, 1461-1464. doi: 10.1007/BF02577838.
- Huang, W.N., Sun, X.Z., 2000. Adhesive properties of soy proteins modified by sodium dodecyl sulfate and sodium dodecylbenzene sulfonate, *Journal of the American Oil Chemists Society* 77, 705-708. doi: 10.1007/s11746-000-0113-6.
- Jagadish, R.S., Raj, B., Parameswara, P., Somashekar, R., 2010. Effect of glycerol on structure - property relations in chitosan/poly(ethylene oxide) blended films investigated using wide-angle X-ray diffraction, *Polym. Int.* 59, 931-936. doi: 10.1002/pi.2808.
- Kalapathy, U., Hettiarachchy, N., Myers, D., Hanna, M.A., 1995. Modification of Soy Proteins and their Adhesive Properties on Woods, *Journal of the American Oil Chemists Society* 72, 507-510. doi: 10.1007/BF02638849.
- Kato, A., 1991. Significance of Macromolecular Interaction and Stability in Functional-Properties of Food Proteins, *ACS Symp. Ser.* 454, 13-24.
- Kinsella, J.E., 1979. Functional-Properties of Soy Proteins, *Journal of the American Oil Chemists Society* 56, 242-258. doi: 10.1007/BF02671468.
- Kumar, R., Choudhary, V., Mishra, S., Varma, I.K., Mattiason, B., 2002. Adhesives and plastics based on soy protein products, *Industrial Crops and Products* 16, 155-172. doi: 10.1016/S0926-6690(02)00007-9.

Lambuth, A.L., 1977. Soybean glues. In: Skeist, I. (Ed.), Handbook of Adhesives. Van Nostrand Reinhold Co., New York, pp. 172-180.

Mo, X.Q., Sun, X.S., Wang, Y.Q., 1999. Effects of molding temperature and pressure on properties of soy protein polymers, *J Appl Polym Sci* 73, 2595-2602. doi: 10.1002/(SICI)1097-4628(19990923)73:13<2595::AID-APP6>3.3.CO;2-9.

Soares, R.M.D., Soldi, V., 2010. The influence of different cross-linking reactions and glycerol addition on thermal and mechanical properties of biodegradable gliadin-based film, *Materials Science & Engineering C-Materials for Biological Applications* 30, 691-698. doi: 10.1016/j.msec.2010.02.026.

Song, F., Tang, D., Wang, X., Wang, Y., 2011. Biodegradable Soy Protein Isolate-Based Materials: A Review, *Biomacromolecules* 12, 3369-3380. doi: 10.1021/bm200904x.

Sothornvit, R., Krochta, J.M., 2000. Plasticizer effect on oxygen permeability of beta-lactoglobulin films, *J. Agric. Food Chem.* 48, 6298-6302. doi: 10.1021/jf000836l.

Sun, X.Z., Bian, K., 1999. Shear strength and water resistance of modified soy protein adhesives, *Journal of the American Oil Chemists Society* 76, 977-980. doi: 10.1007/s11746-999-0115-2.

Sun, X.S., 2011. Soy Protein Polymers and Adhesion Properties, *Journal of Biobased Materials and Bioenergy* 5, 409-432. doi: 10.1166/jbmb.2011.1183.

Wihodo, M., Moraru, C.I., 2013. Physical and chemical methods used to enhance the structure and mechanical properties of protein films: A review, *J. Food Eng.* 114, 292-302. doi: 10.1016/j.jfoodeng.2012.08.021.

Wolf, W.J., 1970. Soybean Proteins - their Functional, Chemical, and Physical Properties, *J. Agric. Food Chem.* 18, 969-&. doi: 10.1021/jf60172a025.

Wu, W.U., Hettiarachchy, N.S., Qi, M., 1998. Hydrophobicity, solubility, and emulsifying properties of soy protein peptides prepared by papain modification and ultrafiltration, *Journal of the American Oil Chemists Society* 75, 845-850. doi: 10.1007/s11746-998-0235-0.

Wu, Y.V., Inglett, G.E., 1974. Denaturation of Plant Proteins Related to Functionality and Food Applications - Review, *J. Food Sci.* 39, 218-225. doi: 10.1111/j.1365-2621.1974.tb02861.x.

Yan, Q., Hou, H., Guo, P., Dong, H., 2012. Effects of extrusion and glycerol content on properties of oxidized and acetylated corn starch-based films, *Carbohydr. Polym.* 87, 707-712. doi: 10.1016/j.carbpol.2011.08.048.

Zhang, H., Deng, L., Yang, M., Min, S., Yang, L., Zhu, L., 2011. Enhancing Effect of Glycerol on the Tensile Properties of Bombyx mori Cocoon Sericin Films, *International Journal of Molecular Sciences* 12, 3170-3181. doi: 10.3390/ijms12053170.

Zhong, Z.K., Sun, X.Z.S., Fang, X.H., Ratto, J.A., 2001. Adhesion strength of sodium dodecyl sulfate-modified soy protein to fiberboard, *J. Adhes. Sci. Technol.* 15, 1417-1427. doi: 10.1163/156856101753213277.

Figure 5.1 The regression model between tensile strength (TS) and dry (a) and wet (b) shear adhesion strength.

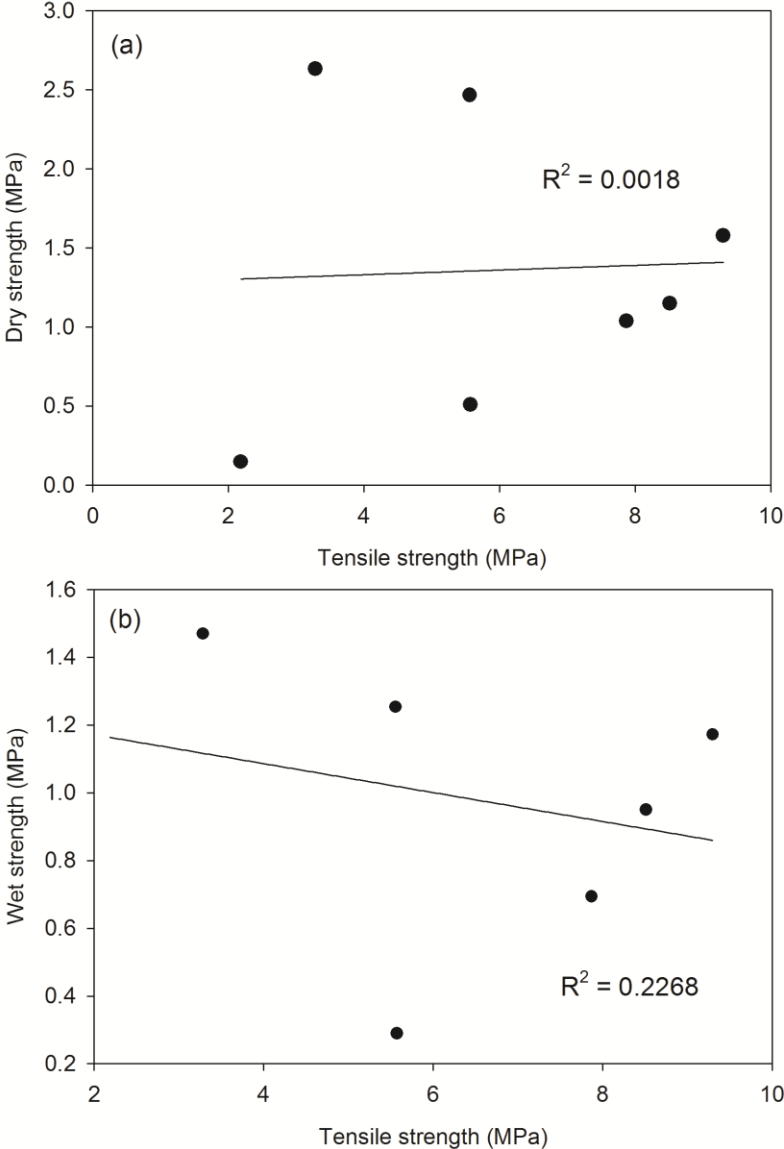


Figure 5.2 The regression model between water resistance and dry (a) and wet (b) shear adhesion strength.

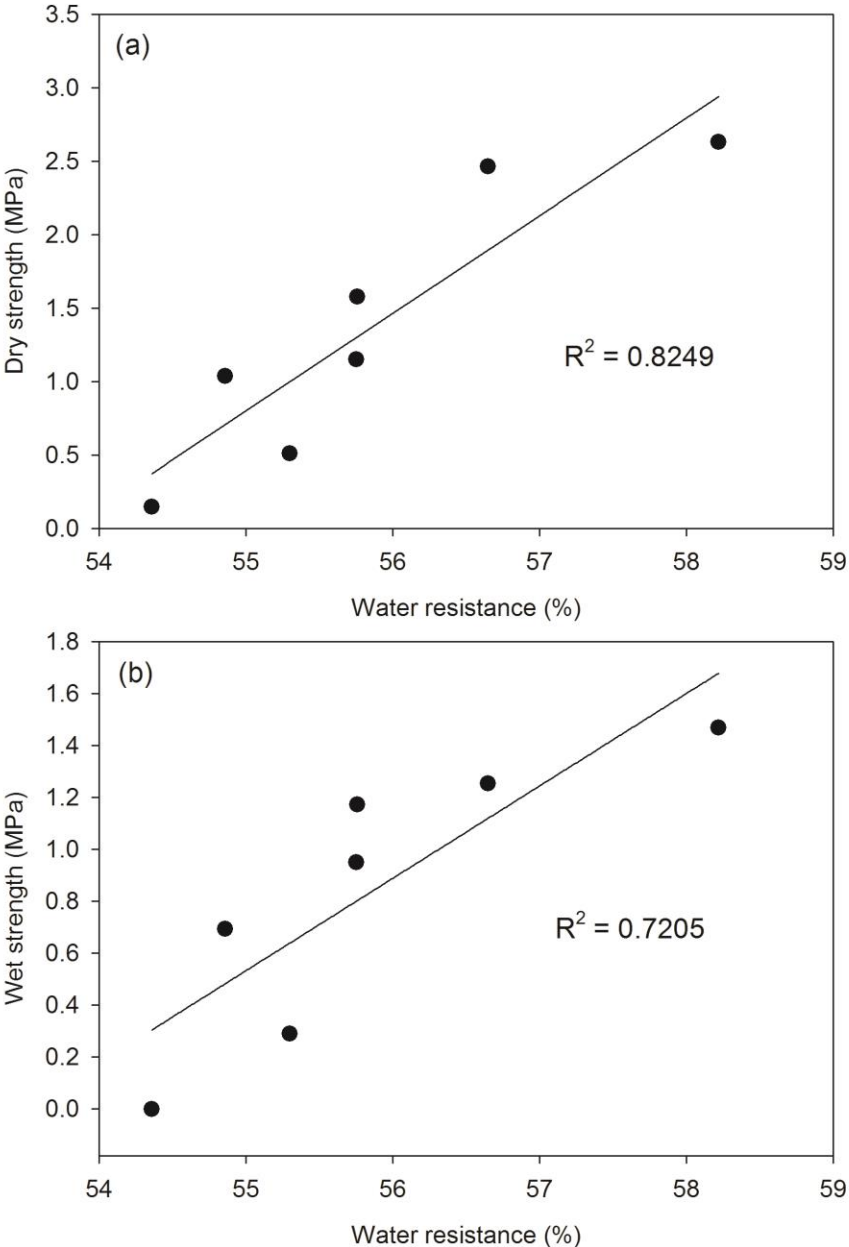


Table 5.1 The dry and wet shear adhesion strength of soy protein polymers with various concentrations of NH₂-PPG-NH₂.

Concentration of NH ₂ -PPG-NH ₂	Dry strength (MPa)	Wet strength (MPa)
0% (Control SPI)	0.147±0.074	-
1%	0.510±0.192	0.290±0.197
5%	1.037±0.407	0.694±0.177
10%	1.150±0.418	0.950±0.459
20%	1.578±0.223	1.172±0.231
30%	2.466±0.395	1.253±0.121
40%	2.632±0.366	1.469±0.264

Table 5.2 Tensile strength (TS) and elongation at break (EB) of films from soy protein biopolymers with various concentrations of NH₂-PPG-NH₂.

Concentration of NH ₂ -PPG-NH ₂	Tensile strength (MPa)	Elongation at break (%)
0% (Control SPI)	2.18 ± 0.32	0.51 ± 0.01
1%	5.57 ± 0.60	1.02 ± 0.04
5%	7.87 ± 0.44	1.40 ± 0.02
10%	8.51 ± 0.22	1.19 ± 0.01
20%	9.30 ± 0.39	4.40 ± 0.05
30%	5.56 ± 0.24	8.51 ± 0.04
40%	3.28 ± 0.49	7.75 ± 0.09

Table 5.3 Water resistance (%) of films from soy protein biopolymers with various concentrations of NH₂-PPG-NH₂.

Concentration of NH ₂ -PPG-NH ₂	Water resistance (%)
0% (Control SPI)	54.36 ± 0.46
1%	55.30 ± 0.33
5%	54.86 ± 0.18
10%	55.75 ± 0.21
20%	55.76 ± 0.30
30%	56.65 ± 0.37
40%	58.22 ± 0.22

Chapter 6 - CONCLUSION

In this work, soy protein-based adhesives have been modified with inorganic calcium silicate hydrate (CSH) to improve adhesion performance and water resistance. The crosslinking agent (APTES) played an important role in forming a crosslinked interface between organic soy protein polymeric matrix and inorganic calcium silicate hydrate, which could help attachment to the wood surface, which consequently leads to the improvement of bonding strength compared to unmodified soy protein. Also, the reduction of water-sensitive functional groups by reacting with the crosslinking agent could contribute to better wet adhesion strength of soy protein-based adhesives.

In addition, we attempted to find reliable indicators to represent shear adhesion strengths of soy protein by establishing the correlation of the physical and mechanical properties with shear adhesion performance of soy protein. This would eventually help industries in the field with quality control and product development. We investigated the correlation between the physical properties such as viscosity, tacky force, and water resistance and adhesion properties of ESP. Viscosity can be used to predict the dry adhesion strength; on the other hands, tacky force and water resistance can be good indicators of wet adhesion strength.

Furthermore, we attempted to build relationships between film and adhesion strength of soy protein as a part of the effort to find reliable predictors for adhesion strength of soy protein. The results revealed the weak correlation between film strength and adhesion strength of soy protein based on low value of R^2 and would be due to the fact that different curing parameters could contribute to different curing quality and strength, which greatly affect the cohesion and adhesion mechanism for each film and adhesive application. Therefore, similar curing

conditions should be required to accomplish the correlation between film and adhesion strength of soy protein.